W-Pos71 THE EFFECT OF CHOLESTEROL ON MODEL MEMBRANE PHASE TRANSITIONS DETECTED BY DEHYDROERGOSTEROL AND ALPHA PARINARIC ACID. Greg Smutzer and Philip L. Yeagle, Dept. of Biochemistry, State University of New York at Buffalo, Buffalo, New York 14214.

The fluorescent probes 9-dehydroergosterol and α-parinaric acid were employed to detect phase transitions by fluorescence depolarization in multilamellar vesicles of L-α-dimyristoylphosphatidylcholine (DMPC) as a function of membrane cholesterol concentration. In the absence of cholesterol, dehydroergosterol fluorescence was characterized by a rise in polarization anisotropy through the phase transition; this rise was observed over a 0.6-1.0° C increase in temperature with the T_m of the lipid at 23.6° C. Addition of one mole% cholesterol caused a marked decrease in total anisotropy change through the phase transition while 5 mole% cholesterol caused a further decrease in amplitude and a broadening of dehydroergosterol polarization anisotropy change. Ten mole% cholesterol completely obliterated the dehydroergosterol-detected phase transition in these multilamellar vesicles. The lipid probe α-parinaric acid exhibited a characteristic decrease in polarization anisotropy through the phase transition with the change occurring over a 2.0° C temperature range. Addition of cholesterol produced a less drastic effect upon changes in polarization anisotropy since 10 mole% cholesterol decreased fluorescence depolarization primarily below the T_m resulting in an approximate 40% decrease in amplitude of the phase transition itself. The opposing direction of the amplitude changes through the T_m as well as the different effect of membrane cholesterol upon these two fluorescent probes indicate that α-parinaric acid and dehydroergosterol are probing different regions of the membrane bilayer. These results further indicate that dehydroergosterol is likely probing the cholesterol-rich regions of the membrane. Supported by NIH grant HL 23853.

W-Pos72 HYDROPHOBIC ION SPIN LABELS AS PROBES OF DISPLACEMENT CURRENTS IN MEMBRANES Ross F. Flewelling and Wayne L. Hubbell, Jules Stein Eye Institute, UCLA School of Medicine, Los Angeles, CA 90024

Protein-bound charge and dipole motions in biological membranes are crucial for a variety of membrane functions, including the opening and closing of channels (gating) and the functioning of electrically active membrane proteins. Such motions have previously been inferred from current-voltage relations obtained from conventional electrical measurements.

We have studied the effect of membrane charge displacement in reconstituted and model systems on the transmembrane relaxation processes of charged spectroscopic probes. Paramagnetic hydrophobic ion spin labels (such as triphenylnitroxylphosphoniums) were rapidly mixed with sonicated lipid vesicles in concentration ranges where their relaxation across the membrane was limited by their own diffusion potential. The rate and equilibrium state for the relaxation are quantitatively dependent on the presence of polarizable elements in the membrane. For example, displacement currents due to membrane-bound hydrophobic ions such as tetraphenylboron and triphenylalkylphosphoniums can be measured by this method down to levels as low as one electronic charge per 1000 lipids. Studies in model systems with the introduction of molecular dipoles and relevant membrane proteins (e.g., alamethicin and rhodopsin) will also be reported. Preliminary results on the measurement of displacement charge are consistent with theoretical calculations based on kinetic equations assuming an Eyring barrier model. The goal of this work is to develop a molecular approach for measuring gating charge movement and capacitance in membranes of isolated and reconstituted systems where microelectrode methods are generally inapplicable. (NIH EY05216)

W-Pos73 FLUORESCENCE LIFETIMES AND FLUORESCENCE YIELDS OF CARBOCYANINE PROBES IN PHOSPHOLIPID BILAYERS. Beverly S. Packard[β] and David E. Wolf[ψ] Division of Chemical Biodynamics, Lawrence Berkeley Laboratory, University of California, Berkeley, CA. 94720[β] and Worcester Foundation for Experimental Biology, Shrewsbury, MA. 01545[ψ].

We have measured the fluorescence lifetimes and fluorescence yields of the 1,1'-dialkyl-3,3,3',3'-tetramethylindocarbocyanine (C_NDiI)-C_3 (N = 12, 18, and 22) probes in a series of phospholipid bilayer environments. The effects of the phospholipid physical state, DiI chain length, charge and H-bonding characteristics of the head group region, and DiI concentration were examined. All decays were best fit by a sum of two exponentials. Consistent with scanning calorimetry and fluorescence recovery after photobleaching (FRAP) data, the magnitude and percentage of the long lifetime component as well as the fluorescence yield increased with the degree of order in the bilayer fluorophore microenvironment. Thus, either phospholipids in the gel state with chain lengths approximating those of DiI or the addition of phosphatidylethanolamine (a phospholipid with a(n) H-bonding headgroup) caused increases in both the fluorescence lifetime and fluorescence yield. Modification of charge in the head group region by the addition of phosphatidic acid or stearylamine to phosphatidyl choline liposomes did not significantly affect the lifetimes but did cause a decrease in the measured fluorescence yield. Both lifetimes and fluorescence yield were found to be dependent on DiI concentration. Understanding the factors which affect fuorescence lifetimes and yields may help to elucidate the partitioning of these probes among domains in biologic membranes.

W-Pos74 THERMODYNAMICS AND KINETICS OF PHOSPHOLIPID MONOMER-VESICLE INTERACTION.
J. Wylie Nichols. Dept. Physiol., Emory University Sch. Med., Atlanta GA 30322.

Resonance energy transfer between 1-palmitoyl-2-(12-(7-nitro-2,1,3-benzoxadiazol-4-yl)amino) caproyl)phosphatidylcholine (P-C_6-NBD-PC) and N-(lissamine rhodamine B sulfonyl)dioleoylphospatidyl-ethanolamine (N-Rh-PE) was used to monitor the rate of P-C_6-NBD-PC transfer between two populations of dioleoylphosphatidylcholine (DOPC) vesicles. The rate-limiting step for this process is the dissociation of the monomer from the vesicle. An Arrhenius plot of the temperature dependence of the dissociation rate constant can be interpreted according to Eyring's activated complex theory to give the standard Gibbs free energy ($\Delta G^{\ddagger o}$= 19.4 kcal/mole), enthalpy ($\Delta H^{\ddagger o}$= 16.4 kcal/mole) and entropy ($T\Delta S^{\ddagger o}$=-3.0 kcal/mole) of activation.

Resonance energy transfer was also used to determine the soluble concentration of P-C_6-NBD-PC in equilibrium with DOPC vesicles. Vesicles were prepared containing small percentages of P-C_6-NBD-PC and N-Rh-PE. The vesicle concentration of P-C_6-NBD-PC was determined from the extent of energy transfer and the vesicle concentration of N-Rh-PE from direct fluorescence. When small amounts of vesicles were added to buffer, the amount of P-C_6-NBD-PC relative to N-Rh-PE decreased, indicating that P-C_6-NBD-PC molecules were being lost from the vesicles to solution. With a 0.04 mole fraction of P-C_6-NBD-PC to DOPC, the concentration of soluble P-C_6-NBD-PC was 3.6 x 10^{-10} M. The molar partition coefficient (K_p) is equal to 4.9 x 10^9 and thus the standard Gibbs free energy (ΔG^o) between a monomer residing in a vesicle versus free in solution can be calculated (ΔG^o=RT lnK_p = 13.2 kcal/mole at 25°C). These data indicate that the free energy of activation for monomer-vesicle dissociation is much larger than the free energy difference between the two states at equilibrium. (Supported by NIH grant GM 32342-01)

W-Pos75 HYDROSTATIC PRESSURE DEPENDENCE OF PLANAR BILAYER LIPID MEMBRANE CONDUCTANCES.
M. Morrone and R.I. Macey, Dept. of Physiology-Anatomy, Univ. of California, Berkeley, CA 94720.

A gas-free high pressure cell has been designed and constructed to measure planar bilayer conductances induced by hydrophobic ions and ionophores as a function of hydrostatic pressure. Plots of conductance versus pressure for valinomycin and nonactin mediated potassium transport in egg phosphatidyl choline-decane membranes give straight lines over a range of 1 to 816 atm. Calculated activation volumes do not significantly differ for valinomycin and nonactin yielding values of 40 cc/mole and 37 cc/mole, respectively. The former value agrees closely with that obtained by Johnson and Miller (BBA 375:286,1975) for K^+-valinomycin transport in liposomes. Steady-state conductance and relaxation experiments are in progress to determine activation volumes for the elementary translocation steps associated with membrane permeation by valinomycin and nonactin as well as hydrophobic ions, tetraphenyl boron and a positively charged analogue, tetraphenyl arsonium. (Supported by NIH Grant #GM18819.)

W-Pos76 THEORY OF FLUORESCENCE DEPOLARIZATION IN MACROMOLECULES AND MEMBRANES. Attila Szabo, Laboratory of Chemical Physics, National Institute of Arthritis, Diabetes, and Digestive and Kidney Diseases, National Institutes of Health, Bethesda, Maryland 20205.

A comprehensive formalism is developed to describe the decay of the fluorescence emission anisotropy, r(t), in macroscopically isotropic systems where both excited state and orientational dynamics contribute to the depolarization. It is shown how energy transfer, heterogeneity, interconversion of excited states with different emission characteristics as well as both overall and internal reorientation, can be treated in a unified way. Such an extension of existing theory is required to analyze situations where, for example, the total fluorescence intensity is multiexponential or where r(t) depends on the excitation frequency. A systematic treatment of the influence of internal motions is presented. First, the geometry of the transition dipoles is explicitly "factored out" and general expressions for r(t) are obtained for several cases including when the motion occurs about a fixed axis and an axis which in turn can "wobble" about a director. Then, a variety of dynamical models (e.g. discrete jumps, free and restricted Langevin motion about an axis, diffusive motion of an axis in an orienting potential) are used to obtain the time dependence of the relevant correlation functions which appear in the above general expressions. In this way, one can obtain r(t) for a large class of models. Of particular interest, is an approximate analytic expression for r(t), valid for any orientation of the transition dipoles and restricting potential, of a cylindrical probe in a membrane. The influence of collective (hydrodynamic) fluctuations of the membrane director are also considered.

W-Pos77 STEROL EXCHANGE BETWEEN UNILAMELLAR VESICLES. INFLUENCE OF PHOSPHOLIPID AND STEROL STRUCTURE AND CHOLESTEROL CONTENT. Lillian Fugler-Domenico, Sanda Clejan, and Robert Bittman, Department of Chemistry, Queens College of the City University of New York, Flushing, NY 11367.

The extent to which phospholipid structural features affect cholesterol (Chol) exchange rate between membranes is not well established. We have studied the rate of [4-^{14}C]Chol exchange between small unilamellar vesicles (SUV) prepared with different phosphatidylcholines (PCs) and with different Chol/PC molar ratios. Donor vesicles containing 15 mol % dicetyl phosphate were separated from an excess of uncharged acceptor vesicles on DEAE-Sepharose CL-6B. Chol exchange between vesicles was first order, with the following $t_{1/2}$ values (min) at 37°C(6 mol % Chol): egg PC, 96 ± 6; diphytanoyl PC, 68 ± 1; diarachidonyl PC, 78 ± 8; dipalmitoyl PC, 128 ± 4; di-O-hexadecyl PC, 112 ± 8; 1-stearoyl-2-oleoyl PC, 199 ± 6; 1-oleoyl-2-stearoyl PC, 180 ± 6. [^{14}C]Chol underwent faster exchange from large unilamellar vesicles prepared from dimyristoyl PC with 6 mol % Chol than from SUV. We conclude that highly branched or unsaturated fatty acyl chains in PC result in weakened Chol/PC interactions; the molecular packing is similar in bilayers of Chol and ether - vs. ester-linked PCs; Chol desorption is sensitive to surface curvature but not to positional distribution of the saturated and unsaturated acyl chains in PC. [^{14}C]-β-Sitosterol (which has a 24 α- ethyl group) underwent exchange between egg PC bilayers containing 20 mol % sterol at the same rate as Chol. The rate of [^{14}C] Chol exchange decreased as the membrane lipid order increased. The following $t_{1/2}$ values (37°C) show that Chol desorption from egg PC SUV took place more readily at Chol content < 20 mol %: 1 mol %, 62 ± 4; 3%, 85 ± 6; 6%, 96 ± 6; 10%, 104 ± 18; 15%, 142 ± 20; 17.5% 158 ± 18; 20%, 191 ± 12; 30%, 199 ± 33; 40%, 193 ± 25. [Supported by NIH Grant HL 16660]

W-Pos78 ELECTROPHORETIC MOBILITIES OF MIXED-PHOSPHOLIPID LIPOSOMES AS A FUNCTION OF PHOSPHOLIPID COMPOSITION, Ca^{+2}, AND pH. James W. Klein and B. R. Ware, Department of Chemistry, Syracuse University, Syracuse, New York 13210, and Howard Petty, Department of Biological Sciences, Wayne State University, Detroit, Michigan 48202.

Electrophoretic light scattering (ELS) has been used to measure the electrophoretic mobility distributions of unsonicated multi-lamellar liposomes. The primary constituents of the liposomes were dimyristylphosphatidylcholine (DMPC) or Egg phosphatidyl choline (PC). Zero to thirty mole percent phosphatidyl serine (PS) was incorporated into these membranes. Their electrophoretic mobilities were measured at pH 5.5 and 7.3 in the presence and absence of 1.5mM $CaCl_2$. The mobility of pure PC membranes in low salt (12.5mM NaCl) is negative and small. This low but non-zero mobility is likely due to a small amount of contaminants not detected by thin layer chromatography, but is consistent with the presence of membrane-bound free fatty acids inferred from pH titration data. The electrophoretic mobility is dependent upon titration data. The electrophoretic mobility is dependent upon the bulk pH, fatty acyl chain length, presence of Ca^{+2}, and mole percent PS. At pH 5.5 and 7.3 the electrophoretic mobilities of DMPC liposomes increased as the mole percent PS was increased. The magnitude of the change in electrophoretic mobility however is markedly reduced by Ca^{+2}. Egg PC gave similar results to DMPC. For pure dipalmitoylphosphatidylcholine (DPPC) liposomes the electrophoretic mobilities at pH 5.5 and 7.3 changed from negative to positive upon addition of Ca^{+2}. The magnitude of the electrophoretic mobility reduction with Ca^{+2} increased as the mole percent of PS, a negatively charged lipid, was increased.

W-Pos79 ELECTROPHORETIC MOBILITIES OF CHARGED LIPOSOMES IN RELATION TO CONTENT OF INCORPORATED STEROLS. Lindsay Plank and B. R. Ware, Department of Chemistry, Syracuse University, Syracuse, New York 13210, and C. E. Dahl, James Bryant Conant Laboratories, Department of Chemistry, Harvard University, Cambridge, Massachusetts 02138.

Electrophoretic light scattering (ELS) was used to study the effects of sterols on the surface charge properties of unsonicated phospholipid bilayer membranes. The motivation for this study was to examine the relationship between sterol molecular conformation and the packing density of phospholipids in charged bilayer membranes. The initial surface charge density was determined by the ratio of negatively charged egg phosphatidylglycerol to zwitterionic egg phosphatidylcholine. Replacement of a portion of the phosphatidylcholine in phosphatidylglycerol:phosphatidylcholine liposomes by cholesterol was observed to cause a significant increase in electrophoretic mobility. This result is consistent with the smaller area occupied by a cholesterol molecule relative to the phospholipid. By contrast, an equivalent portion of lanosterol, which has a bulkier molecular geometry, did not produce an increase in electrophoretic mobility.

We have also used the ELS technique to probe the kinetics of cholesterol exchange between phospholipid vesicles by monitoring the changes in frequency shift of distinct vesicle populations as a function of time. For a surprisingly broad set of experimental conditions, the ELS spectra indicate no detectable exchange of cholesterol among liposome populations. Supported by NIH Grant GM 27633.

W-Pos80 BINDING OF CATIONIC ANTIBIOTICS TO LIPOPOLYSACCHARIDES. Arnold A. Peterson*, Robert E. W. Hancock+, and Estelle J. McGroarty*, *Michigan State University, East Lansing, MI, +University of British Columbia, Vancouver, British Columbia CANADA.

Cationic antibiotics have been shown to work, in part, by altering the permeability of gram-negative bacterial membranes, possibly by binding to the anionic lipopolysaccharide (LPS). We have characterized the interactions of LPS with cations such as aminoglycosidic and peptide antibiotics, and naturally occurring polyamines to determine cation induced changes of LPS structure leading to antibiotic permeability and toxicity. The partitioning of the cationic spin probe 4-dodecyldimethyl ammonium-1-oxyl-2,2,6,6-tetramethyl piperidine (CAT_{12}) was used to measure the binding of cations to isolated and purified LPS of Pseudomonas aeruginosa. Electron spin resonance spectra indicated that increasing concentrations of cations competitively displaced bound probe into the aqueous environment. This ability to displace CAT_{12} is affected by the charge of the competing cation, with higher charged molecules displacing a greater amount of probe. The toxicity of some aminoglycoside and peptide antibiotics was shown to correlate with the ability to bind to LPS. In addition, the mobility of the LPS head group, as detected with this probe, was shown to be altered by the addition of cations; high levels of polyamines increased mobility while the antibiotics decreased mobility, indicating differences in binding between the two groups. For all cations tested the ability to perturb LPS head group structure was independent of charge and affinity. We propose that the disruption of outer membrane integrity and permeability by cationic antibiotics may result from the anionic phosphate and carboxyl groups on the LPS binding these cations, and in turn altering the conformation of the LPS.

W-Pos81 RED-EDGE EXCITATION OF FLUORESCENCE AND THE DYNAMIC PROPERTIES OF PROTEINS AND MEMBRANES, by Susan Keating-Nakamoto and Joseph R. Lakowicz, University of Maryland, School of Medicine, Department of Biological Chemistry, Baltimore, Maryland 21201.

We used red-edge excitation of fluorescence to study the dynamics of solvents, model membranes and the protein apomyoglobin which were labelled with 2-p-toluidinyl-6-naphthalene sulfonic acid, (TNS). Red-edge excitation results in a shift of the emission maximum to longer wavelengths, (excitation red shifts); the magnitude of the shifts depend on the dynamic properties and polarity of the surrounding solvent. Using phase modulation fluorometry, the observed spectral shifts and lifetime behavior indicate the selective excitation of a subclass of solvent-relaxed fluorophores. The extent of solvent relaxation can be inferred from the magnitude of excitation red shifts. The red shifts of TNS in propylene glycol were correlated to the solvent relaxation times estimated by phase sensitive detection of fluorescence for TNS in propylene glycol at the same temperatures. The data obtained for TNS in propylene glycol was compared to the excitation shifts for TNS bound to the macromolecules and used to estimate the relaxation rates of the environments surrounding the probe. The comparison indicates rapid relaxation of TNS bound to lipids, 5 nanoseconds, and slower relaxation, 8 nanoseconds, of TNS bound to the heme site of apomyoglobin. An advantage of this method is that time-dependent information can be estimated using only steady state measurements.

W-Pos82 THE CONCEPT OF CRITICAL COAGELIZATION AND CRITICAL MICELLIZATION PRESSURE OF BIOLOGICAL SURFACTANTS.

Patrick T.T.Wong and Henry H.Mantsch
National Research Council of Canada, Ottawa, K1A 0R6, CANADA

We have investigated the Raman spectra of monoacyl phospholipids as a function of pressure,at constant temperature,up to pressures of 25 kbar.The critical pressure at which the clear micellar solution transforms into an opaque coagel,i.e.,a poorly hydrated solid phase,we have designated as the critical coagelization pressure. In the case of aqueous palmitoyl lysophosphatidylcholine this pressure was found to be 2 kbar. The transition has first order characteristics as demonstrated by the discontinuity of vibrational energies at the critical coagelization pressure. The transitions exhibits a very high hysteresis as the coagel phase does not transform back to the micellar phase until the pressure is reduced to values as low as 0.5 kbar. This critical pressure we have designated as the critical micellization pressure.

W-Pos83 EXCIMER FORMATION OF A PYRENEMETHYL CHOLESTEROL ADDUCT IN SINGLE BILAYER LIPOSOMES. Lesley Davenport and Ludwig Brand; Biology Department, The Johns Hopkins University. Baltimore, MD 21218.

1-Pyrenemethyl 3-β-hydroxy-22,23-bisnor-5-cholenate (PMC), a fluorescent cholesterol analogue, may be incoroporated within single bilayer dimyristoyllecithin (DML)vesicles, by cosonication from aqueous dispersions. Solubility of PMC within buffer is poor and background fluorescence is therefore insignificant. With increasing labelling ratios of PMC to phospholipid, excited-state dimers (excimers) are formed (PMC to lipid > 1:100; < 1 mole% cholesterol) similar to the closely related pyrene molecule. The broad structureless excimer fluorescence (λ max 480nm) is readily distinguished from the highly structured monomer fluorescence and compares favourably to the emission spectrum reported for that of pyrene. The process of excimer formation for PMC is significantly lower than for the corresponding pyrene concentrations, when embedded in the bilayer. The dimer to monomer fluorescence emission intensity ratio (I_{480}/I_{396})shows saturation-like deviations from linearity with increasing PMC concentrations indicative of non-random distributions of PMC within the bilayer. Consistent with the kinetic nature of excimer formation, increasing the temperature of the bilayer vesicles, above the phospholipid phase transition temperature (34°C) results in an increase in excimer fluorescence. Introduction of cholesterol (20 and 33 mole%) into the bilayer results in an increase in the I_{480}/I_{396} fluorescence ratio,with a greater effect for the higher cholesterol content. Above the phospholipid phase transition temperature the trend is identical. This is in contrast to pyrene which shows a decrease in the I_{480}/I_{396} ratio with increasing cholesterol. Interpretations of this data with respect to bilayer inhomogeneity will be discussed.

W-Pos84 OXYGEN QUENCHING OF PYRENE-LIPID FLUORESCENCE IN PHOSPHATIDYLCHOLINE VESICLES. A PROBE FOR MEMBRANE ORGANIZATION. P.L.-G. Chong and T.E. Thompson, Department of Biochemistry, University of Virginia, Charlottesville, VA 22908.

Oxygen quenching has been employed as an alternative method to study the temperature dependence of the excimer formation constant, k_{dm}, of N-(10-[1-pyrene]-decanoyl)-sphingomyelin (PyrSPM) in 1-palmitoyl-2-oleoyl-L-α-phosphatidylcholine (POPC) multilamellar vesicles. In conjunction with the lifetime of PyrSPM monomer in the absence of excimer and oxygen, K_{dm} can be determined from the measurements of the monomer intensity as a function of oxygen concentration. The great advantage of this method is that k_{dm} can be determined without knowledge of the excimer lifetime and intensity. Our results show that k_{dm} changes abruptly at temperatures around 40±5 °C which corresponds to the temperature range of the phase transition (T_m) of PyrSPM determined by differential scanning calorimetry. This suggests the existence of PyrSPM enriched domains in POPC vesicles. In addition to k_{dm}, the oxygen quenching method also permits the determination of the product of oxygen-monomer quenching rate and oxygen concentration, $k^*_{+,m}*[O_2]$. This product exhibits a progressive change at a temperature close to the T_m of PyrSPM, suggesting that the oxygen permeability through membranes depends upon the physical state of the local domain. This observation leads us to suggest that oxygen permeability through the entire membrane composed of different domains may be heterogeneously regulated. In contrast, no abrupt change with temperature in either k_{dm} or $k^*_{+,m}*[O_2]$ was observed in the case of 1-palmitoyl-2-[10-(1-pyrenyl) decanoyl] phosphatidylcholine (PyrPC). Thus the miscibility of PyrPC and POPC appears much better than that of PyrSPM and POPC. (Supported by USPHS grants HL-17576 and GM-14628.)

W-Pos85 PHOSPHOLIPID TRANSFER BETWEEN APOLIPOPROTEIN-PHOSPHOLIPID RECOMBINANTS: PRESSURE EFFECTS William W. Mantulin and Henry J. Pownall, Baylor College of Medicine and The Methodist Hospital, Department of Medicine, 6565 Fannin, M.S. A-601, Houston, Texas 77030.

The spontaneous passive transfer of phospholipids between membrane compartments is an important metabolic pathway. Kinetic transfer experiments for phospholipids support the mechanism in which the rate limiting step involves monomeric phospholipid dissociation from the lipid surface into the aqueous phase, followed by rapid uptake. We now report that high hydrostatic pressure (up to 1500 bar) slows the rate of transfer for a pyrene labeled fluorescenct phospholipid (1-myristoyl-2[9'(3'-pyrenyl)nonanoyl]phosphatidycholine, MPNPC) between recombinant complexes of human plasma apolipoprotein A-I (apo A-I) and 1-palmitoyl-2-oleoyl (POPC) phosphatidylcholine. The experimental protocol involves mixing donor complexes of POPC/apo A-I containing MPNPC in a pressure chamber with an excess of acceptor complexes. The decay rate of pyrene excimer fluorescence is a measure of the rate of change in the microscopic concentration of MPNPC. The kinetics of MPNPC transfer under pressure remain first order and thus we conclude that the mechanism of transfer through the aqueous phase is maintained. In the pressure-temperature domain of our experiments neither apo A-I nor POPC undergo a phase transition, since the logarithm of the transfer rate versus plots of pressure show no discontinuities. The activation volume and free energy for the transfer reaction are positive and the latter is approximately 23 kcal/mol. The positive activation volume presumably corresponds to the work necessary to overcome pressure induced compression of the recombinant donor complex prior to MPNPC transfer.

W-Pos86 THE EFFECT OF POTENTIAL-SENSITIVE MOLECULAR PROBES ON THE ^{31}P NMR SPECTRUM IN DIMYSTEROL PHOSPHATIDYLCHOLINE VESICLES. J.C. Smith and J. Brand, Department of Chemistry and Laboratory for Microbial and Biochemical Sciences, Georgia State University, Atlanta, GA 30303.
The nature of the charge gradients to which extrinsic molecular probes are sensitive (i.e., local, surface, transmembrane, etc.) in energy transducing systems is in part determined by the location of these dyes in the membrane bilayer. The location issue has been explored by monitoring the effect of several polyene dyes on the ^{31}P NMR spectra at 24.15 MHz in model phospholipid vesicles. A minimum of two Lorentzian lineshape functions is required to fit the data satisfactorily. The ^{31}P chemical shift relative to an external TMP reference is essentially insensitive to the presence of any probe thus far employed at the indicated resolution; changes of 0.05 PPM or less have been routinely observed. Anionic probes such as oxonals V, VI, and X (the t-butyl derivative) and the merocyanine M540 induce changes of ten percent or less in the linewidth and spin lattice relaxation time (1.5 sec). In contrast, the cationic dye diS-C_3-(5), when added to the vesicle suspension, markedly increases the spectrum linewidth; a reduction in the T1 value of nearly 30 percent relative to that for dye-free vesicles is also observed. The anionic probes may be unable to sufficiently penetrate the model membrane headgroup region to significantly perturb the phosphorous moiety whereas the cationic probe is. Since the phosphorous is expected to bear a negative charge, electrostatic repulsion in the case of the oxonols and M540 and charge attraction in the diS-(C_3-(5) case may be important in determining the locations assumed by these probes. When oxonol V or M540 is present during the sonication of the lipid suspension to form vesicles, the T1 value is reduced to less than 1 sec and the linewidth markedly broadened, suggesting that these probes are not expelled from the immediate ^{31}P local as the vesicle is formed. Higher resolution measurements and a more detailed analysis of the effect of the several polyenes on the two Lorentzian components are in progress. Support: NIH grants GM 30552 and RR 09201.

W-Pos87 THE LATERAL DIFFUSION OF DiI FROM A LABELED MEMBRANE TO AN UNLABELED MEMBRANE FOLLOWING ELECTRIC FIELD INDUCED FUSION: A NEW QUANTITATIVE TECHNIQUE. Arthur E. Sowers, American Red Cross Blood Services Laboratories, Bethesda, Maryland 200814.
The lateral mobility of membrane components has been previously studied by observing the movement of mobile components from labeled membranes to unlabeled membranes following fusion. This approach has been recently termed the fluorescence redistribution after fusion (FRAF) method. (Schindler et al. PNAS 77, 1457). Because fusion in these systems proceeds in a statistical manner, the initial instant that fusion takes place cannot be determined accurately other than by back extrapolation or by happenstance early discovery of a fusion event. On the other hand, fusion induced by an electric field offers the possibility of high fusion yields and simultaneous fusion at a known time. The purpose of this study was to evaluate the feasibility of using an electric field protocol to induce fusion events and also trigger a recording device to accurately determine the moment the diffusion process begins. Red cell ghosts and intact red cells were used as model membranes and a lipid soluble fluorescent dye (DiI) was used as a label. Lateral concentration gradients at a precisely known pre-equilibrium time were recorded on film, measured by densitometry, and compared with a mathematical model. Electric field protocols which induced fusion were as previously described for red cell ghosts (Sowers, J.C.B, 97, 178a) and mitochondrial inner membranes (Sowers, BBA, in press). A preliminary estimate for D of about $2x10^{-8}cm^2/sec$ for DiI has been found.

W-Pos88 PYRENEDODECANOYL-CoA AND CARNITINE: KINETICS OF INTERVESICULAR TRANSFER. P.E. Wolkowicz, H.J. Pownall, D.F. Pauly, and J.B. McMillin-Wood. Baylor Coll. Med. Houston, TX 77030

Factors that control the interaction of lipid amphiphiles with membranes may play a role in the partitioning of these molecules between metabolic pools. The CoA (PDCoA) and carnitine (PDC) esters of the fluorescent palmitate analogue, pyrenedodecanoic acid (PDA) were employed to measure membrane vesicle association and the kinetics of intervesicular transfer. Accessibility of PDCoA and PDC to a water-soluble quencher was measured in the presence of 1-palmitoyl-2-oleoylphosphatidylcholine single bilayer vesicles, liver and heart mitochondria (LM, HM) and liver and heart reticulum (ER, SR). The majority of probe (99.9%) was associated with the membranes. Although an increase in the vesicle radius decreases intervesicular transfer rates (k) (PDC:36% of small vesicles; PDCoA:60% of small vesicles) transfer rates from ER/SR membranes are further reduced compared to large vesicles (PDC: 22-33% of the large vesicle value; PDCoA: 15-38% of the large vesicle value). Despite a significantly smaller radius of curvature of LM/HM, k values are only reduced a further 8-20% over k for ER/SR. No large effects of ER/SR vesicles compared to large vesicles (67-79%k) on transfer are seen with PDA. The decreased rates of transfer from natural membranes are also associated with decreased enthalpy and increased free energy of transfer compared to large vesicles. A role for membrane protein as an additional vector affecting amphiphile desorption is proposed.
Supported by HL-30186.

W-Pos89 MEASUREMENT OF TRANS-MEMBRANE pH GRADIENTS USING THE FLUORESCENT PROBE DANSYL-GLYCINE.

Stacey Drant & John Bramhall; Microbiology and Immunology Department, UCLA Medical School and UCLA Cancer Center, Los Angeles, California 90024.

The amphiphilic fluorescent dye dansyl-glycine appears to have practical use for monitoring the magnitude and stability of trans-membrane proton gradients. Although freely soluble in aqueous media the dye readily adsorbs to the surfaces of lipid vesicles. Because membrane-bound dye fluoresces at a higher frequency, and with greater efficiency, than dye in aqueous solution it is easy to isolate the light emission from those dye molecules adsorbed to the lipid surface. When dansyl glycine is mixed with phospholipid vesicles the dye molecules attain a partition equilibrium between buffer and the outer, proximal, surface of the vesicles. This is a rapid, diffusion-limited process which is indicated by a fast phase of fluorescence intensity increase. In a second step, the inner, distal, surface of each vesicle becomes populated with dye, a process which involves permeation through the lipid bilayer and which is generally much slower than the original adsorption step. The dansyl-glycine permeates as an electrically neutral species, the flux is thus strongly dependent on the degree of protonation of the dye's carboxylate moiety, and hence upon pH. When the external pH is lower than that of the vesicle lumen the inward flux of dye is greater than that on the opposite direction; as a consequence, dye accumulates in the lumen. Because dye partitions very rapidly into the membrane hydrophobic domain this local elevation of dansyl-glycine concentration leads to an increase in the dye concentration in the inner membrane monolayer, which in turn leads to an elevated fluorescence intensity proportional to the membrane pH gradient.

W-Pos90 SOLID-STATE NMR STUDIES OF THE MOLECULAR DYNAMICS AND PHASE EQUILIBRIA OF MIXED-CHAIN PHOSPHATIDYLCHOLINES, B.A. Lewis, S.K. Das Gupta, and R.G. Griffin. Francis Bitter National Magnet Laboratory, M.I.T., Cambridge, MA 02139

Solid state ^{13}C, ^{31}P, and ^{2}H NMR experiments on aqueous dispersions show that 1-myristoyl 2-palmitoyl phosphatidylcholine (MPPC) and 1-myristoyl 2-stearoyl PC (MSPC) have no stable $L\beta'$ phase, but rather undergo a transition directly from the subphase (L_C phase) to the $P\beta'$ phase. For MSPC the ^{13}C spectra also show that the conformation at the sn-2 carbonyl group in the $P\beta'$ and L_α phases differs from that of MPPC, DPPC, and other diacyl lipids previously examined. The full rigid lattice powder pattern is observed in the sn-2 $^{13}C{=}O$ spectra of MPPC, MSPC, and dipalmitoyl PC (DPPC), and in the ^{31}P spectra of MPPC and MSPC, at temperatures above 0°C when the samples have been stored at lower temperatures for sufficient periods. Thus motion at these positions is in the slow limit ($\tau_c << 10^4$ sec^{-1}). At higher temperatures the sn-2 carbonyl spectra of MPPC and MSPC show superpositions of two components as seen before in the $P\beta'$ phase of diacyl PCs, and the rigid component disappears only after the appearance of the narrow, isotropic component, indicating that these lipids go directly from the subphase to the $P_{\beta'}$ phase. ^{2}H spectra of 2(12,12-d_2) MPPC show substantial motion even at 2° after annealing at low temperature. This motion presumably results from trans-gauche isomerization along the acyl chain, since overall molecular motion is ruled out by the ^{13}C and ^{31}P spectra. (Supported by NIH grants GM-23289, GM-25505, RR-00995; NSF grant DMR-8211416; and USPHS Fellowship GM-09062.)

W-Pos91 RESOLUTION LIMITS OF 1,6-DIPHENYL-1,3,5-HEXATRIENE FLUORESCENCE HETEROGENEITY IN LIPID VESICLES BY PHASE AND MODULATION DECAY MEASUREMENTS: David A. Barrow and Barry R. Lentz, Biochemistry Department, University of North Carolina, Chapel Hill, NC 27514

Measurement of multiple fluorescence decay times of 1,6-diphenyl-1,3,5-hexatriene (DPH) in membranes can theoretically be used to investigate lipid bilayer structural domains. To assess the practical feasibility of such measurements by the phase and modulation techniques, we reduced as much as possible experimental errors that are specifically associated with performing these measurements in lipid vesicles. Next, we used measurements of single DPH fluorescence decay times (7-8 nsec) in liquid-crystalline-phase, single-component lipid bilayer vesicles to determine empirically the level of precision obtainable for these measurements. These precision limits were used in theoretical calculations to assess the practicality of dual lifetime resolution in membrane samples containing several pairs of lifetime components. For the specific precision limits determined here (using the commercially available phase and modulation instrument), we conclude that two coexisting decay times must differ by at least a factor of 1.3 if they are to be resolved reliably.

To demonstrate experimentally that such resolutions could be accomplished accurately, populations of DPH-containing lipid vesicles with single (or nearly single) decay times were mixed together. The resulting heterogeneous fluorescence of such mixtures was then resolved in terms of two component lifetimes, each of which was in good agreement with measured values in the individual vesicle populations. Finally, DPH fluorescence decay measurements were correlated with phase behavior in well-characterized lipid systems. Both long (10-12 nsec) and short (3-6 nsec) lifetime components for DPH were observed in the gel-phase of all vesicles examined.
Supported by NSF grant PCM-79-22733.

W-Pos92 THE EFFECTS OF BUTYLATED HYDROXYTOLUENE ON THE STATIC AND DYNAMIC PROPERTIES OF DIPALMITOYLPHOSPHATIDYLCHOLINE LIPOSOMES-A FLUORESCENCE STUDIES

Kwan-Hon Cheng and James R. Lepock, Department of Physics,University of Waterloo,Waterloo,Canada (KHC present address:Department of Pathology,University of Virginia Medical Center,Charlottesville, Virginia)

The antioxidant butylated hydroxytoluene(BHT) is a common food additive. In addition to its antioxidant activity it appears to perturb lipid bilayers and has been shown to increase Na^+ permeability(M.Singer and J.Wan,Biochem. Pharmacol.26,2259-2268,1977),decrease killing of mammalian cells at low temperatures,increase the repair of radiation damage and increase Con A mediated agglutination(Rule et al.,Biochim. Biophys. Acta.556,399-407,1979).Measurements were made of fluorescence lifetime(τ),steady state polarization(r),and differential phase polarization (Δ) of diphenylhexatiene(DPH) in dipalmitoylphosphatidylcholine(DPPC) multilamellae liposomes with different amount of incorporated BHT. The order parameter (S) and rotational rate (R)of DPH were calculated using the theory of differential polarized phase fluorometry. The following conclusions were drawn:1)In the gel phase of DPPC liposomes,the progressive changes of r,s, τ and R of DPH as the amount of BHT incorporated is increased clearly indicate that BHT decreases the order packing and changes the mode of motion of the fatty acyl chains of the lipid bilayer of DPPC liposomes 2) In the liquid crystalline phase of DPPC liposomes,the invariance of r,S, and τ and the slight increase in the R of DPH suggest the lack of a perturbing effect of BHT in that region of the liposomes and/or a change in the partition of DPH such that it is less affected by the BHT. Similar studies via spin labelling and D.S.C. provide further evidences on the above conclusions.

W-Pos93 SPIN-LATTICE RELAXATION IN THE GEL PHASE OF [7,7-$^2H_2$] N-PALMITOYLGALACTOSYLSPHINGOSINE (NPGS) AND [7,7-$^2H_2$] DIPALMITOYL PHOSPHATIDYLCHOLINE (DPPC): A SOLID STATE ^2H NMR LINE-SHAPE STUDY.

D.J. Siminovitch, E.T. Olejniczak, M.J. Ruocco, S.K. Das Gupta and R.G. Griffin. F. Bitter Nat'l Magnet Laboratory, M.I.T., Cambridge, MA 02139.

Spin-lattice relaxation experiments have been carried out on hydrated [7,7-$^2H_2$] NPGS and DPPC bilayers to compare the dynamics of the two lipids at the same position in the hydrocarbon chain. Of the 5 possible relaxation times which can be measured for a spin I=1 nucleus, we report here on measurements of the spin-lattice relaxation times T_1 and T_{1Q}. T_1 characterizes the rate of return of Zeeman energy to its equilibrium value, while T_{1Q} is associated with the decay of quadrupolar energy. T_1 was measured using the inversion recovery sequence [180-τ-90_x-t-90_y]; after a variable delay τ following the inverting pulse, the recovery of magnetization was monitored by Fourier transformation of the quadrupole echo. T_{1Q} was measured using the Jeener-Broekaert sequence [90_x-t-45_y-τ-45_y]; after a variable delay τ, the decay of quadrupolar order was monitored by Fourier transformation of the spin alignment echo following the 45° detection pulse. For both lipids, the τ-dependence of the powder pattern lineshapes obtained in these experiments reveal a strong orientation dependence of the spin-lattice relaxation times. However, the orientation dependence in the cerebroside NPGS is very different from that observed in the lecithin, DPPC. Simulation of the partially relaxed lineshapes indicate that the anisotropy of T_1 and T_{1Q} in the gel state of either lecithin or cerebroside is the direct result of molecular reorientation of the C-D bond among a discrete number of sites, and that the differences in relaxation behavior between cerebroside and lecithin can be satisfactorily accounted for without any long-axis rotation in cerebroside. The spin-lattice relaxation results supplement information obtained from lineshape analysis of quadrupole echo spectra.

W-Pos94 PARTITION OF AMPHIPHILIC MOLECULES INTO PHOSPHOLIPID VESICLES AND HUMAN ERYTHROCYTE GHOSTS: MEASUREMENTS BY ULTRAVIOLET DIFFERENCE SPECTROSCOPY.

Ruth Welti, Lee J. Mullikin, Tetsuro Yoshimura, and George M. Helmkamp, Jr., Dept. of Biochemistry, University of Kansas Medical Center, Kansas City, KS 66103

Molar partition coefficients for chlorpromazine and methochlorpromazine between phospholipid vesicles or human erythrocyte ghosts and buffer were determined by ultraviolet difference spectroscopy. This technique involves use of tandem cells and a double beam spectrophotometer for titration of an amphiphile solution with vesicles or ghosts. The molar partition coefficients determined with 10 μ M amphiphile between small unilamellar egg PC vesicles and buffer at pH 7.4 are 4.4×10^5 for chlorpromazine and 0.8×10^5 for methochlorpromazine. An increase in the partition of chlorpromazine into vesicles was seen as pH was increased to the pK_a of chlorpromazine at 9.2. Chlorpromazine also partitions preferentially into fluid phase phospholipid compared to solid phase. Molar partition coefficients for 10 μ M amphiphile between unsealed human erythrocyte ghosts and buffer at pH 8.0 were determined to be 6.5×10^5 for chlorpromazine and 2.5×10^5 for methochlorpromazine. Difference spectroscopy is an equilibrium technique which does not require separation of bound from free amphiphile, as do many other methods of determining membrane-buffer partition coefficients. This method is useful for any amphiphile which has an appreciable absorbance below its critical micelle concentration.

This work was supported by Grant GM24035 from the National Institutes of Health and postdoctoral fellowship PD82-01 from the American Heart Association, Kansas Affiliate, Inc.

W-Pos95 DETERMINATION OF THE PARTITION COEFFICIENT FOR A FLUORESCENT LIPOPHILE PROBE IN LIPID VESICLES BY DIRECT OBSERVATION OF PROBE DISTRIBUTION IN VESICLE POPULATIONS. J.K. Allen, D.K. Dennison and J.D. Morrisett, Baylor College of Medicine, Houston, Texas 77030.

Determining the vesicle/aqueous phase partition coefficient for lipophilic molecules is difficult because (1) of the great difference in solubilities of probe in the lipid and aqueous phases, (2) it is difficult to determine when equilibrium has been reached and (3) because true model systems are difficult to find. At equilibrium, probe molecules are incorporated into lipid vesicles following a Poisson distribution. If $V_n + A \underset{k_-}{\overset{k_+}{\rightleftharpoons}} V_{n+1}$ n=0,1,2,...where V_n is a vesicle with n probe molecules, A is free probe, k_+ and k_- are the forward and reverse rate constants and $(k_+/k_-) = K$, the partition coefficient, then, as shown by Tachiya and Almgren [J. Chem. Phys. (1981) 75: 865-870]: $P_n = (P/n!)(K[A]^n \exp(-K[A])$, which describes a Poisson distribution with a mean of K[A]. 1-Palmitoyl,2-oleoyl-phosphatidylcholine/cholesterol vesicles incorporating the fluorescent probe 1-palmitoyl-2-12-[N-4-nitrobenzo-2-oxa-1,3-diazole]-aminocaproyl phosphatidylcholine, NBD-PC, have been studied. The distribution of probe in vesicles is directly observed using flow microfluorometry, FMF. The sensitivity of an Ortho 50-H Cytofluorograf was improved to permit the direct observation of these small vesicles (r_{av}=134 nm). The equilibrium probe distributions are shown to be consistent with a Poisson distribution, and the maximum likelihood mean values are calculated for the observed truncated distributions. For this NBD-PC probe, K= (8.02 ± 2.17) x 10^{-9} (s.d.)(n=4).

This research was supported by grants HL-07282 and HL-27341 (Project V) from the NIH.

W-Pos96 ORDER IN SUPPORTED PHOSPHOLIPID MONOLAYERS DETECTED BY THE DICHROISM OF FLUORESCENCE EXCITED WITH POLARIZED EVANESCENT ILLUMINATION. Nancy L. Thompson*, Thomas P. Burghardt# and Harden M. McConnell*. Dept. Chemistry, Stanford Univ., Stanford, CA 94305* and CVRI, Univ. California, San Francisco, CA 94143#.

We describe a technique for measuring the average orientation of absorption dipoles in a two-dimensional system. A laser beam is totally internally reflected at the interface between a glass slide and aqueous solution, which creates a thin layer of evanescent illumination that excites fluorescent molecules near the interface. Fluorescence is collected with an inverted microscope using a high aperture objective. Dipoles with different tilt from the normal to the interface are preferentially excited when the laser polarization is rotated. The fluorescence intensity vs. polarization curve gives the "order parameter" γ (equal to the Y_{20} moment of the average distribution of dipoles expressed as an expansion in spherical harmonics). We have applied this technique to dipalmitoylphosphatidylcholine monolayers made at an air/water interface and transferred under water to hydrophobic glass microscope slides. The monolayers contain 2 mole % phosphatidylethanolamine labelled with the fluorescent group NBD either on one acyl chain or at the head group. For chain-labelled lipid, γ equals .36 ± .01; γ decreases slightly for monolayers with increasing surface pressure from 10 to 40 dynes/cm. For head-labelled lipid, γ drops from .27 ± .01 to .03 ± .01 with increasing pressure from 10 to 40 dynes/cm. We interpret the data in terms of probe partitioning into fluid and gel phases. The technique presented here may prove useful for detecting order in the arrangement of proteins specifically bound to or incorporated into monolayers or multibilayers. Supported by Runyon-Winchell DRG-593, AHA 82 071 and NIH 5R01 AI13587.

W-Pos97 A STRUCTURAL STUDY OF LIPID AGGREGATES CONTAINING RADIOCONTRAST AGENTS FOR CT SCANNING. Gordon L. Jendrasiak, Department of Physics and School of Medicine, East Carolina University, Greenville, NC, G. Donald Frey, Department of Radiology, Medical University of South Carolina, Charleston, SC, Robert C. Heim Jr., The Citadel, Charleston, SC.

We have used aggregates of phospholipid and the iodolipid radiocontrast agents, ethiodol and iodocholesterol, to visualize the rabbit liver by means of CT scanning. Proton and phosphorous NMR spectroscopic studies of the aggregates were done with a view toward determining their structure. The NMR studies strongly support the hypothesis that the aggregates containing iodocholesterol are in the liposomal configuration. The measurements suggest that the ethiodol containing aggregates are either in the liposomal configuration or in a liposome-emulsion combination arrangement, depending on the ratio of ethiodol to phospholipid and the presence of phosphatidic acid. Electron microscopy has provided complimentary structural information. The iodocholesterol containing liposomes exhibit different NMR spectra when exposed to chaotropic anions than do cholesterol containing liposomes. One possible reason for this behavior is that the iodocholesterol may "sit" somewhat differently in the liposome than does cholesterol. Of interest here is that liver imaging by CT scanning is not enhanced by injection of iodocholesterol containing liposomes whereas it is significantly enchanced by ethiodol containing liposome injection. Since we have used this image enchancement as a diagnostic test for liver cancer, the structure of the aggregates is of some importance.

W-Pos98 ANTIBODY-HAPTEN INTERACTIONS ON MODEL MEMBRANES: EFFECTS OF MEMBRANE COMPOSITION. A. Petrossian & J. C. Owicki, Dept. of Biophysics & Medical Physics, Univ. of CA, Berkeley, CA 94720.

Antibody binding to antigens on cell membranes is crucial to immune recognition. We modeled this phenomenon by studying the interactions of monoclonal anti-fluorescein IgG and Fab fragments with a fluorescent lipid hapten (fluorescein-chlorotriazine-triglycine-dipalmitoyl-phosphatidylethanolamine, FG3P) incorporated as a minor component into liposomes, at 25°C. Antibody binding quenches the hapten fluorescence. The kinetics of the binding of IgG or Fab to haptenated liposomes prepared from branched or unsaturated phosphatidylcholines was distinctly biphasic (see figure). That for saturated (DMPC or DPPC) phosphatidylcholines and for DPPC:cholesterol mixtures was much less so. The affinity of Fab for hapten in DPPC:cholesterol (2:1) vesicles was approximately equal to that for NaFluorescein; it was up to 60 times less for the other lipids studied. The avidity of IgG binding was also maximal for DPPC:cholesterol vesicles. We hypothesize that the haptens exist in at least two states: extended away from the membrane, and sequestered at the membrane surface or in the bilayer (where antibodies cannot bind them). The equilibrium and kinetic aspects of interconversion between these states depend sensitively on the chemical and physical states of both the head-group and hydrocarbon regions. Of the membranes studied, sequestration is least for those made of DPPC:cholesterol mixtures. Preliminary theoretical analysis of this model yields kinetic results that are consistent with the figure. The figure shows fluorescence intensity vs. time (min.) for IgG binding to dioleoyl-phosphatidylcholine vesicles with 2.7nM FG3P; [IgG]/[FG3P]=1, 5, & 15 for curves a, b, & c.

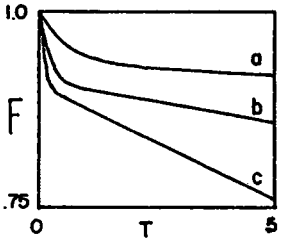

W-Pos99 ELECTROSTATIC POTENTIALS ADJACENT TO BILAYER MEMBRANES CONTAINING THE GANGLIOSIDE G_{M1}. R.V. McDaniel, A.C. McLaughlin and S.G.A. McLaughlin. Department of Physiology and Biophysics, HSC, SUNY Stony Brook, N.Y. 11794 and Department of Biology, Brookhaven National Laboratory, Upton, N.Y. 11973.

Although the Gouy-Chapman-Stern theory of the aqueous diffuse double layer provides a good description of the electrostatic potential adjacent to charged phospholipid bilayer membranes, it does not adequately describe the zeta potential of biological membranes: the zeta potential of an erythrocyte is about 1/2 the value predicted from the theory using the known density of negatively charged sialic acid residues. We formed membranes from mixtures of the zwitterionic lipid phosphatidylcholine, PC, and the glycolipid G_{M1} to mimic the electrostatic properties of the erythrocyte. G_{M1} has one negative charge, which is located about 1 nm from the surface. In a decimolar monovalent salt solution, where the Debye length is about 1 nm, the electrophoretic mobilities of the PC:G_{M1} vesicles are 1/2 the mobilities of PC:PS or PC:PG vesicles of equivalent composition. When the salt concentration decreases and the Debye length increases the mobilities of the three model membranes are similar. We also measured both the nonactin and FCCP conductance of planar bilayer membranes and the ^{31}P NMR spectra of sonicated vesicles containing the ganglioside. These measurements indicate that the potentials both within the GM1:PC membrane and at the phosphate group of PC are also less than the values predicted from the theory in a 0.1 M salt solution. This work supported by NSF grant PCM8340253 and NIH grant GM24971.

W-Pos100 THE ADSORPTION OF THE TETRAVALENT CATIONS GENTAMICIN AND SPERMINE TO BILAYER MEMBRANES CONTAINING NEGATIVE LIPIDS. L. Chung, G. Kaloyanides, R.V. McDaniel, A. McLaughlin, and S. McLaughlin, Departments of Physiology and Medicine, SUNY at Stony Brook, N.Y. 11794.

The Gouy-Chapman-Stern theory can describe the binding of gentamicin or spermine to membranes containing bovine brain phosphatidylserine (PS) or triphosphoinositide (TPI). The intrinsic 1:1 association constants were derived from the concentration of tetravalent cation that caused the charge of a multilamellar vesicle formed from a dilute mixture of PS or TPI in phosphatidylcholine (PC) to reverse sign. Neither cation binds to PC. The 1:1 association constants of both these cations (10 M^{-1} for PS and 1000 M^{-1} for TPI) are orders of magnitude less than those derived by other investigators, who ignored the accumulation of cation in the aqueous double layer and described the data by Scatchard plots. The Gouy-Chapman-Stern theory also accounts for the observed slopes (12-15 mV/decade) of both the zeta and surface potential vs. log [tetravalent cation] curves, which were determined from electrophoresis and nonactin conductance measurements. We determined the binding of gentamicin to multilamellar vesicles formed from PS, DMPS, and PC-PS mixtures and to sonicated PS vesicles by means of electrophoresis and NMR measurements. When the surface concentration of PS was high, the binding of gentamicin to the membranes increased 100 fold as the area per PS molecule decreased by about two fold, which suggests that higher order complexes form between one gentamicin and more than one PS molecule. Supported by NSF grant PCM8340253 and NIH grant GM24971.

W-Pos101 FLUORESCENCE POLARIZATION OF PARINARIC ACID PROBES IN MODEL MEMBRANES COMPOSED OF PHOSPHATIDYLCHOLINE AND GANGLIOSIDE GM1. Brook Redd, Blake Wendelburg, and David A. Rintoul, Division of Biology, Kansas State University, Manhattan, KS (Intr. by Lyn Yarbrough)

Ganglioside GM1 is a glycosphingolipid which is found at the surface membrane of eukaryotic cells, and is thought to be the membrane receptor for the enterotoxin elaborated by Vibrio cholerae. Since the details of glycolipid motion in biological membranes are unknown, we have investigated the effects of varying amounts of GM1 on the phase transitions of defined phosphatidylcholine (PC) species. Steady state fluorescence polarization of cis and trans parinaric acid, and glycolipid probes containing an N-acyl parinaric acid chain, was measured while heating and cooling liposomes composed of pure PC species and GM1. These experiments indicated the presence of a more ordered lipid phase at temperatures above the phase transition temperature of the PC alone. No phase transition was detected in pure GM1 alone over the temperature range of 5 - 70 deg. C. This novel ordered lipid phase was most apparent at GM1/PC ratios (mole/mole) of 1/3; at higher ratios the phase transition due to ganglioside in the bilayer disappears. This ratio was the same for all PC species examined. Our data are consistent with the notion that glycolipids can exist as phase-separated domains in PC bilayers at mole ratios of up to 1/3 (GM1/PC). Details of the preparation of the N-parinaroyl glycolipid probes will also be presented.

W-Pos102 LATERAL DIFFUSION IN BOVINE ROD OUTER SEGMENT PHOSPHOLIPID MONOLAYERS. P. Tancrède*, J. Teissié and J.F. Tocanne, *University of Quebec, Photobiophysics Research Centre, Trois-Rivières (Québec), Canada G9A 5H7 and Laboratoire de Biochimie Cellulaire (C.N.R.S.), 31062 Toulouse, France.

We have undertaken a study of the molecular dynamics of the main lipid components of the rod outer segment disk membranes, phosphatidylethanolamine (PE), phosphatidylcholine (PC) and phosphatidylserine (PS). The phospholipids were spread as monolayers at the nitrogen-water interface, the subphase being either 0.1 M NaCl or 0.1 M NaCl + 0.01 M $CaCl_2$ at pH=5.6 and T=21 ± 0.5° C. The lateral diffusion coefficients (D) in the monolayers were calculated from fluorescence recovery after photobleaching (FRAP) measurements using 12-9 anthroyl-stearic acid as a probe dispersed (1%, mole/mole) in the lipids before spreading. D was determined for each phospholipid at four different surface pressures, 5, 15, 25 and 35 mN/m. Our results show that both the fluorescence at zero time illumination and dimerisation constant of the probe in the film are not affected by the nature of the host lipid nor by the ionic composition of the subphase, therefore suggesting that the spectroscopic properties of the probe are independent of the lipid environment. On the other hand, D varies markedly for the three phospholipids: $1.8 \times 10^{+3}$, $0.50 \times 10^{+3}$ and $0.20 \times 10^{+3}$ $\mu m^2 . sec^{-1}$ for PE, PC and PS, respectively, for all the surface pressures studied. In the presence of calcium ions, these values decrease roughly by a factor of 3 for PE and PS and remain constant for PC. These observations provide new evidences for the modulation of the lateral diffusion in membranes by the nature of the polar heads of the lipids and the possible functional consequences of this effect for the disk membranes are discussed.

W-Pos103 MULTIPLE ENVIRONMENTS IN LIPID BILAYERS: EFFECTS ON FLUORESCENCE LIFETIMES AND POLARIZATION ANISOTROPY DECAYS. Anthony Ruggiero, Richard Ludescher, and Bruce Hudson, Institute of Molecular Biology and Department of Chemistry, University of Oregon, Eugene, Oregon 97403.

The fluorescence lifetime of the probe parinaric acid depends on its local environment. A much longer lifetime is observed when this tetraene fatty acid is present in solid phase lipid bilayers than when the bilayer is fluid. Studies of nominally "one-component" bilayers such as DPPC above 45 degrees reveal multiple lifetime components in picosecond laser excitation-single photon counting fluorescence experiments. When the temperature is varied between 40 and 65 degrees, the lifetimes obtained from a three component fit remain relatively constant but the amplitudes of each component vary considerably, especially near 48 degrees. The interpretation of this behavior will be discussed.

Fluorescence polarization anisotropy decays observed for parinaric acid in egg PC/cholesterol mixtures exhibit strong upward curvatures after an initial decay to a minimum. This anisotropy behavior is a systematic function of the cholesterol content. The only consistent explanation of these results is that there are two environments present at cholesterol contents less than about 20-30% such that a cholesterol-rich phase provides an environment resulting in a long fluorescence lifetime for the probe and a high limiting anisotropy (little angular mobility).

W-Pos104 PATCH CLAMP STUDY OF THE LIGHT RESPONSE OF ISOLATED FROG RETINAL RODS. R.D. Bodoia and P.B. Detwiler. University of Washington, Dept. of Physiol. & Biophys., Seattle WA 98195.

Photocurrents were recorded simultaneously from the inner segment by a suction electrode and from the outer segment by a patch electrode. Inner segment photocurrent was not affected when a patch pipet formed a giga seal to the outer segment membrane (cell-attached recording) but disappeared when the patch membrane was ruptured (whole-cell recording) and the rod was voltage-clamped at the pipet potential. Light suppressed an inward membrane dark current which appeared as a reduction of a steady current flowing out of the pipet in cell-attached recordings and into the pipet in whole-cell recordings. This steady current reversed sign at a membrane potential of +8mV. In darkness the steady-state I-V relation showed marked outward rectification. In both recording conditions steady bright lights were associated with a reduction in current noise. The power spectrum of the light sensitive noise was the sum of two components. The low frequency component could be fit by a single Lorentzian having a cut-off frequency of about 0.6 Hz, and noise power of about 0.5 pA^2. In whole-cell recordings this component was seen to increase in dim lights while cell-attached recordings from a small fraction of outer segment membrane failed to show such an increase. The second component of the light sensitive noise has a noise power of about 0.5 pA^2 and rolls off around 400 Hz. This component is seen to decrease with progressively brighter lights in both whole-cell and cell-attached recordings. Neither component of the light-sensitive noise is voltage-dependent.

W-Pos105 MEMBRANE CURRENT NOISE IN ROD PHOTORECEPTORS EXPOSED TO LOW EXTERNAL CALCIUM. Gary G. Matthews, Department of Neurobiology and Behavior, SUNY, Stony Brook, NY 11794

Outer segment membrane current of isolated toad rods was recorded with a suction electrode in 10^{-8} M Ca. During the large transient dark current immediately after exposure to low Ca (Yau *et al.*, *Nature, 292,* 502), pronounced light-suppressable noise in membrane current was seen. The noise power spectrum was fitted by a single Lorentzian with corner frequency 39.6 ± 9.9 Hz (mean ± S.D., N=10). After the dark current declined to a steady level, bright-flash responses were often followed by a transient increase in dark current lasting 30-50 sec, accompanied by single-Lorentzian noise similar to that described above but with corner frequency of 27.3 ± 5.3 Hz (N=15). The noise could arise from fluctuations in light-sensitive channels or in voltage-sensitive channels in the inner segment. Results of 2 experiments favored the latter. (1) Bathing the inner segment with a cocktail of agents (Cs, TEA, Co) known to block the voltage-sensitive conductances (Bader *et al., J. Physiol., 331,* 253) eliminated the noise during increased dark current following bright flashes. (2) With low Ca inside the electrode, rods attached to pieces of retina showed increased dark current following bright flashes, but the noise was absent or attenuated. Attached rods are electrically coupled to other rods in the piece (Nunn *et al., Fed. Proc., 39,* 2066) and voltage changes associated with increased dark current would be attenuated. Thus, the noise is likely due to voltage-sensitive conductances responding to voltage changes during the increased dark current. In this view, the corner frequencies reflect membrane time-constant, and the briefer time-constant immediately after exposure to low Ca may indicate higher outer segment conductance at that time. (Supported by USPHS Grant EY03821 and by the Alfred P. Sloan Foundation)

W-Pos106 SUBPICOSECOND EXCITED STATE PROCESSES IN VISUAL PIGMENTS, A. G. Doukas[+], M. R. Junnarkar[+], R. R. Alfano[+], R. H. Callender[+], T. Kakitani*, B. Honig*, M. Okabe[x], V. Balogh-Nair[x], and K. Nakanishi[x], [+]Department of Physics, The City College of New York, N.Y. 10031, *Department of Biochemistry and [x]Department of Chemistry, Columbia University, New York 10027

The fluorescence quantum yields for bovine and squid rhodopsin have been measured using picosecond spectroscopy. Both pigments yield similar results with an average value of $(1.2\pm0.5)\times10^{-5}$. Since the estimated radiative lifetime of rhodopsin is 5 nanoseconds the rate constant of the process that competes with the fluorescence must be of the order of 100 femtoseconds. Given the large quantum yield of isomerization the process is likely to correspond to the motion along the C11-C12 torsional coordinate that leads to cis-trans isomerization. In addition, preliminary low temperature experiments show that the fluorescence from bovine rhodopsin remains unresolved (less than 15 psec) even at 4 K. Substitution of H_2O with D_2O has no effect in the fluorescence lifetime in contrast to the effect observed in the formation of bathorhodopsin. These measurements imply that proton translocation does not take place in the excited state of rhodopsin or at least during the fluorescence process.

This research is supported by NIH.

W-Pos107 A KINETIC ANALYSIS OF PHOSPHODIESTERASE ACTIVATION IN ROD DISC MEMBRANES. Richard T. Klingbiel, David F. O'Brien, Patricia N. Tyminski, Eastman Kodak Company, Research Laboratories, Rochester, NY 14650.

A quantitative assessment of the phosphodiesterase-activation mechanism believed operative in photoreceptors is described. Two successive mathematical methods are utilized. First, the rate equations are integrated for the special cases of very low bleach or steady-state phosphodiesterase activity. The resulting analytical expressions are used to derive a set of approximate rate constants from a series of experiments of varying chemical constraints. Second, this set of kinetic rate constants is used to generate exact numerical solutions to the rate equations. In this way the set of rate constants are refined until the generated behavior agrees with experiment. The numerical solutions exhibit initial rate, induction time, saturation behavior, photo-sensitivity as well as first and second-stage gain in reasonable agreement with experiment. The light titration curve is calculated accurately from the analytical results for all bleach levels. The dependence of sensitivity on PDE, G-binding protein, phosphorylation of bleached rhodopsin and membrane size is discussed.

W-Pos108 ATP-DEPENDENT CALCIUM UPTAKE INTO NATIVE DISC MEMBRANES. K.L. Puckett, E.T. Aronson, and S.M. Goldin (Intr. by K. Miller) Harvard Medical School, Boston, MA 02115

An ATP-dependent Ca^{++} uptake activity has been identified in preparations of native disc membranes from bovine rod outer segments (ROS). Discs isolated from ROS by hypoosmotic shock and floatation on 5% Ficoll were further purified by separation into two distinct subpopulations on a linear 5-20% Ficoll gradient. The major subpopulation, the "R" band, contained ~85% of the total protein, and ≥90% of the bleachable and regenerable rhodopsin. The minor membrane component, the "W" band, contained ~15% of the total protein, and <1% of the total rhodopsin. Both subpopulations showed an ATP-dependent Ca^{++} uptake activity; the "W" band had ~10 fold higher specific activity as compared to the "R" band. To determine whether the association of this Ca^{++} uptake activity with the "R" band was merely coincidental, we exploited the osmotic properties of these disc membranes. The sedimentation rate of the "R" band discs varied with the osmotic strength of the gradient solution. On each gradient, the Ca^{++} uptake activity always precisely co-migrated with the rhodopsin containing membranes. This result suggests that the ATP-dependent Ca^{++} uptake activity was associated with intact disc membranes. The ATP-dependent Ca^{++} uptake activity of the "R" band was further characterized. The K_m of Ca^{++} [6 μm] for uptake was determine using an EDTA/Ca^{++} buffering system. Vanadate inhibited Ca^{++} uptake with a $K_I \sim 20$ μm. Ruthenium red [10 μm], did not inhibit this Ca^{++} uptake activity, suggesting insignificant mitochondrial contamination. Neither GTP [2mM] nor AMP-PNP [2mM] were able to support Ca^{++} uptake. The amount of Ca^{++} uptake activity in the "R" band, and it's affinity for Ca++, was sufficient, in principle, to account for a role of this Ca^{++} "pump" in the regulation of cytosolic Ca^{++} levels in rod cells *in vivo*.

W-Pos109 PHOSPHORYLATION OF RIM PROTEIN IN THE DISCS OF FROG RODS. E. Z. Szuts, Marine Biological Lab., Woods Hole, MA 02543

Bullfrog outer segments contain a protein kinase that phosphorylates the rim protein (RP) of rod discs. RP is an intrinsic membrane protein with a mol. wt. of ~250K Da (220K on 6% Laemmli; 240K on 10% Laemmli). Its reaction is light dependent, observed when fresh broken outer segments are incubated with either [γ^{32}P] ATP or [^{35}S]ATP-γ-S. Radioactive labeling of proteins was measured using SDS-PAGE. Freezing cell suspension prior to incubation, reduced extent of labeling by 60%. No labeling occurred when [^{3}H]ATP or [^{35}S]ATP-α-S was used as substrate donor, excluding nucleotide-binding with the previous nucleotides as the mechanism for labeling.

Identity of phosphorylated protein as RP was verified by 1) coincidence of radioactivity with Coomassie-stained band (acid and Laemmli gels), 2) coincidence of radioactivity with con-A labeled band, 3) constant radioactivity of RP-band (cpm/μg RP) as discs were purified by density centrifugations and as peripheral membrane proteins were extracted, and 4) identical mobility shifts for radioactive and stained bands with SH-oxidation prior to SDS-PAGE. With flash stimulation, extent of phosphorylation saturated with a 17% bleach, with largest levels of incorporation so far being 0.1 mol phosphate/mol RP (0.1 mM ATP) and 0.01 mol thiophosphate/mol RP (1 mM ATP-γ-S). Radioactive incorporation followed first-order reaction with a half-time of 1 min (substrate donor conc. 30nM).

Light also initiates phosphorylation of a ~270K Da protein, whose concentration is 10-30% of RP. It also copurified with discs during density centrifugations, but appears to be separate from RP, because it was extractable with low-μ buffer and its phosphorylation relative to RP varied with the concentration and identity of substrate donor. (Supported by NIH grant EY02399 and private sources)

W-Pos110 PHOTOTRANSDUCTION IN RODS DOES NOT REQUIRE A CHANGE IN CYTOPLASMIC pH.

S. Yoshikami and W.A. Hagins Lab. of Chem. Physics, NIADDK, NIH, Bethesda, MD 20205

When live rat rods are perfused with 1 mM Ca^{++} Ringers to which 10 mM NH_4Cl is suddenly added from a fluid jet, the dark current increases and light responses become larger for 1-2 m., then return slowly to their original size. When the jet is removed, the dark current stops and light responses cease for 2-3 m. Both then slowly recover. But if the retina is first equilibrated for 10 m. with a Ringers containing 20 mM imidasole, a membrane-permeable weakly basic buffer (pK 6.9), the effect of NH_4Cl removal on the dark current or light responses is reduced by 85%. Since NH_4Cl increases the pH of rod cytoplasm when applied and decreases it when removed (Hagins & Yoshikami, *Vertebrate Photoreception*, Academic, 1976), it is likely that its effect on the dark current is at least indirectly a pH effect. Imidasole, acting as a buffer, suppresses the pH change. Imidasole itself affects the dark current like NH_4Cl but much more weakly. After equilibration, imidasole does not alter the amplitude-intensity relation of the photocurrent as Ca^{++} buffers do. *Thus it is likely that light controls the dark current by a mechanism that does not require a change in cytoplasmic pH as an essential intermediate step.*

Does the decrease in pH_i suppress the dark current by inhibiting the Na:Ca exchange pump of the outer segment plasma membrane and thus raising $[Ca^{++}]_i$? NH_4Cl removal greatly reduces and prolongs the light-stimulated efflux of Ca^{++} from the outer segments and increases the photocurrent duration. NH_4Cl removal also causes a 10 μM decrease in $[Ca^{++}]_{est.}$ at 95 μM suggesting that it is an inward movement of extracellular Ca^{++} that suppresses the dark current. Reducing the $[Ca^{++}]_{est.}$ from 1 to 0.1mM decreases by 50 % the effect of cytoplasmic acidification on the dark current but does not shift to higher values the light needed to suppress the dark current by 1/2. Thus pH changes affect the dark current by influencing the Na:Ca exchange pump in the plasma membrane, causing a net inward movement of extracellular Ca^{++} and not by mobilising Ca^{++} from internal stores.

W-Pos111 RHODOPSIN BEHAVIOR IN A HIGH CHOLESTEROL ENVIRONMENT

Arlene D. Albert, Durriya Safiuddin and Andrew Behnke, Biochemistry Dept. SUNY/Buffalo School of Medicine, Buffalo, NY 14214.

Recombined bovine disk membranes were produced by solubilization of the membrane in dodecyltrimethylammonium bromide followed by dialysis. When cholesterol was added after solubilization recombined membranes could be produced in which the cholesterol content was approximately ten times that found in native disk membranes. Papain proteolysis produced the same fragments in both the high cholesterol recombined membranes and the disk membranes. The photolytic properties of rhodopsin in high and low cholesterol recombined membranes were compared. Absorbance spectra of the high and low cholesterol membranes were taken before illumination, immediately after the flash and at 5, 10, 20, and 30 minute time intervals after the single flash. The low cholesterol membrane exhibited the spectral shifts characteristic of the Meta I to Meta II to Meta III transition. The high cholesterol membrane, however did not exhibit these shifts. After an initial shift in the peak position from 498nm to 480nm no additional shifts were observed. Spectra were taken at temperatures between 7°and 34°C. The high cholesterol recombined membranes were not as thermally stable as the low cholesterol membranes. (Supported by RO1 EY03328.)

W-Pos112 A 3-DIMENSIONAL RECONSTRUCTION OF CRYSTALLINE RHODOPSIN MEMBRANES.

B.L. Scott, K.A. Taylor and J.M. Corless, Dept. of Anatomy, Box 3011, Duke Univ. Med. Ctr., Durham, NC 27710

Tween-80 treatment of bullfrog photoreceptor membranes has yielded 2-dimensional crystals of rhodopsin [PNAS, USA 79:1116 (1982)]. The rhodopsin molecules pack as dimers within an orthorhombic unit cell, which measures 47 X 151 Å. The 2-sided plane group is $p22_12_1$. A 3-dimensional reconstruction of negatively stained crystals has been completed at ~25 Å resolution, allowing us to visualize general structural features of the membrane surfaces. Crystal preparations were applied to carbon-coated grids, stained with uranyl acetate, and examined with a Philips EM 400T electron microscope equipped with low-dose kit and ± 60° eucentric goniometer stage. Projections from specimens tilted up to 60° were analyzed and merged using programs provided by the MRC Laboratory of Molecular Biology, Cambridge, U.K. The resulting map has the following features. Along the z-axis (perpendicular to membrane plane), the staining contrast profile shows three minima: one in the center of the membrane, and two located ± 30 Å from the center. Thus, the crystalline sheet is about 60 Å thick. The two principal maxima are located ± 16 Å from the center. Within these high contrast regions, each rhodopsin dimer defines two stain-excluding domains (see Figure). At one surface of the crystal (+20 Å from center), the dimer has a bi-lobed shape. Directly below, at the other surface (-20 Å), it is distinctly tri-lobed in appearance. Each shape is quite representative for each surface of the dimer. X-axis (scale) = 75 Å. The orientation of the dimer with respect to the orientation of rhodopsin in native disk membranes will be discussed. (Support: NIH Grant EY-01659 to JMC)

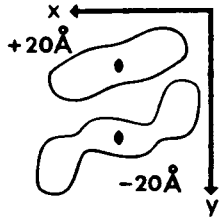

W-Pos113 3-DEHYDRORETINAL CHROMOPHORE OF THE GOLDFISH PORPHYROPSIN Andrew T.C. Tsin and Frank Santos, Division of Life Sciences, The University of Texas at San Antonio, San Antonio Texas 78285

The isomeric configuration of the 3-dehydroretinal chromophore of the goldfish porphyropsin was determined by visual pigment regeneration and by the Hplc (High performance liquid chromatography) analysis of the extracted 3-dehydroretinal chromophore. Rod outer segments (ROS) were prepared from the retinas of dark-adapted goldfish using discontinuous sucrose gradients. In one experiment, 7.2 nm of bleached porphyropsin (in the ROS) were regenerated with 13 nm of 11-cis 3-dehydroretinal and a 60% regeneration of the goldfish porphyropsin was obtained after two hours of incubation at room temperature. When the ROS were extracted with methanol, reacted with hydroxylamine and then extracted with methylene chloride, one major peak was observed in the Hplc profile of this extract. This peak coeluted with authentic 11-cis 3-dehydroretinyl oxime. These results, together with recent results of others, provide strong evidence that the chromophore of the goldfish porphyropsin is 11-cis 3-dehydroretinal.
Supported by the NSF (8023064) and the NIH (RR08194).

W-Pos114 THE VISUAL CHROMOPHORE 11-CIS RETINAL: DISTRIBUTION OF 12s-TRANS AND 12s-CIS CONFORMERS IN SOLUTION. ASSIGNMENT OF THE 255nm ABSORPTION BAND. Walter Sperling (introduced by Walther Stoeckenius). Cardiovascular Research Institute, UCSF, San Francisco, CA 94143.

The absorption spectra of 11-cis retinal in solution show a temperature dependence consistent with a Boltzmann distribution between 3 states, one planar ground state (12s-trans) and two degenerate higher states with a twisting of ca. $\pm 140^0$ about the 12s bond (12s-cis). Planar refers to the planarity of the conjugated side-chain only. The segment C12/O points either below (l) or above (r) the plane of the paper. At room temperature about 1/3 of the molecules are in the 12s-trans, 1/3 in the 12s-cis(l), and 1/3 in the 12s-cis(r) state. At 80 K most molecules are in the 12s-trans state. For both temperatures, 80 K and 293 K, the theoretical limits for the Boltzmann distributions at 0 K (100% s-trans; 0% s-cis) and ∞K (1/3 s-trans; 2/3 s-cis) are nearly achieved. One conclusion is that the side chain of the 11-cis,12s-trans conformer (low-temperature form) deviates from planarity to about the same extent as do trans retinal and the other mono-cis retinals. The band at 255nm increases and decreases concomitantly with the break in coplanarity at the 12s bond. This band is not the "cis peak" ($^1A_g^- \rightarrow {}^1A_g^{+*}$), but rather arises from the twisting of the molecule about the 12s bond, i.e. it is due mainly to the "partial chromophore" character of the segments of the side chain of the 12s-cis conformers.

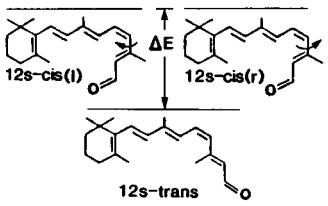

W-Pos115 RETINOL FLUORESCENCE IS UNIFORM ALONG ROD OUTER SEGMENT AXIS.
Michael W. Kaplan, Neurological Sciences Institute, Good Samaritan Hospital & Medical Center, Portland, OR 97210.

Rhodopsin concentration and dichroism are uniform along the axis of amphibian rod outer segments (ROSs) (1). However, visual pigment regeneration (2) and recovery of function (3) following intense, uniform bleaches is axially dependent. In this study the equilibrium distribution of retinol, the final photoproduct of rhodopsin's 11-cis retinal chromophore, has been investigated. Dark-adapted retinas were isolated from Rana pipiens and bleached (3.6×10^3 lux for 1 hr) to allow equilibrium formation of retinol. Isolated ROSs were viewed using an epi-fluorescence microscope (Zeiss G365 excitation filter, LP420 barrier filter) fitted with a silicon-intensifier-tube television camera. Data were recorded using a video analyzer system. Fluorescence was uniform along the ROS axis, and quickly faded to a uniform background level of approximately 10% of the initial intensity. Dark-adapted control cells showed only the background level fluorescence, suggesting that retinol is the fluorophore. The uniform equilibrium distribution of retinol implies that older disk membranes at the distal tip of the ROS contain functional oxidoreductase enzymes. No correspondence with axial birefringence gradients was found. The kinetics of retinol formation as a function of axial position remains to be resolved. (Supported by USPHS grant EY01779 and the Oregon Lions Sight and Hearing Foundation).

1. M. W. Kaplan, M. E. Deffebach and P. A. Liebman 1978. Biophys. J. 23:59-70.
2. T. P. Williams 1982. Invest. Ophthalmol. Vis. Sci. 22:229a (ARVO suppl.).
3. D. A. Baylor and T. D. Lamb 1982. J. Physiol. (Lond.) 328:49-71.

W-Pos116 SIMULTANEOUS PHOTOCURRENT AND CALCIUM RELEASE MEASUREMENTS FROM SINGLE ROD PHOTORECEPTORS. D.L. Miller and J.I. Korenbrot. Dept. of Physiology, Univ. of Calif., San Francisco,CA 94143

We have developed a technique for measuring individual rod photocurrents while simultaneously measuring the concentration of Ca^{2+} in a small volume surrounding that rod's outer segment (ROS). The entire ROS is drawn into a snug-fitting pipette that allows the measurement of the rod photocurrents (Baylor, et.al., J. Physiol. 288, 589 ('79)). A small (∿12μm) pipette containing the Ca^{2+} sensor di(octylphenyl)phosphate/dioctyl phenylphosphonate/PVC at its tip is introduced coaxially within the current-measuring electrode and placed near the tip of the ROS. This arrangement enables us to measure light-dependent changes in Ca^{2+} concentration in normal (110 mM) NaCl and 0.1 mM $CaCl_2$ without any interference from photovoltages in the calcium electrode signal.

We have confirmed, using retinas obtained from Bufo marinus, that upon illumination Ca^{2+} is released specifically from the rod's outer segment (Yoshikami, et.al., Nature 286, 395 ('80), and Gold and Korenbrot, PNAS 77, 5557 ('80)). The Ca^{2+} release begins essentially simultaneously with the photocurrent. The amount of Ca^{2+} released is linear up to a few hundred absorbed photons/rod, and is approximately $2x10^4$ Ca^{2+} released/Rh*. Interestingly, at any given intensity tested, the amount of Ca^{2+} released is nearly constant from cell to cell (e.g. 10% variation), whereas the photocurrent can vary significantly from cell to cell (e.g. peak current 7-17 pA, given nearly identical membrane-electrode seal resistances and fraction of ROS length within the electrode).

It was also found that the amount of Ca^{2+} released continues to increase with light intensity up to intensities $>10^5$ Rh*/rod, or an averageof 50 Rh*/disc. That is, a single Rh*/disc is insufficient to saturate the Ca^{2+} release, and is not the limiting unit of control of Ca^{2+} available for release.

W-Pos117 LIGHT-DEPENDENT RELEASE OF CA FROM RODS MEASURED BY LASER MICRO MASS ANALYSIS. By W.H. Schröder and G.L. Fain, Institut für Neurobiologie, KFA, Jülich, Federal Republic of Germany and the Jules Stein Eye Institute, UCLA.

We have measured light-dependent Ca efflux from shock-frozen rods in isolated toad retina by means of laser micro mass analysis. Dark-adapted rod OS's contain 4 - 5 mM Ca per l, of which about 50 % can be released by illumination. In steady dim light (68 Rh*/rod) the light-dependent efflux is about 10^4 Ca per Rh*. In bright light the rate per Rh* decreases but the total efflux increases to at least 3×10^7 Ca/rod · sec. The influx rate in darkness is about 10^5 Ca/rod · sec and is not increased significantly in steady illumination. Thus in bright light most of the light-sensitive pool is depleted in a very short time (< 60 sec). Ca depletion can also be observed in intact animals, since the outer segments of thoroughly light-adapted toads contain about 50 % of the Ca of dark-adapted animals. Where does this Ca go? Some goes into the mitochondria of the inner segment. In bright light as much as 5 % of Ca released from the OS's is rapidly absorbed by the mitochondria and then slowly released again, presumably to be expelled from the cell. However most of the Ca from the OS's is extruded by Na/Ca exchange, since replacement of choline for Na reduces the rate of light-dependent efflux by at least 90 %. It is possible that all of the Ca released from the OS's can be accounted for by these two mechanisms (mitochondrial buffering and Na/Ca exchange), though we cannot completely exclude the possibility of Ca pumps or other forms of Ca extrusion.

W-Pos118 INVESTIGATION OF THE LOW TEMPERATURE "RIGOR"STATE IN RABBIT PSOAS MUSCLE FIBERS. John W. Shriver, (Intr. by Wayne Bolen), Dept. of Medical Biochemistry and Dept. of Chem. & Biochem., Southern Illinois University, Carbondale, IL 62901.

Single rabbit psoas muscle fibers have been chemically skinned (170 mM propionate, 5 mM EGTA, 2 mM $MgCl_2$, 2 mM Na_2ATP, 5 mM imidazole, 4°C; Wood et al. Science 187, 1075 (1975)) and mounted onto a computer controlled position and force transducer (Cambridge Technology, Model 303) using aluminum foil T-clamps (1 mm x 1 mm, Kem-Mil Co., CA; after a design supplied by Y. Goldman) to mechanically attach the fiber, obviating the need for glue. The fiber (length 2-3 mm; sarcomere length = 2.5 μ) was suspended in a water jacketed 1.0 ml flow cell allowing rapid solution changes to be performed without pulling the fiber through the solution surface. Ionic strength of solutions was determined using an iterative computer program taking into account the heats of protonation and complexation of all species involved. After incubation of the fiber in relaxing solution (μ=0.10; $MgCl_2$ 2.06 mM, K•PIPES 0.05 M, Na_2ATP 1.06 mM, K_2EGTA 1 mM, KCl 0.0552 M, pH 7.1) the solution was changed to a rigor solution (μ=0.10; $MgCl_2$ 1.06 mM, K•PIPES 0.050 M, Na_2ATP 0.0 mM, K_2EGTA 1.0 mM, KCl 0.0595 M, pH 7.10) at the same temperature. The force resulting from imposition of rigor was significantly temperature dependent with the force approaching zero at low temperature (2°C). There was essentially no change in stiffness as measured by 10 msec linear length changes (5μ excursion). Thus, to the extent that the stiffness is a reflection of the number of crossbridges attached to actin, the negligible rigor force produced at low temperature does not appear to be due to decreased numbers of attached crossbridges. It may be due to the inability of the crossbridges to perform a powerstroke. (Supported by Research Corporation).

W-Pos119 EFFECTS OF TEMPERATURE ON V_o, FORCE, STIFFNESS AND ENERGY LIBERATION IN FROG SKELETAL MUSCLE. D.M. Burchfield and J.A. Rall, Physiol. Dept., Ohio State University, Columbus, OH, 43210.

Velocity of unloaded shortening (V_o) and steady rate of energy liberation (S.R.E.L.) depend on the rate of ATP hydrolysis by cross-bridges. Experiments were designed to determine if V_o and S.R.E.L. maintain a fixed relationship to each other when both parameters are altered. When the temperature of semitendinosus muscle is increased from 0 to 10°C, peak tetanus force increases by 45 ± 4% (n = 15) and S.R.E.L. increases by 462 ± 11% (n = 10). V_o, measured at peak force by the slack step technique, increased by 252 ± 27% (n = 9). The increase in S.R.E.L. was significantly greater than the increase in V_o but account must be made for the increase in force. The usual procedure is to divide S.R.E.L. by force, assuming that force is proportional to number of attached cross-bridges. This point was examined by determining the ratio of peak muscle stiffness, using ramp releases, at 0 and 10°C. This ratio is 1.10 ± 0.05 (n = 7). Thus S.R.E.L. should be normalized by stiffness. Before a comparison can be made between V_o and cross-bridge energy liberation, the temperature dependence of Ca^{2+} cycling energy liberation must be known. This was determined by measuring S.R.E.L. at a sarcomere length of 3.8 μm at 0 and 10°C. The rate of Ca^{2+} cycling energy liberation increased by 569 ± 28% (n = 5). Assuming that Ca^{2+} cycling energy liberation is not altered by muscle length, cross-bridge energy liberation can be determined by subtracting S.R.E.L. at 3.8 μm from that at 2.4 μm. Cross-bridge energy liberation increases by 350% from 0 to 10°C. This increase is greater than the increase in V_o. These results suggest that V_o and cross-bridge energy liberation are not two measures of the same reaction sequence. (Supported by NIH grant AM20792).

W-Pos120 SHORTENING SLOWS THE DECLINE OF THE Ca^{++} TRANSIENT OF CARDIAC MUSCLE WHETHER OR NOT SHORTENING DEACTIVATION OCCURS.
P.R. Housmans, N.K.M. Lee and J.R. Blinks, Dept. of Pharmacol., Mayo Fdn., Rochester, MN 55905.

In many kinds of striated muscle the total duration of mechanical activity during a twitch is less when the muscle is allowed to shorten than when it contracts isometrically ("shortening deactivation" or SD). SD is pronounced in frog skeletal muscle and mammalian cardiac muscle, but nearly absent in frog ventricular muscle (J. Physiol. 152: 30, 1960 and 283: 469, 1978). In mammalian heart muscle SD can be diminished or abolished by caffeine. We have shown (Science 221: 159, 1983) that in the cat papillary muscle isotonic shortening is accompanied by a slowing of the decline of the intracellular Ca^{++} transient, and have suggested that this and SD might both result from a decrease in the Ca^{++} affinity of troponin C during shortening. Now we have studied the influence of isotonic shortening on intracellular Ca^{++} transients and mechanical activity under conditions in which SD does not occur. Frog ventricular strips and cat and ferret papillary muscles were microinjected with the Ca^{++}-sensitive bioluminescent protein aequorin; the papillary muscles were studied before and after exposure to caffeine. Shortening slowed the decline of the aequorin signal whether or not SD occurred. The duration of the aequorin signal was longer, both in absolute terms and in relation to that of mechanical activity, under conditions in which SD did not occur. When SD was absent, the aequorin signal always outlasted the period of active shortening, but did not necessarily outlast the total period of length change. Support: USPHS Grant HL12186 and International Research Fellowship TW 03046.

W-Pos121 LENGTH- AND TEMPERATURE-DEPENDENCE OF ACTIVATION AND TENSION PRODUCTION BY FROG ATRIAL TRABECULAE. P.J. Reiser and B.D. Lindley, Dept. of Physiology, Case Western Reserve Univ., School of Medicine, Cleveland, Ohio 44106.

Single atrial trabeculae (50-150 um diam.) were isolated and mounted for measurement of isometric tension. Na-withdrawal contractures were used to study the effects of muscle length (ML) and temperature (T) on activation and tension development. The $[Na]_o$ in the contracture solutions was adjusted to grade the level of activation during different contractures. Contracture tension was studied at several ML's and at cold (4-6°C) and warm (20-24°C) T's. The sigmoidal relationship between normalized peak contracture tension (the peak tension at each ML in 0 mM Na Ringer being set = 100%) and $[Na]_o$ was shifted to lower $[Na]_o$'s at ML's less than L_o and to greater $[Na]_o$'s at ML's greater than L_o at the warm T. That is, stretched cardiac muscle is more sensitive to Na-withdrawal. Rapid T-jumps from cold to warm T's (complete within 400 ms) led to tension transients involving an initial abrupt increase in tension followed by a decrease, with the magnitude of the latter being dependent on ML and the $[Na]_o$ of the contracture solution. For a given $[Na]_o$ the T-jump resulted in a greater decrease in tension during the transient at lengths $<L_o$ compared to the transients at lengths $\geq L_o$. The results demonstrate that activation and tension development of atrial trabeculae are length- and temperature-dependent. More specifically, the observed length-dependency suggests that the force generating mechanism of frog cardiac muscle becomes more sensitive to the intracellular calcium concentration at longer ML's. Supported by USPHS (HL 19848) and Northeast Ohio Affiliate, American Heart Association.

W-Pos122 INTERNAL WALL MECHANICS DURING CARDIAC CONTRACTION. Henry H. Gale, Department of Physiology, Creighton University Medical School, Omaha, Nebraska 68178.

According to the prevailing view (Handb. Physiol., The Heart, ch. 4) the thickening and thinning of the wall during the cardiac cycle is mostly caused by cells sliding between their neighbors without changing the cross-sectional shapes of the cells. The wealth of interfiber connections (Robinson and Winegrad, 1981) and the highly irregular projecting shapes of the fibers suggest that sliding may not occur. Mechanical analysis shows that sliding fibers are inefficient in coupling fiber tension to compression of the blood. Also the weaving of sliding fibers around the numerous lateral cell anastomoses creates local areas of high stress concentration and deformation. Another model for accomodating wall shape change assumes that the cells are strongly linked together forcing the cells to deform along with the wall (Gale, 1979). Here stress and deformation are more evenly spread through the cell. But, altering the cross-sectional profile of a fiber requires overcoming active lateral forces exerted by the fiber. This occurs in the heart wall where the crossing of fibers in nonparallel adjacent layers opposes the longitudinal tension of one fiber to the transverse expansion forces of its crossing neighbors. A third concept (Spotnitz et al., 1974) proposes that groups of interconnected fibers slide past each other moving along macroscopic cleavage planes in the wall. During changes in wall thickness, adjoining bundles of muscle, separated by the slippage planes, tilt like the slats of a venetian blind. But myocardial wall fibers do not all run in parallel paths. At different depths in the wall the direction of the fiber paths is different. Any gross cleavage plane penetrating into the wall will parallel the fiber paths of one layer but must transect the fiber paths of the other layers. The transected fiber paths are mechanically uncoupled from the load, blood.

W-Pos123 EXTRACTION AND FUNCTIONAL RECONSTITUTION OF THE CARDIAC A-BAND. J. Krueger, S. Margossian, & B. London. The Albert Einstein Col. of Medicine & Montefiore Medical Center, Bronx, N.Y.

Single cardiac muscle cells were enzymatically isolated from rat ventricles and permealyzed with a non-ionic detergent (Brij 58, 0.5% w/v). The distribution and concentration of cell protein were measured with an interference microscope coupled to a high contrast video system. The mean protein concentration of the intact cells (28.4g/100 ml) decreased by 54% after treatment with detergent. Correcting for an observed 22% increase in the cell's lateral dimensions gave 66% of the cardiac cell protein as nonsoluble or myofibrillar. The A-band was selectively removed by wash with a sol'n containing 2 mM Mg-acetate, 5 mM ATP, 5 mM EGTA, 10 mM imidazole pH 7.2, and 0.35 to 0.5 M K-proprionate. At a sarcomere length of 1.9 um, the ratio of protein in the wide/narrow bands was 0.66 in the high salt extracted cells vs 1.3 in intact cells and 1.7 in the permealyzed cells. The extracted cells were exceedingly compliant, and their contractile response to iontophoretically applied Ca^{2+} was lost. A-bands of 1.5 um in length reformed upon incubation of the extracted cells with dog myosin (2.5 mg/ml prepared by ion-exchange chromatography). The protein ratio was restored to 1.4 and the A-bands were well registered laterally (but occasionally uncoupled serially). Reconstructed sarcomeres shortened and relengthened spontaneously in response to brief pulses of iontophoretically applied Ca^{2+}, and the degree and speed of shortening were related to the amount of Ca^{2+} delivered to the cell. These results demonstrate an experimental model for replacement of the cardiac A-band as a means of defining the role of thick filament chemistry to cardiac function. Supported, in part, by the N.Y.H.A. and HL 21325, HL18824, and HL 26569.

W-Pos124 AN ANALYTICAL EVALUATION OF ISOMETRIC RELAXATION IN TERMS OF THE CROSS-BRIDGE CYCLE IN ISOLATED HEART MUSCLE. J.Krueger & K. Tsujioka, The Albert Einstein College of Medicine, Bronx, N.Y. 10461

We utilized the dynamic properties of the cardiac sarcomere and a generalized model of the cross-bridge cycle to infer the molecular events underlying the time course of contraction in isolated heart muscle. Thin papillary muscles or cardiac trabeculae were isolated from rats and electrically stimulated to contract (24/min, 27° C, 1.9 mM $CaCl_2$). Sarcomere length, measured by light diffraction, was held constant until preselected moments in contraction, after which point the sarcomeres were either (1) shortened at constant velocity, or (2) shortened or stretched isotonically. The measured velocity of unloaded shortening, sarcomeric elasticity, and preaccepted ultrastructural dimensions were incorporated into a generalized cross-bridge model developed by H.M. Lacker & C. Peskin (N.Y.U. Courant Inst.). Consideration of the full, instantaneous force-velocity relation distinguished between alternative interpretations of the model. Changes in the shape of the observed force-shortening velocity relation require only that the rate of cross-bridge dissociation changes during isometric relaxation, whereas agreement with the simultaneous relations for sarcomere lengthening requires also that the orientation of the cross-bridge change. The completed model then predicted the slowing of the time constant for tension recovery after quick stretches or releases as relaxation progresses. Independent of thin filament activation, changes in the properties of the actomyosin complex appear sufficient to quantitatively account for the time course of truly isometric contraction in heart muscle. Supported, in part, by the N.Y.H.A. and HL 21325.

W-Pos125 TEMPERATURE DEPENDENCE OF SPONTANEOUS CONTRACTILE ACTIVATION AND SARCOPLASMIC RETICULUM TRANSPORT IN DISSOCIATED MYOCYTES. A. Turk, H. Gonzalez-Serratos, P. Paolini, J. Swanson, S. Padilla and G. Inesi. Dept. of Biology and SDSU Heart Institute, San Diego State University, San Diego, CA 92182. Dept. of Biophysics and Dept. of Biochemistry, School of Medicine, University of Maryland, Baltimore, MD 21202.

Functionally skinned single myocytes were prepared by perfusing rat hearts with collagenase. In the presence of micromolar calcium, the myocytes exhibited spontaneous contractile activation with beating rates varying between 10-40 per minute and propagation of activation wave proceeding throughout the myocyte at constant velocity. Beating rates, velocity of sarcomere shortening, velocity of propagation or activation wave were obtained by manual measurements and with automatic evaluation. The contracting cells were studied over a 6 to 35° C temperature range and recorded on 16 mm film, using a 400 frame/second camera connected to a microscope equipped with a temperature controlled stage. Three different techniques of analysis produced equivalent results. First, measurements were made manually from a projected image. Second, a digitizer tablet interfaced to a microcomputer was used to determine the sarcomere distances between cursor positions read from the image projected onto the tablet. Third, film frames were subjected to computer image analysis procedures including sarcomere edge detection and superposition of computer generated lines representing the sarcomere orientation within a user defined window on the image. Velocity of propagation and beat frequency were evaluated as a function of calcium concentration. In these comparative experiments it was found that the spontaneous contractile activation of the myocytes exhibited a temperature dependence similar to that manifested by the velocity of calcium transport by sarcoplasmic reticulum in the myocytes in situ. (Supported in part by USPHS grant HL27867 (G.I.), NIH grant 3ROI NS17048 (H. G-S) and AHA, Calif. Affil., grant 80-S129 (P.P.)).

W-Pos126 THE EFFECTS OF PARTIAL EXTRACTION OF TNC UPON THE TENSION-PCA RELATION IN SKINNED SINGLE FIBERS FROM RABBIT PSOAS MUSCLE. Marion L. Greaser and Richard L. Moss, Department of Physiology and the Muscle Biology Laboratory, University of Wisconsin, Madison, WI 53562.

The regulation of contraction in vertebrate skeletal muscle is believed to involve the binding of Ca^{2+} to the TnC subunit of troponin. We have begun studies to investigate possible cooperative interactions between adjacent functional groups (composed of 7 actin monomers, 1 troponin, and 1 tropomyosin) along the thin filament. Segments of skinned single fibers from rabbit psoas muscles were mounted in an experimental chamber and sarcomere length was set to 2.4-2.5 μm by adjusting overall length. Isometric tension was measured at 15°C in solutions containing maximally (pCa 5.49) and submaximally (pCa 7.00-5.95) activating levels of free Ca^{2+} (1) in control fiber segments, (2) in the same segments following partial extraction of TnC, and finally, (3) following recombination of TnC into the segments. The extraction was done at 11-13°C in 20 mM Tris, 5 mM EDTA, pH 7.8 (Cox, et al., Biochem. J., 195: 205) for 120'. Extraction of TnC resulted in reductions in tension during maximal Ca^{2+} activation to levels that were 28-42% of control values. The relative tension-pCa relation was shifted to lower pCa's by approximately 0.3 pCa unit. Readdition of TnC to the fiber segments resulted in recovery of tension to near control levels and in the return of the tension-pCa relation to its original position. This shift was not affected by the concentration of free Mg^{2+} in the activating solution (either 0.05 or 1.0 mM). A straightforward conclusion on the basis of these findings is that the Ca^{2+} sensitivity of a functional group within the thin filament may vary depending upon the state of activation of immediately adjacent groups. (Supported by grants from the NIH and the American Heart Association).

W-Pos127 INTERSARCOMERE DYNAMICS OF ISOMETRIC SINGLE FIBERS FOLLOWING A RAPID RELEASE. R.J. Baskin, W. Zagotta*, and K. Burton, Department of Zoology, University of California, Davis, CA 95616.

Linear releases, imposed during the plateau of an isometric tetanus often result in a decrease in tension. This has posed a problem since shorter sarcomeres should develop more tension. It has been argued however, that this is a complicated situation in which there exist populations of both shortening and lengthening sarcomeres at very different sarcomere lengths. Thus linear releases may not be uniformly distributed along the fiber. Using a laser diffraction technique, we have measured sarcomere length at different locations along a single fiber during and immediately following a linear release of 1-2% of initial sarcomere length. While sarcomeres at the released end of the fiber usually shorten, other fiber regions exhibit a variable response. Central regions of the fiber generally maintain a pattern of slow sarcomere lengthening. An isometric region is usually found between the middle of the fiber and the end. The location of this "isometric" region varies with time, usually moving towards the end of the fiber in the early seconds on the tetanus. As a result of the small, rapid releases studied in this investigation, the sarcomere length at different fiber regions varied. The particular pattern of the regional variation was not uniform from fiber to fiber. These results support the notion that small, rapid releases are not uniformly distributed along the length of a fiber.

W-Pos128 THE EFFECT OF PRIOR SHORTENING ON ISOTONIC SHORTENING VELOCITY AND ON FORCE MAINTENANCE DURING ISOVELOCITY SHORTENING IN THE CHICK ANTERIOR LATISIMUS DORSI (ALD) MUSCLE. Peter L. Becker and Richard A. Murphy, Department of Physiology, University of Virginia, Charlottesville, VA. 22908.

The shortening velocity of the tetanically stimulated 1 to 3 day old chick ALD following an isotonic release declines with distance shortened, independent of muscle length or rate of shortening. This phenomenon was studied during isovelocity releases using a microcomputer-controlled electronic lever. The muscle was given a step-shortening to discharge the SEC followed immediately by an isovelocity shortening of various lengths and at rates from 0.05 to 0.5 V_{max}. The force fell rapidly to an equilibrium value which declined during the isovelocity shortening. (If the step was too great, force fell sharply and then rose briefly before declining during the remainder of the isovelocity shortening.) The decline in force was dependent on the magnitude of shortening but not on the rate or on the absolute muscle length. The force seen during these isovelocity shortenings represented the force the muscle could maintain at that particular velocity, and the decline in force reflects an impaired force generating capacity. When an isovelocity shortening was terminated by an isotonic release to a smaller load, the velocity observed at any time following the release was dependent on the total distance (isovelocity and isometric) of prior shortening. These results demonstrate that shortening inhibits both the rate of isotonic shortening and the isovelocity force generating capacity of the muscle. This effect is proportional to the distance shortened, rather than the absolute muscle length or the rate of shortening. The phenomenon may be due to shortening-dependent inactivation or to the imposition of an internal load on the contractile component of the muscle. Supported by NIH grant 5 P01 HL19242.

W-Pos129 THE MAXIMUM SPEED OF SHORTENING IN LIVING MUSCLE FIBERS OF R. TEMPORARIA. Rome, LC Striz, S and Julian, FJ, Dept Anes Res Labs, Brigham and Women's Hospital, Boston, MA

Estimates of the unloaded speed of shortening (V_u) exceed estimates of the speed of shortening of isotonic contractions at loads approaching zero (V_{iso}), by 5-30% in living fibers and up to 50% in skinned fibers (Julian & Moss J Physiol 311 1981). Typically V_u is estimated by the "slack test" and V_{iso} is estimated by extrapolation to load (P)=0 of linearized Hill curves fit to data at .05 P_o < P < .8 P_o. The discrepancy between estimated V_u and V_{iso} could be explained by: 1) the "slack test" is not an accurate estimate of V_u, 2) extrapolation from the linearized Hill curves is not an accurate estimate of V_{iso}, or 3) V_u actually exceeds V_{iso}. We obtained improved estimations of V_u and V_{iso} by measuring V_u directly by photographic techniques and by measuring force-velocity relations during isotonic and isovelocity contractions at very low P (.005 to .05 P_o). Estimates of V_u varied by 50% depending upon the criteria chosen to identify the point on the force record corresponding to the time at which the imposed slack had been taken up (T_s). To determine the actual T_s, photographs of the fiber were taken at different times following various imposed amounts of slack. T_s was found to correspond to the point on the force record where the rate of tension development was 5-10 P_o/s, thereby enabling us to calibrate the readings of the "slack test". In all cases, estimates of V_{iso} made by extrapolating (to P=0) a line fit to data at P=0.02 to 0.005 P_o exceeded estimates of V_{iso} from the linearized Hill curves fit to P= 0.05 to 0.6 P_o. No difference was observed between these improved estimates of V_u and V_{iso} (V_u/V_{iso} = 1.01 ± SD = 0.04, n = 14) suggesting that fibers have a unique maximum speed of steady shortening irrespective of the technique by which it is determined. This remains to be tested in skinned preparations. Supported by NIH Grants HL30133 (FJJ) & AM07046 (LCR).

W-Pos130 THE FENN EFFECT IN VASCULAR SMOOTH MUSCLE: PHOSPHAGEN BREAKDOWN DURING MAXIMUM POWER OUTPUT IN PORCINE CAROTID ARTERY. **Joseph M. Krisanda and Richard J. Paul. Department of Physiology, University of Cincinnati College of Medicine, Cincinnati, Ohio 45267 USA.**

One characteristic of chemomechanical transduction in most striated muscle is an increase in energy liberation with increased work output. Little is known about the efficiency in work producing contractions (work per ATP) in vascular smooth muscle (VSM), although smooth muscle is known to exhibit a high economy (isometric force per rate of ATP breakdown). Recent studies on visceral smooth muscle (Butler et al., AJP 244:C234, 1983) suggested that its efficiency was much lower than striated muscle. We conducted experiments on VSM shortening under conditions of maximum power output (P_{max}). Strips (n=6) of porcine carotid artery were incubated in MOPS-buffered PSS and stimulated isometrically with KCl (+50 mM) at 37°C. The unloaded shortening velocity (V_{us}) and active isometric force, measured after 10 minutes of stimulation, were 0.015±.005 l_o/s and 124±12 mN/mm^2. On a subsequent contraction after 10 minutes of stimulation, measurements of phosphagen breakdown ($\Delta \sim P$) were made following a 10s isovelocity shortening at $0.28 \cdot V_{us}$ (= P_{max}). Control levels of ATP and PCr were 0.40±.02 and 0.60±.04 μmol/g. Total phosphagen utilized during the 10s experimental period, calculated from measurements of $\dot{J}_{O_2}$ and $\Delta \sim P$ was 0.299±.036 μmol/g and the work output was 2.4±.24 mJ/g. Work per $\Delta \sim P$ was 8.2±.68 kJ/mol, which when corrected for the work due to series and parallel elastic elements yielded an active work per $\Delta \sim P$ of 2.43±.47 kJ/mol. The ratio of ATP utilization under maximum power to that under isometric conditions was 3.5±0.4. These data indicate that a Fenn Effect can be observed in VSM and that its efficiency is substantially less than striated muscle. Supported in part by NIH R01 23240, 22619, F32 HL06051 (JMK) and an Established Investigatorship of the American Heart Association (RJP).

W-Pos131 CROSS-BRIDGE ELASTICITY IN SINGLE SMOOTH MUSCLE CELLS. F.S. Fay, and D.M. Warshaw Dept. of Physiology, Univ. of Mass. Med. Sch., Worcester, MA 01605

Previous studies (Warshaw & Fay, J. Gen. Physiol. 82:157, 1983) of fiber elasticity in single smooth muscle cells (SMC) isolated from toad (Bufo marinus) stomach muscularis suggest that the elastic response to a step change in length may originate within the cross-bridges (X-B). To further define the extent to which changes in X-B length are responsible for the observed elastic response, we compared the relation of stiffness (E) to force (F) during F development following activation (increasing number of X-Bs) to that in a fully activated fiber (constant number of X-Bs) immediately after a quick release (QR) of varying magnitude (0.5→2.0% L_{cell} in 2.0 ms). Assuming the existence of an elasticity in series (SEC) with the X-Bs, comparison of E vs F during activation and after a QR provides an estimate of X-B stiffness. The results indicate that X-B stiffness is 1.5 ± .28 (S.D. N=4) times the maximum fiber stiffness at peak isometric force. Assuming a linear X-B length:force (L:F) relation during the length step itself, the resultant SEC L:F is of the form $F/F_{max} = 0.07 (e^{321 \times \Delta L/L_{cell}} - 1)$. This study suggests that the total fiber compliance is distributed between an exponential SEC and linear X-B extended by 0.84% L_{cell} and 0.63% L_{cell} respectively at peak isometric force. Knowing the precise L:F for both SEC and X-B, meaningful insight into X-B kinetics during F development, and during F redevelopment following A QR may be obtained. (Supported by: DMW, MDA; FSF, NIH, HL14523).

W-Pos132 A THERMODYNAMIC MODEL OF CROSS-BRIDGE ELASTICITY AND KINETICS FROM SINGLE SMOOTH MUSCLE CELLS. D.M. Warshaw, R. Bisk, F.S. Fay, Dept. of Physiology, Univ. of Mass. Med., School, Worcester, MA 01605.

To help explain smooth muscle's (SMC) slow, economical contractile capabilities, we have developed a thermodynamic model (T.L. Hill, 1974, 1975) consisting of a cross-bridge (X-B) cycle having two detached (refractory (R) and nonrefractory (N))states going to two attached (low (L) and high (H) force) X-B states in series with an exponential elasticity. The model relates X-B free energy and kinetics to characteristics of the tension transients described in our previous work (Warshaw and Fay, J. Gen. Physiol. 82:157, 1983). In order to accommodate observed differences between smooth and skeletal muscle mechanics, energetics, and kinetics of actomyosin ATPase, we have modified the model for the X-B cycle in skeletal muscle so that all transitions between X-B states are slowed with most significant slowing between attached H and detached R states. The model indicates that the X-B cycle in SMC as compared to fast striated muscle: 1) is much longer; 2) has X-Bs spending a greater proportion of the total cycle time in the H state; 3) has X-Bs spending less time in both the detached and L state. These characteristics of the X-B cycle in our model provide important new insights into factors contributing to SMC's economical but slow contraction. (Supported by: DMW, MDA; FSF, MDA and NIH HL14523).

W-Pos133 FORCE RECOVERY FOLLOWING SMALL AMPLITUDE RAMP RELEASES IN OSMOTICALLY COMPRESSED CARDIAC TRABECULAE. Michael Roy Berman (Intr. by R.Z. Litten, III), Department of Physiology and Biophysics, University of Vermont, Burlington, Vermont 05405.

Force recovery following small amplitude (0.2-0.4% Lo) ramp releases was studied as a function of ramp duration (5 ms to 15 sec) in normal width (Wo) and radially compressed (0.7-1.0 Wo) muscles. Right ventricular trabeculae from adult male Wistar rats were chemically skinned (250 µg/ml saponin, 1 hour), osmotically compressed (4-18 g/100 ml Dextran T-500), then activated (pCA 5) while compressed. At the force plateau 8 identical releases were applied at 10 second intervals and the force responses were averaged. Groups of 8 releases were then performed for different ramp durations. The difference in force between the beginning and end of the release ramp (Fs) and the magnitude of the force recovery following the end of the release ramp (Fr) were measured. Recovery following rapid (5 ms) releases was fit to a single exponential and the rate constant was determined. In normal width trabeculae Fr/Fs was near 1 (0.8-1) for rapid releases; as ramp duration increased Fr and Fs decreased, approaching zero for ramp durations > 160 ms. Fr/Fs for compressed muscles was low (0.3-0.5) following rapid releases. As ramp duration increased Fs fell, but not by more than 50%, even for releases talking 15 seconds to complete; Fr fell to near zero for release durations > 620 ms. The rate constant of force recovery following rapid releases (25-45 per second) was not correlated with relative muscle width. These results are consistent with the existence of "hindered" crossbridges in compressed muscles (Berman & Maughan, Pflugers Arch 393:99-103, 1982). Further, the observation that the recovery rate constant does not change with compression suggests that crossbridge cycling rate is not altered by changes in filament lateral separation. Supported by PO1-HL-28001-02/P4.

W-Pos134 STIFFNESS MEASUREMENTS DURING THE RELAXATION PHASE OF THE ISOMETRIC TETANUS. L.A. Dusik and B.H. Bressler. Dept. of Anatomy, University of British Columbia, Vancouver, Canada.

The instantaneous stiffness to tension relationship has been studied during the relaxation phase of the isometric tetanus in single muscle fibers from frog semitendinosus. Stiffness measurements were made using small amplitude (<6nm/half sarcomere) lengthening and shortening steps complete in 500µsec. During the plateau of the tetanus a good correlation was seen between tension and stiffness. However, for the same amplitude of length change, rapid stretch produced a consistently higher tension change than a rapid release. Moreover, the magnitude of the difference was dependent on the amplitude of the applied step. During the early phase of relaxation, prior to the 'shoulder', the change in stiffness was seen to lag the tension change. Following the shoulder, there was a rapid fall in stiffness which corresponded to a similar decline in tension. Our data would suggest that during the initial phase of relaxation, there was a slow decline in the tension per cross-bridge without any significant decrease in the number of attached cross-bridges. This could be due to the intracellular Ca^{++} concentration remaining near saturation levels during this phase as has been proposed by Edman and Flitney (J. Physiol. (1982):329,1-20). Following the shoulder, a marked decrease in intracellular Ca^{++} would lead to a rapid detachment of cross-bridges which is reflected in a precipitous drop in both stiffness and tension. The apparent difference in measured stiffness values between stretch versus release was also significantly reduced during this phase. As this difference is most pronounced when the fiber is fully activated, we propose that it may be due in part to an alteration in the amount of Ca^{++} bound to the myofilaments as a result of the length step. (Supported by the M.R.C. and M.D.A.C.)

W-Pos135 SUPPRESSION OF ACTIVE CROSS BRIDGE MOTIONS OF ISOLATED LIMIULUS THICK FILAMENTS BY D_2O. S.-F. Fan, M.M. Dewey, D. Colfleah and R. Greguski, Department of Anatomical Sciences and B. Chu, Department of Chemistry, SUNY at Stony Brook, NY 11794.

The twitch of muscle is considerably depressed after soaking in D_2O-Ringer's solution. It was believed that the main action of D_2O is on the process of signal transferring from the depolarized T-system to the sarcoplasmic reticulum. The effect of D_2O on the contractile system is small (S. Ebashi, Ann. Rev. Physiol. 38:293, 1976). However, in those experiments the preparations were exposed to D_2O for only less than one hour. The active cross bridge motions of the isolated thick filaments of Limulus striated muscle detected by quasi-elastic light scattering method (S.-F. Fan, et al., Biophys. J. 41:261a, 1983; K. Kubota et al., J. Mol. Biol. 166:329, 1983) are suppressed when 50% H_2O of the suspending medium (100 mM KCl, 2 mM $MgCl_2$, 5 mM $CaCl_2$, 2 mM ATP, 0.1 mM EGTA, 5 mM Tris, pH 7.0) is replaced by D_2O. The effect has a latent period of 3 to 5 hours, reaches its maximum effect after 15 to 20 hours. The maximum degree of suppression may be close to 100%. It is reversible with comparable time course. The myosin ATPase activity is not affected as determined in our case (after 20-30 hour of treatment with D_2O) by following H^+ release and by K. Hotta and M.F. Morales, J. Biol. Chem. 235:PC 61, 1960. It seems that the conformational changes caused by the H-D exchange of either the contractile proteins and/or the proteins of the calmodulin-phosphorylation system are responsible for the mentioned suppression effect.

W-Pos136 THE MECHANICAL PROPERTIES OF SKINNED SKELETAL MUSCLE FIBERS FOLLOWING ACTIVATION IN SOLUTIONS CONTAINING ATPγS. Richard L. Moss, Gary G. Giulian, and Marion L. Greaser, Department of Physiology and the Muscle Biology Laboratory, University of Wisconsin, Madison, WI 53706.

There has been growing interest in the use of ATPγS in studies of phosphorylation reactions, primarily due to the virtual irreversibility of thiophosphorylation. We have done experiments to determine the mechanical properties of skinned fibers from rabbit psoas muscles following incubations in solutions containing ATPγS. Fiber segments were placed in an experimental chamber and activated at 15°C in solutions as previously described, except as follows: pCa 4.50, 4.1 mM ATP, 1 mM free Mg^{2+}. The maximum velocity of shortening (V_{max}) was measured using the slack test, and these records were also used to measure steady isometric tension (P_0). The segments were then placed in activating solution containing calmodulin and ATPγS (no ATP). Immediately upon activation, tension transiently increased to near 0.5 P_0 before attaining a steady value of about 0.2 P_0. Contractions in control solutions following a 15' incubation in ATPγS showed little change in V_{max} or P_0; however, prolonged incubations of up to 120' resulted in progressive decreases in V_{max} to values as low as 20% of control, with much lesser declines in P_0. Since some myosin LC_2 thiophosphorylation (as determined by IEF) was observed during the incubations, several additional fibers were bathed for 5' in ATPγS solutions containing myosin light chain kinase and calmodulin at pCa 4.50. Under these conditions, LC_2 thiophosphorylation was 80-90% complete, and yet no changes were observed in V_{max} or P_0 relative to control. Thus, the observed effects of incubation in the presence of ATPγS do not appear to involve LC_2, and may suggest the presence of an additional, as yet unidentified, thiophosphorylated site. (Supported by grants from the NIH and the American Heart Association).

W-Pos137 CROSSBRIDGE ARRANGEMENTS IN SHORTENED LIMULUS THICK FILAMENTS. Rhea J. C. Levine and Robert W. Kensler. Dept. of Anatomy, The Medical College of PA, Philadelphia, PA 19129.

Thick filaments isolated from living fiber bundles of Limulus telson muscles that have been stimulated are 25-30% shorter (3.0μm) than those isolated from unstimulated muscle (4.1-4.3μm). We have examined short thick filaments by negative staining and/or metal shadowing combined with optical diffraction in order to determine whether filament shortening is accompanied by a rearrangement of the crossbridge helix. Although negatively stained short filaments frequently display regions that look "swollen" in the middle of each arm, optical transforms of such images are qualitatively similar to those from long filaments, consisting of a series of layer lines indexing on orders of $1/43.5nm^{-1}$ and having meridional reflections at $1/14.5nm^{-1}$ and $1/7.2nm^{-1}$. Analysis of the 50-60% of transforms that display order indicates that the greatest crossbridge mass lies at the same radius from the center of the filament backbone as it does in long filaments (15.5±1.3nm S.D.; range 13.1-17.8nm) and the rotational symmetry, estimated from the calculated crossbridge radius (r) and measurement of the radial positions of the primary maxima on the 1st and 4th layer lines (R) ($J_n=2\pi rR$; $Jn=5.4\pm0.59$ S.D.) is 4 ($J_4=5.32$). If there is any increase in the diameter of short filaments, it is very small (3-4nm) and lies within the "swollen" regions. There is no apparent difference between long and short filaments with respect to the number of crossbridges/crown. Shadowed short filaments have a right-handed surface helix of subunits and by optical filtration 6-7 such subunits are resolved/strand, similar to the situation in long filaments and consistent with a 4-stranded crossbridge helix. We are examining the possibility that filament shortening may involve disaggregation of myosin and paramyosin, which may be transiently reflected by the disorder in the lattice we have observed. Supported by USPHS grants: AM30443 and HL15835 to the Pennsylvania Muscle Institute.

W-Pos138 MECHANICAL POWER OUTPUT OF MUSCLE DURING CYCLIC CONTRACTION, Robert K. Josephson, Department of Psychobiology, University of California, Irvine, CA 92717 (Intr. S.E. Fraser)

The mechanical power output of muscle was determined by measuring tension as the muscle was subjected to sinusoidal length change and stimuli which occured at a selected phase of the length cycle. The area of the loop formed by plotting muscle tension against length over a full cycle is the work done on that cycle; this times the cycle frequency is the mechanical power output. Power output can be positive (done by the muscle) or negative (done on the muscle) depending on the phase between muscle length and stimulation. In flight muscles of the tettigoniid insect Neoconocephalus triops examined at the normal wing stroke frequency during flight (25 Hz) and operating temperature (30°C), the work output at optimal excursion amplitude and stimulus phase is 1.52 J/kg/cycle (s.e. = 0.8, n =22) with single stimuli per cycle. This is a power output of 38 W/kg. The maximum power occurs at a phase such that the onset of the twitch coincides with attainment of the longest muscle length. The optimum excursion amplitude with single stimuli is 5.7% of rest length (peak to peak). With greater excursion, work output declines because of the decreasing muscle force associated with the more rapid shortening velocity. Work output can be increased above that obtained with single stimuli by using bursts of stimuli on each cycle. In these muscles the maximum power output at 25 Hz is about 76 W/kg which is achieved with a bursts of 3 stimuli separated by 4 msec intervals and an excursion amplitude of 6.0% of rest length. Supported by NSF Grant PCM-8201559.

W-Pos139 EFFECTS OF pH, Mg^{2+}, AND DEUTERIUM OXIDE (D_2O) ON CONTRACTILE ACTIVATION OF SKINNED FIBERS FROM THICK- AND THIN-FILAMENT REGULATED MUSCLES. R.E. Godt, J.L. Morgan, F.A. Honkanen, D.J.E. Luney & E.D. Stevens*. Dept. of Physiology; Medical College of Georgia; Augusta GA 30912, and *Dept. of Zoology; Univ. of Guelph; Guelph, Ontario.

We compared the effects of pH, Mg^{2+}, and D_2O, agents known to influence contractile activation, on the force-pCa relation of skinned fibers from frog semitendinosus, a thin-filament regulated muscle, and from striated adductor of the sea scallop (Placopecten magellanicus), which is regulated at the thick filament. In both muscle types, calcium sensitivity increased with increasing pH, although their responses were strikingly different. The force-pCa curve of the frog shifted markedly to the left as pH increased from 6.5 to 7 or 7.25, but increasing pH to 7.5 or 7.75 had no further effect. That of the scallop, however, shifted only slightly when pH increased from 6.5 to 7, while a further increase to 7.5 caused a marked leftward shift. The responses to Mg^{2+} and D_2O, on the other hand, were similar in frog and scallop. Increasing Mg^{2+} from 60 uM to 1 mM caused calcium sensitivity to decrease, shifting the force-pCa curves to the right by about 0.2 log units (frog) or 0.3 log units (scallop). Replacement of solvent water by D_2O also decreases calcium sensitivity. Comparing pH and pD of 7, the force-pCa relation shifted to the right by about 0.5 log units (frog) or 0.7 log units (scallop). In both species, maximal calcium-activated force was increased by 20% in D_2O. These data argue that Mg^{2+} and D_2O influence contractile activation by acting at molecular sites which are common to both thick- and thin-filament regulated muscles. (Supported by NIH grant AM 31636 and a Dean's Student Research Fellowship. R.E.G. is an Established Investigator of the American Heart Association.)

W-Pos140 pH SHIFT OF THE FORCE-pCa RELATION IN SKINNED FIBER BUNDLES FROM THE ANTERIOR BYSSUS RETRACTOR MUSCLE (ABRM) OF MYTILUS. P. Bryant Chase, Department of Biological Sciences, Univ. of Southern California, Los Angeles, CA 90089.

Thin (minimum dimension <120μm) strips of ABRM fibers, skinned with 0.1% (w/v) saponin, have been used to study the effect of pH on steady-state active force generation. The force-pCa relation of the ABRM is shifted to higher $[Ca^{2+}]$ by increasing $[H^+]$; the pK's determined were 6.6 (pH 7.5), 6.3 (pH 6.8), and 5.9 (pH 6.15). K and n were determined by unweighted linear least squares regression using a linearized form of the binding equation:

$$F/Fmax = (1 + (K/[Ca^{2+}])^n)^{-1}$$

The force-pCa relation also becomes less steep with increasing $[H^+]$; n's were 4.4 (pH 7.5), 2.1 (pH 6.8), and 1.6 (pH 6.15). The first n is surprisingly large, if it is interpretted as the minimum number of Ca-binding sites involved in force regulation. These experiments, performed to further the understanding of active contraction of a thick filament regulated muscle, suggest a close interrelationship between Ca^{2+} and H^+ binding.
All solutions contained 2mM Mg-ATP, 10mM EGTA, 25mM pH buffer (TES (pH 7.5), PIPES (pH 6.8), or MES (pH 6.15)), 5mM Mg^{2+}, 82-128mM K^+, and 46-82mM Cl^- (ionic strength = 140mM). Ion-ligand binding for Ca^{2+}, H^+, and Mg^{2+} was calculated from binding coefficients published by Martell and Smith (1974-1982, Critical Stability Constants, V1-5. Plenum Press, NY) and by Good et al. (1966, Biochem. 5:467-477). This work was supported in part by a Grant-in-Aid of Research from Sigma Xi, the Research Society.

W-Pos141 DIRECT AND EXTRAPOLATED DETERMINATIONS OF MAXIMUM SHORTENING VELOCITY OF WHOLE SKELETAL MUSCLES. Dennis R. Claflin. Bioengineering Prog., U. of Michigan, Ann Arbor, MI 48109.

The maximum shortening velocity of skeletal muscle preparations is traditionally estimated by extrapolating to the velocity at zero load (V_{max}) along a hyperbola fitted to velocities at non-zero afterloads. The "slack test" is a technique for measuring unloaded shortening velocity (V_o) directly by applying a series of quick releases to a fully activated muscle preparation and measuring the time required to take up the imposed slack. The V_o is not different from V_{max} in single skeletal muscle fibers. The hypothesis tested was that V_o is greater than V_{max} for whole skeletal muscles in which the fiber population is heterogeneous with respect to intrinsic shortening velocity. The hypothesis was based upon the assumptions that: (1) the V_{max} of a heterogeneous whole muscle is influenced by the force-velocity characteristics of all fibers, whereas (2) the slack test measures only the unloaded shortening velocity of the fastest fibers within a whole muscle. The hypothesis was tested in vitro at 20°C on soleus muscles from 4 week old female rats. The heterogeneity of the soleus muscle is indicated by the wide range of isometric twitch contraction times among its motor units. A computer algorithm was developed to provide an unbiased, least squared error fit of a rectangular hyperbola to the force-velocity data. The V_{max} was 3.3 ± 0.1 (mean ± S.E.M., n=10) fiber-lengths/s while V_o measured on the same muscles was 5.0 ± 0.1 fiber-lengths/s. The ratio of V_o/V_{max} was 1.6 ± 0.1. A comparison of these results with the distribution of contraction times reported for rat soleus muscles supports assumptions (1) and (2). The results support the hypothesis that V_o is greater than V_{max} in heterogeneous whole muscles. (Supported by USPHS Grant NS17017.)

W-Pos142 DO SEGMENT LENGTH MEASUREMENTS SHOW STEPWISE SHORTENING? H.L.M. Granzier, F. Brozovich, S. Rowinski, J. Myers & G.H. Pollack, Div. of Bioengineering & Dept. of Anesthesiology WD-12, Univ. of Washington, Seattle, WA 98195.

We have developed a segment length monitoring system to explore the dynamics of shortening in fiber segments. The method is similar to that used by Edman and colleagues, except that we have been able to achieve substantially higher resolution. Thin hairs, approximately 30 - 40 μm wide, and 70 - 100 μm long are placed along the upper surface of the fiber, perpendicular to its long axis. The image of a section of the fiber containing two hairs is split such that one hair is projected onto one photodiode array (Reticon, 256 element), while the other is projected onto a second array. A processing circuit computes the area under the image of the marker, from which the median location is computed. Because this method is integrative, the location of the median is computed with a resolution considerably better than the spacing between individual photodiode elements. The difference between medians of the two markers is then computed every 256 microseconds. The observed noise level for detection of individual markers is considerably better than 1 μm. In the four unstimulated fibers we have been able to study to date, release and stretch imposed on the fiber resulted in clear pauses in the segment length record. We have not yet carried out enough controls to rule out artifact, e.g. 2 fibers did lose their excitability prior to the time the records could be obtained; however, the pause durations (1-2 msec) and step sizes (ca. 1%) were similar to those measured previously under comparable loading conditions by diffraction and by phase locked loop analysis of the striation pattern.

W-Pos143 FORCE DECAY FOLLOWING SMALL STRETCHES OF FRESHLY SKINNED RABBIT PSOAS FIBERS IN RIGOR, PP_i, AND AMPPNP SOLUTIONS. M. Schoenberg and E. Eisenberg†. NIADDK and NHLBI†, NIH, Bethesda, MD

To study crossbridge detachment rates, we examined the rate of force decay for 180 s following a 2 nm stretch (step time, 0.8 ms) of freshly skinned rabbit psoas fibers in rigor, pyrophosphate (PP_i), and adenyl-5'-yl-imidodiphosphate (AMPPNP) solutions at ligand concentrations of 0.25, 1, and 4 mM, with 1 mM EGTA, 10 mM imidazole, 90 mM KCl and 2 mM free Mg^{++}. Sarcomere length was monitored by laser diffraction. In each solution studied, a stretch of 2 nm/half-sarcomere produced a force of ~ $0.3P_o$, suggesting that, in each case, the number of attached crossbridges was approximately the same. The force decay appeared to be linearly related to the logarithm of time after stretch over many decades of time (Kuhn, Biophys. Struct. Mechanism 4:159:1978), suggesting a wide range of detachment rateconstants. For 4 mM PP_i, the fastest rateconstant was 100-1000 times greater than the slowest one. Force decayed over ~ 5 decades, reaching half its initial value in $\tau_{1/2}$ ~ 0.2 s. Decreasing PP_i to 1 mM or 0.25 mM decreased the rate of force decay, increasing $\tau_{1/2}$ to 1.5 s and 7 s respectively, suggesting either that PP_i binding is not saturated at 1 mM or detachment rate is a very nonlinear function of % saturation. In 4 mM AMPPNP, the decay of force was also slower than in 4 mM PP_i, by 1.5 - 2 orders of magnitude, even though the *in vitro* binding constant of S-1 to actin probably differs < 2-fold in the two solutions. There was also a very slow logarithmic decay in rigor, even when allowance was made for changes in sarcomere length during the plateau of stretch. The decay was 20% in 3.5 s, with $\tau_{1/2}$ ~ 1 hr. We conclude that, while individual detachment rateconstants vary greatly, all the strained crossbridges in freshly skinned rabbit psoas fibers detach and reattach in positions of lesser strain, resulting in tension decay to F = 0. The rates of detachment are very rapid in 4 mM AMPPNP or PP_i compared to rigor.

W-Pos144 ELLIPSOMETRY STUDIES ON THE DIFFRACTION ORDERS OF A SINGLE SKINNED FIBER UNDERGOING CALCIUM ACTIVATED CONTRACTION. R. J. Baskin, M. Jones, Z. C. Xu and Y. Yeh, Departments of Zoology and Applied Science, University of California, Davis, California 95616.

Optical ellipsometry measurements have been made on the diffraction orders of a single skinned fiber undergoing calcium activated contraction. A rapidly oscillating photoelastic modulator (PEM) is used to follow the dynamic changes of the ellipsometry signal as calcium is introduced into the relaxing solution with 4 mM ATP. The time period for a complete cycle of the PEM is 20 μsec. Signals are captured in that time or multiples of this basic period for digital signal averaging. Ellipsometry data is analyzed by direct curve fitting and by spectral analysis methods. The calcium activated state shows an increase in the phase shift over that of the relaxed state. Furthermore, the activated state also exhibits a small but discernable change in the absolute values of the differential polarizabilities between those along and perpendicular to the fiber axis. This latter observation is unique to the present experiment, and was not observed in the relaxed-to-rigor transition studies.[1] If our interpretation of the relaxed-to-rigor transition data is correctly attributable to the tilting motion of the anisotropic S-2 elements, then the present result suggests that additional dynamics and other sarcomeric moieties have been observed by this technique. We shall explore some of these possibilities in relationship to the sliding filament theory of muscle contraction. (Supported in part by grants NSF PCM 8300046 to RJB and NIH AM 26817 to YY.)

1. Y. Yeh, M. E. Corcoran, R. J. Baskin, and R. L. Lieber, Biophys. J. 44, December, 1983 (in press).

W-Pos145 CA^{++} ACTIVATION OF SKINNED SMOOTH MUSCLE CELLS FROM AMPHIUMA STOMACH IS EXCLUSIVELY MYOSIN-LINKED. John Caffrey* and Alan Magid. Depts. Physiol. & Anat., DUMC, Durham, N.C. 27710

Smooth muscle activation is dominated by a calmodulin-dependent myosin phosphorylation mechanism, but an actin-linked mechanism might operate as well. We have looked for dual regulation in single smooth cells isolated enzymatically from Amphiuma stomach, and then chemically skinned with Triton X-100, saponin, or digitonin. To provide unloaded conditions, cells were attached to a single tether in a chamber through which test solutions were flushed. Cell dimensions were recorded by photo- or TV-micrography. Detergent caused rapid, complete loss of contractile response to Ca^{++} (Act, pCa < 6). Unresponsive cells in Act did, however, contract promptly and completely when calmodulin (CMD, 10 μM) was added to the superfusate. Ca^{++} alone is therefore unable to effect shortening. It might maintain attachment of activated crossbridges. This seems ruled out by experiments where cells were skinned directly into Act containing 15 mM P_i. They initially contracted fully (to about 0.3 L_o) as when MOPS buffer is used, but then they completely relaxed. Calcium might activate non-cycling bridges. The expected increase in fiber stiffness was sought by using the PVP osmotic stress technique to squeeze the cells. Cells in Ri were much stiffer than in Rel, but in Act, cells were as or more compliant than relaxed ones. Troponin-tropomyosin-linked inhibition is unlikely: Cells did not contract when MgATP was lowered to 10 μM or washed out. Further, skinning cells in 10 mM Mg^{++}, hoping to retain labile proteins (Lehman, BBA 745: 1), did not preserve sensitivity to Ca^{++} alone. Taken together, these observations strongly suggest that active shortening in this preparation is regulated solely by a calcium/calmodulin-dependent system. Supported by NIH.

W-Pos146 EFFECTS OF VASODILATORS ON $[Ca^{++}]_i$ IN VASCULAR SMOOTH MUSCLE. Kathleen G. Morgan, James P. Morgan*, and Tia T. DeFeo*. Dept. of Medicine, Beth Israel Hospital, Harvard Medical School, Boston, MA 02215.

The purpose of the present study is to determine if all vasodilators relax vascular smooth muscle (VSM) solely by a decrease in $[Ca^{++}]_i$. The bioluminescent Ca^{++} indicator aequorin was loaded into smooth muscle cells of the ferret portal vein (FPV) by a recently described chemical loading procedure. The FPV has little intrinsic tone, so the effects of vasodilators were determined against a background of 33 mM K+-depolarization (K). K produces easily detectable, sustained, parallel increases in L (Ca^{++}-induced light) and F (force). The effects of the vasodilators were most pronounced when added to the muscle before the addition of K but were also detectable when added after the development of tone with K. L and F were decreased in a parallel manner by Ca-depleted physiological saline solutions (Ca-D), verapamil (V), and Na nitroprusside (NPR); but, in the presence of isoproterenol, papaverine and forskolin L was either unchanged or increased as the muscle relaxed. Additionally, with the agents that decreased L, the F/L ratio, measured in the steady state after relaxation of the muscle, was found to decrease in the order of Ca-D >V> NPR. These results suggest that vasodilators have effects other than to decrease $[Ca^{++}]_i$ and that these agents can affect the $[Ca^{++}]_i$-myofilament interaction. Since V is the only drug which has been reported capable of entering cells, it seems likely that the other drugs are acting through second messengers. Supported by NIH grants HL 31704, HL 31117, and an American Heart Association grant in aid.

W-Pos147 THE 110-KDALTON ACTIN- AND CALMODULIN-BINDING PROTEIN FROM INTESTINAL BRUSH BORDER IS AN ATPase. Jimmy H. Collins, Chris Borysenko, Jye-Ping Chiao, Brendon Lamperski and Hunter Martin; Department of Biochemistry, University of Pittsburgh School of Medicine; Pittsburgh, PA 15261.

The 110-kdalton protein present in chicken intestinal brush border microvilli may laterally link the actin filament bundle that forms the structural core of the microvilli with the microvillar plasma membrane. We have obtained highly purified preparations of the 110-kdalton protein from brush borders by extraction with buffer containing 0.6 M KCl and 5 mM ATP, followed by gel filtration chromatography, sedimentation of the 110-kdalton protein as a complex with exogenous actin, dissociation and solubilization of the 110-kdalton protein with ATP and hydroxyapatite-agarose chromatography. Purified preparations contained variable amounts of an 18-kdalton protein identified as calmodulin by comigration on SDS-polyacrylamide gels in the presence of either Ca^{2+} or EGTA and by Ca^{2+}-dependent, trifluoroperazine-sensitive stimulation of bovine brain cAMP phosphodiesterase. The purified 110-kdalton protein bound F-actin in the absence but not the presence of ATP. It had Ca^{2+}-ATPase (0.2 μmol/min/mg) and K^{+}, EDTA-ATPase (0.2 μmol/min/mg) activities and Mg^{2+}-ATPase (0.03 μmol/min/mg) activity that was not altered by added bovine brain calmodulin or trifluoroperazine. The actin-binding and ATPase activities of the 110-kdalton protein were similar to those of purified brush border myosin. However, immunoblot analysis showed no crossreactivity between the 110-kdalton protein and pololyclonal antibody against purified chicken brush border myosin. Also, peptide maps of 110-kdalton protein and myosin obtained by limited proteolysis with V-8 protease had few, if any, peptides in common. Thus, this protein appears to be chemically distinct but enzymatically similar to brush border myosin. We are presently attempting to further characterize the molecular properties of the 110-kdalton protein.
Supported by NIH Grant GM 32567, Grant Z-87 from the Health and Human Services Foundation of Pittsburgh, and a Basil O'Connor Starter Grant from the March of Dimes to J.H.C.

W-Pos148 STUDIES ON THE PHOSPHORYLATION SITES OF MACROPHAGE MYOSIN HEAVY CHAINS. J.A. Trotter and I. Walkiw, University of New Mexico School of Medicine, Albuquerque, NM 87131.

Macrophages contain at least two myosins (FEBS Lett. 156: 135, 1983), the heavy chains of which have at least one phosphorylation site, which is located on the rod portion of the molecule (Biophys. Biochem. Res. Comm. 106: 1071, 1982). When myosin is purified from rabbit alveolar macrophages which have been incubated in the presence of $^{32}PO_4$, both heavy and light chains are phosphorylated. The heavy and light chains are separated from one another by a modification (D. Hathaway, personal communication) of the Method of Perrie and Perry (Biochem. J. 119: 31, 1970), followed by partial acid hydrolysis (6NHCl, 110°C, 2 hr) and TLE. Autoradiography shows that all the radioactivity of heavy and light chains comigrates with the phosphoserine standard. After cleavage of the heavy chain at cysteine residues with 2-nitro-5-thio-cyanatobenzoic acid (Jacobsen et al, J. Biol. Chem. 248: 6583, 1973), the heavy chain radioactivity is associated with peptides that migrate in SDS-PAGE with apparent molecular weights of 73, 135 and 145 kDa. Quantitative densitometry of stained gels and autoradiographs shows that the amount of radioactivity per molecular equivalent of protein in the 73kDa band is approximately 1.7x that associated with the 135 or 145 kDa bands, while the latter two are approximately equal, both in terms of protein and radioactivity. Since we have previously shown that all heavy chain ^{32}P is associated with the 132 kDa myosin rod, we hypothesize that the 73 kDa NTCB peptide is a fragment of the 135-145 kDa peptide, and that phosphorylation of one or more sites on the 135-145 kDa fragment promotes cleavage at a cysteine residue near the middle of that peptide.

Supported by PHS Grant #GM 31363.

W-Pos149 SKELETAL MYOSIN S-1 INDUCES FORMATION OF ACTIN FILAMENT BUNDLES. Toshio Ando and Dan Scales*. Cardiovascular Res. Inst., UCSF, San Francisco, CA 94143; *Dept. of Physiology Univ. of Pacific, San Francisco, CA 94115.

It is well known that the light scattering intensity of F-actin solution increases immediately on the formation of the rigor complex with S-1. However, we have observed a peculiar behavior of light scattering from acto-S-1. After initial rise in scattering there was a further gradual increase in the light scattering. The initial rate (v_o) of the gradual increase has a maximum (v_o^m) at molar ratio of S-1 to actin of 1/6-1/7, regardless of [actin], pH(6-8.5) and the ionic strength (up to 0.3 M KCL). Lower pH and higher ionic strength increase v_o^m, and v_o^m is proportional to $[actin]^2$. In order to determine what is happening to acto-S-1 during the gradual increase in the light scattering, we have observed acto-S-1 at different times with an electron microscope. We have seen that regular bundles of actin filaments are gradually formed on adding S-1. Solution conditions which give larger v_o^m favor faster formation of actin bundles. The bundles possess lateral stripes with 350 Å periodicity, and the distance between adjacent actin filaments in the bundles is about 93 Å. In the light of structure and size of actin filaments, these values suggest that in the bundles actin filaments are arranged in register, and contact through S-1. In order to see if S-1 holds two actin filaments together, acto-S-1 was chemically cross-linked with EDC under various conditions, and the cross-linked products were studied on SDS-PAGE. Only one product with apparent M.W. of 200K behaves differently from others. The 200K product is not produced in low ionic solution or when EDC is added to acto-S-1 immediately after mixing S-1 with F-actin, and contains both actin and S-1 HC, suggesting that the 200K comes from S-1 which holds two actin filaments together.

W-Pos150 DETERMINATION OF THE BINDING CONSTANTS OF SMOOTH MUSCLE MYOSIN LIGHT CHAIN KINASE AND VARIOUS PHOSPHATASES TO ACTIN AND MYOSIN. J.R. Sellers, M.D. Pato* and R.S. Adelstein, NHLBI, NIH, Bethesda, MD 20205 * University of Sasakatchewan, Saskatoon, Canada S7NOWO.

We have measured the binding constants of turkey gizzard smooth muscle myosin light chain kinase (MLCK) to smooth muscle myosin and to skeletal muscle actin by assaying for the MLCK activity remaining in the supernatant following sedimentation in an airfuge at 50mM NaCl, 10mM MOPS (pH 7.0), 1mM $MgCl_2$, 0.1mM EGTA, 1mM DTT and 0.5mg/ml BSA. MLCK bound to unphosphorylated myosin with a $K_B = 1.34 \times 10^6 M^{-1}$. Suprisingly, it was found that the presence of Ca^{++}/calmodulin resulted in about a 3-fold decrease in this binding constant. MLCK bound weakly to myosin rod and phosphorylated myosin. In agreement with a report by Dabrowska et al, BBRC 107, 1525, 1982, we found that MLCK also bound to skeletal muscle actin ($K_B = 2.49 \times 10^5 M^{-1}$). When actin was complexed with tropomyosin (TM), the binding constant was increased about 4-fold. Again, the presence of Ca^{++}/CaM weakens the MLCK binding. When the binding constants of MLCK to myosin and actin-TM were measured at higher ionic strengths, it was found that increasing the ionic strength decreased the actin-MLCK binding more than it decreased the myosin-MLCK binding.

We have also measured the binding of various smooth muscle phosphatases to myosin (See Pato and Adelstein, JBC 258, 7047, 1983). SMPIII and SMPIV bound to unphosphorylated myosin with $K_B = 3.7 \times 10^5 M^{-1}$. These phosphatases bound extremely tightly to thiophosphorylated myosin. Neither SMPI nor SMPII (which do not dephosphorylate intact myosin) nor the isolated catalytic subunit SMPI bind appreciably to either unphosphorylated or thiophosphorylated myosin. None of the phosphatases studied bound strongly to actin.

W-Pos151 MONOCLONAL ANTIBODIES TO SMOOTH MUSCLE MYOSIN HEAVY CHAIN SUBFRAGMENTS S-1, S-2, AND LIGHT MEROMYOSIN. M.D. Schneider, J.R. Sellers, Y.A. Preston, and R.S. Adelstein. Laboratory of Molecular Cardiology, NHLBI, NIH, Bethesda, Maryland 20205.

We report the characterization of three hybridoma cell lines secreting antibody directed against identified domains of smooth muscle myosin, produced by polyethylene glycol-induced fusion of P3-X63.Ag8 myeloma cells with spleen cells from mice immunized with a partially phosphorylated chymotryptic digest of purified adult turkey gizzard myosin. Antibody specificities were determined by solid-phase indirect radioimmunoassay and immunoreplica techniques, employing purified turkey gizzard intact myosin, heavy meromyosin (HMM), subfragment S-1, subfragment S-2, rod, light meromyosin (LMM) and 20- and 17-kilodalton (kD) light chains. Hybridoma antibody binding was detected by an ^{125}I-labelled $F(ab')_2$ fragment of affinity-purified sheep IgG directed against mouse immunoglobulins. Antibody 420D3 recognizes a determinant detected on gizzard HMM and its 64-kD degradation product, but not intact or SDS-denatured gizzard myosin, S-1, or rabbit skeletal muscle HMM. Although no binding to intact rod is detected, the antibody binds to the 38-kD S-2 fragment of rod digested with chymotrypsin, as well as to S-2 derived from HMM digested with papain. Antibody 583E3 recognizes gizzard intact myosin, rod, or LMM. Antibody 633E9 binds to gizzard intact myosin, HMM, or S1. The latter two both bind to SDS-denatured homogenates of 20-day embryonic chick gizzard or thoracic aorta and to purified chick intestinal brush border myosin, but not to calf aortic myosin, chick pectoralis myosin, or SDS-denatured homogenates of chick cardiac ventricle, pectoralis, or cerebellum, or of adult rat stomach, uterus, cardiac ventricle, pectoralis, cerebellum, liver, or spleen.

Thus, we have produced monoclonal antibodies that recognize distinct domains of the avian smooth muscle myosin heavy chain, that is, subfragments S-1, S-2 and LMM. The antibodies will be employed as probes of the structure and functional organization of smooth muscle myosin.

W-Pos152 PHOSPHORYLATION OF HEAVY MEROMYOSIN BY Ca^{2+} ACTIVATED, PHOSPHOLIPID-DEPENDENT PROTEIN KINASE (PROTEIN KINASE C). M. Nishikawa, J.R. Sellers, *H. Hidaka and R.S. Adelstein, *Mie University, School of Medicine (JAPAN) and National Heart, Lung, and Blood Institute, NIH, Bethesda, Maryland 20205

Smooth muscle heavy meromyosin (HMM) can serve a substrate for protein kinase C as well as for the Ca^{2+}/calmodulin-dependent kinase, myosin light chain kinase (MLCK). When HMM was incubated with protein kinase C, the 20,000-dalton light chain on HMM molecule was phosphorylated and 1.7-2.2 moles of phosphate was incorporated per mole of HMM. Analysis of the ^{32}P-labelled tryptic peptides following the phosphorylation of HMM showed that the phosphopeptides observed with protein kinase C were different from the phosphopeptide obtained with MLCK, indicating that the two enzymes phosphorylated different sites on the 20,000-dalton light chain of HMM. Phosphorylation of HMM by protein kinase C did not increase the actin-activated MgATPase activity, whereas phosphorylation of HMM by MLCK raised the MgATPase activity markedly. After phosphorylation of HMM with MLCK, addition of protein kinase C resulted in an additional incorporation of 2 mole phosphate/mole HMM. This additional phosphorylation of HMM significantly decreased the actin-activated MgATPase activity of HMM due to an 8 fold increase in the Km for actin. In addition, prephosphorylation of HMM by protein kinase C decreased the rate of phosphorylation of the HMM by MLCK, due to a 7 fold increase in the Km for HMM. This raises the possibility that contractile activity in smooth muscle and non-muscle cells may be modulated by phosphorylation at a number of different sites in myosin.

W-Pos153 STUDIES ON MYOSIN AND MYOSIN LIGHT CHAIN KINASE DURING FETAL DEVELOPMENT OF SMOOTH MUSCLES. P. de Lanerolle, R. Felsen, T. Triche* and R. S. Adelstein, Laboratory of Molecular Cardiology, NHLBI, and *Laboratory of Pathology, NCI, NIH, Bethesda, MD 20205.

We have used affinity purified antibodies to smooth muscle myosin and myosin light chain kinase to study these proteins during fetal development of mammalian and avian smooth muscles. Fluorescein-labelled, affinity purified antibodies to tracheal smooth muscle myosin were used to detect the presence of smooth muscle myosin in sections prepared from frozen tissues. Myosin light chain kinase (MLC kinase) was detected using affinity purified antibodies to turkey gizzard MLC kinase (PNAS 78:4738, 1981) that were visualized using rhodamine-labelled goat anti-rabbit second antibodies. Both myosin and MLC kinase antibodies were detected in vascular smooth muscles in adult sheep hearts. However, only the myosin antibodies were readily visualized in vascular smooth muscle in 45 day old fetal sheep hearts (term = 150 days). Similar results were obtained from studies on fetal chick hearts and gizzards. We also studied MLC kinase activity in fetal chicken gizzard since gizzards represent a relatively homogeneous population of smooth muscle cells. Extracts were prepared from gizzards removed at various times from chick eggs and tested for phosphorylation of myosin light chains. The data, normalized to extractable protein, indicate low levels of MLC kinase activity in gizzards removed from 9-12 day eggs (15-20% compared to adult gizzards). The MLC kinase activity increases with time and the activity in the gizzards removed from newborn chicks is near the level seen in adult gizzards. The significance of this apparently lower level of the MLC kinase activity in fetal smooth muscles is under investigation.

W-Pos154 PURIFICATION AND CHARACTERIZATION OF SMOOTH MUSCLE PHOSPHATASE-IV FROM TURKEY GIZZARDS. M.D. Pato and E. Kerc, Department Of Biochemistry, University of Saskatchewan, Saskatoon, Saskatchewan, Canada S7N 0W0.

There are at least 4 phosphatases in turkey gizzard smooth muscle which dephosphorylate muscle proteins. Smooth muscle phosphatase (SMP) I and II have been purified to apparent homogeneity. SMP-I is a trimer (M_r = 60,000, 55,000 and 38,000) while SMP-II is a single subunit (M_r = 43,000) enzyme. Both SMP-I and II dephosphorylate the isolated smooth muscle myosin light chains but not the intact myosin. However, the dissociated catalytic subunit (M_r = 38,000) of SMP-I is active towards myosin and myosin light chains.

We have now purified SMP-IV, an enzyme which is active against intact myosin and PHMM. SMP-I and IV eluted together from Sephacryl S-300 and DEAE-Sephacel columns but were resolved on ω-aminooctyl Sepharose. Further purification of SMP-IV was carried out by affinity chromatography on myosin-Sepharose and thiophosphorylated myosin light chain-Sepharose. Determination of the subunit composition of the enzyme by electrophoresis on a non-denaturing gel followed by SDS-polyacrylamide gel electrophoresis of the eluted active fraction showed that SMP-IV is composed of two subunits (M_r = 58,000 and 40,000). SMP-IV has high activity towards PHMM and myosin light chains but low activity against phosphorylase a and histone II-A. Activity towards PHMM and myosin light chains are stimulated by Mn^{2+}. Mg^{2+} and Ca^{2+} inhibit the activity against myosin light chains but slightly activate the activity towards PHMM. Both activity are optimal at pH 8.0. SMP-IV binds tightly to myosin but not to actin (See abstract of Sellers, et,al.).

W-Pos155 IDENTIFICATION OF LIGHT CHAIN BINDING SITES ON SMOOTH MUSCLE MYOSIN AND ITS SUBFRAGMENTS USING A LIGHT CHAIN OVERLAY OF SDS-POLYACRYLAMIDE GELS. J.R. Sellers, Laboratory of Molecular Cardiology, NHLBI, NIH, Bethesda, MD 20202 (Introduced by M. E. Payne)

The interactions of smooth muscle myosin and its light chains (LC) have been examined by overlaying SDS-polyacrylamide gels of myosin and its subfragments with labelled 20,000-dalton and 17,000-dalton light chains. The technique involves electrophoresis of myosin and its various proteolytic subfragments in the presence of SDS. The gel is fixed in methanol-acetic acid, washed several times with 0.2M NaCl, 50mM Tris (pH 7.5), 1mM $MgCl_2$, and then incubated for 2 h in 20mg/ml bovine serum albumin, 0.1% gelatin, 0.2M $NaCl_2$, 1mM $MgCl_2$, 50mM Tris (pH 7.5). It is then incubated overnight in the latter buffer containing 0.01-0.05mg/ml of either ^{32}P-labelled 20k LC or ^{14}C-labelled 17k LC. The following day the gel is extensively washed with 1M NaCl, 1mM $MgCl_2$ and 50mM Tris (pH 7.5) prior to staining and destaining. The LC-binding fragments can be visualized by autoradiography. The gel shows that both LC's can rebind to the heavy chains of myosin (200k), HMM (130k) and S-1 (97k) in a ratio of 0.1-0.4mol LC/mol myosin. No binding is observed to rod, LMM or S-2. HMM is split upon prolonged chymotryptic digestion into an N-terminal 66k peptide and a C-terminal 64k peptide which binds LC's. Smooth muscle S-1 can be further cleaved by trypsin to give fragments of 29k, 50k and 26k while skeletal S-1 is cleaved to 27k, 50k and 20k. The LC's bind to the 26k fragment of smooth muscle S-1 and to the 20k fragment of skeletal muscle S-1. These two fragments are located at the C-terminal end of the S-1. The results indicate that a strong light chain binding site exists in the C-terminal region of S-1, but do not exclude the possibility of other interaction sites elsewhere on the S-1 or the S-2 regions of myosin.

W-Pos156 PURIFICATION OF A CALCIUM-CALMODULIN DEPENDENT MYOSIN LIGHT CHAIN KINASE FROM LIMULUS MUSCLE. J.R. Sellers, E.V. Harvey and M. Tannenbaum, National Heart, Lung, and Blood Institute, NIH, Bethesda, MD 20205.

It has previously been shown that the regulatory light chains of myosin from Limulus, the horseshoe crab, can be phosphorylated by either purified turkey gizzard smooth muscle myosin light chain kinase (MLCK) or by a crude kinase fraction prepared from Limulus muscle (Sellers, J. Biol. Chem. 256, 9274, 1981). This phosphorylation was shown to be associated with a 20-fold increase in the actin-activated MgATPase activity of the myosin. We have now purified the Ca^{++}-calmodulin dependent MLCK from Limulus muscle to near homogeneity using a combination of low ionic strength extraction, ammonium sulfate fractionation and chromatography on DEAE-Sephacel and Sephacryl S-300. The final purification was achieved by affinity chromatography on a calmodulin-Sepharose 4B column. An SDS polyacrylamide gel showed a doublet with Mr = 39,000 and 37,000 which comprise 95% of the stained bands. Electrophoresis of the kinase fraction under non-denaturing conditions results in a partial separation of the two major bands each of which has catalytic activity. An SDS polyacrylamide gel overlayed with I^{125}-calmodulin demonstrated that both the 39kd and the 37kd proteins are capable of binding calmodulin. Neither of the bands could be phosphorylated by the cAMP-dependent protein kinase. Using Limulus light chains as a substrate the Vmax was 15.4 umoles/min/mg and the Km was 15.6 uM. The K_D for calmodulin was determined to be 6nM. The enyzme did not phosphorylate various histones, casein, actin or tropomyosin.

W-Pos157 ISOLATION OF THE NATIVE FORM OF CHICKEN GIZZARD MYOSIN LIGHT CHAIN KINASE. Michael P. Walsh and Philip K. Ngai, Dept. of Medical Biochemistry, University of Calgary, Alberta, Canada.

Phosphorylation of a specific serine residue on each of the two 20,000-dalton light chains of smooth muscle myosin is widely believed to be a prerequisite for contraction. This reaction is catalyzed by Ca^{2+}- and calmodulin-dependent myosin light chain kinase (MLCK). Recently, we separated and purified two forms of gizzard MLCK (Walsh et al (1983) FEBS Letters 153, 156): the well-characterized 130,000-dalton enzyme and a form which, following affinity chromatography on calmodulin-Sepharose, consisted of two polypeptide chains of M_r = 136,000 and 141,000. Using a monoclonal antibody to the isolated 130,000-dalton enzyme we have shown that gizzard contains a single form of MLCK of M_r = 136,000 and that the 130,000-dalton form is derived from this native enzyme by proteolysis during isolation (Adachi et al (1983) Biochem. Biophys. Res. Commun., in press). We have since succeeded in separating and purifying the 136,000-dalton MLCK and the 141,000-dalton polypeptide which previously copurified with it. These two polypeptides are shown to be distinct calmodulin-binding proteins: only the M_r = 136,000 protein exhibits MLCK activity; the two proteins present completely different chymotryptic peptide maps; only the M_r = 136,000 protein reacts with a monoclonal antibody to gizzard MLCK in immunoblotting experiments; and only the M_r = 136,000 protein is phosphorylated by cAMP-dependent protein kinase. The 141,000-dalton protein is identified as caldesmon (originally described by Sobue et al (1981) Proc. Natl. Acad. Sci. (U.S.A.) 78, 5652) on the basis of Ca^{2+}-dependent interaction with calmodulin, Ca^{2+}-independent interaction with actin, competition between calmodulin and actin for binding to this protein only in the presence of Ca^{2+}, subunit M_r and tissue content.

W-Pos158 THE EFFECT OF MYOPATHIC HAMSTER PROTEASE ON GIZZARD AND SCALLOP MYOSINS. S.S. Margossian, A. Malhotra, Montefiore Med. Center., Bronx, N.Y.; P.D. Chantler, Med. Col. Penna., Philadelphia, PA.; J.R. Sellers, NIH, Bethesda, MD.; W.F. Stafford, Boston Biomed. Res. Inst., Boston, MA and H. S. Slayter, Dana-Farber Cancer Inst., Boston, MA.

Turkey gizzard and scallop myosins were incubated with the neutral protease from myopathic hamsters in an effort to digest the regulatory light chains. These regulatory light chains exhibited a remarkable degree of resistance to proteolysis. Essential light chains in molluscan myosin were hydrolyzed to the same degree as the regulatory light chains. The heavy chains on the other hand were readily broken down even at relatively high weight ratios of myosin to protease. Digestion of myosin in the presence of Mg^{++} required a tenfold increase in protease concentration to get a comparable breakdown. These modifications did not appear to influence the physical properties of gizzard myosin which remained monodisperse during sedimentation velocity and equilibrium runs in high salt or ATP-containing low salt buffers; in the latter, the characteristic shape change of smooth muscle myosin was preserved as revealed by electron microscopy. The isolated light chains however, were readily hydrolyzed by the protease indicating that the conformation of the intact myosin makes the light chains inaccessible to the protease. A dramatic increase in ATPase activity of phosphorylated gizzard myosin was observed after protease treatment, whereas that of unphosphorylated myosin was unaffected. In scallop myosin, protease treatment resulted in a decrease in Ca-sensitivity brought about by an increase in the actin-activated ATPase in the absence of Ca^{++} and a decrease in this activity in the presence of Ca^{++}. (Supported by NIH grant HL 26569 to SSM).

W-Pos159 DIAZEPAM-INDUCED CHANGES IN CYTOSKELETAL PROTEINS OF CULTURED CHICK HEART FIBROBLASTS. William G. McNett*§ and Robert R. Kulikowski. Department of Anatomy, Mt. Sinai School of Medicine of the City University of New York, New York, NY 10029 and §College of Medicine, Pennsylvania State University, Hershey, PA 17033.

We studied the role of myosin in the generation and maintenance of cell shape by treating fibroblasts with diazepam (Valium, Roche), a putative specific inhibitor of myosin synthesis and accumulation, and by examining the proteins of the detergent resistant cytoskeleton (DRC). Cells were grown in a diazepam-containing medium and labelled for various times with ^{14}C-leucine. Proteins were examined by SDS-polyacrylamide gradient gels and radioautography. Compared to control cultures (vehicle only), the drug-treated cells were less spread upon the substrate. Removal of diazepam reversed this effect. In both control and experimental cultures a minimum of 12 labelled peptides, ranging in molecular weight from 15,000 to 310,000, with prominent bands at 210,000, 195,000 (MHC), 53,000, 50,000, 45,000, and 18-20,000, were detected in the DRC fraction. In the drug-treated cells, when compared to the controls, i) the bands at 210,000, 190,000, and 50,000 were reduced or missing with respect to the actin band (45,000) which remained constant; ii) the MHC band shifted from 195,000 to 200,000. Compared to the DRC MHC, MHC in the detergent soluble fractions of control and experimental cultures had a molecular weight of 195,000. These results suggest that diazepam either interferes with the normal processing of the precursor to MHC, resulting in a larger peptide, or induces the synthesis and accumulation of a different MHC gene product associated with the cytoskeletons of these cells. (Supported by HL 30517).

W-Pos160 IS THERE A DIRECT ACTION OF 4-AMINOPYRIDINE ON INTESTINAL SMOOTH MUSCLE ?

A. Morales-Aguilera and D. González-Ramírez. División de Farmacología, Unidad de Investigación Biomédica del Noreste, I.M.S.S. Apdo. Postal 020-E, 64720, Monterrey, Nuevo - León, México.

The unsolved question of the existence of a purely myogenic activity in intestinal smooth muscle as well as of its possible mechanism, appears recurrently in the literature. 4-aminopyridine (4-AP), which increases transmitter release at synaptic terminals by blocking K^+ conductance and/or potentiating Ca^{++} inward current, increases mechanical activity on spontaneously active rabbit jejunum segments (EC_{50} = 2 x 10^{-5}M). After blockade of all cholinergic activity by ceiling doses of atropine (10^{-4}M), a remarkably constant contractile activity is uncovered. This atropine-resistant activity remains without change in the presence of Tetrodotoxin (10^{-7}M). The atropine-TTX treated preparations are still responsive to 4-AP (10^{-5}M) in a manner qualitatively similar to the drug-free preparation. 4-AP potency is directly proportional to pCA and Verapamil abolishes all contractile activities. The above described facts could be explained by a myogenic activity of intestinal smooth muscle, which is affected by blockade of K^+ and increase of Ca^{++} currents, or by these same actions of 4-AP on TTX-resistant synaptic terminals releasing phasically an hitherto unidentified transmitter.

W-Pos161 CATIONIC LOCAL ANESTHETICS STIMULATE A MEMBRANE-BOUND PHOSPHATASE IN ACHOLEPLASMA LAIDLAWII. P.V. Burke, R. Kanki, and H. H. Wang, Department of Biology, University of California, Santa Cruz, CA 95064.

The plasma membrane p-nitrophenylphosphatase activity of Acholeplasma laidlawii is stimulated by spin-labeled local anesthetics (2- N-methyl-N-(2,2,6,6,-tetramethyl piperidinooxyl) ethyl p-hexyloxybenzoate) abbreviated as C6SL and its methylated quaternary analog, C6SLMeI. The tertiary amine C6SL (at a concentration of $5x10^{-5}$M) is more potent at pH 6.5 than at pH 7.7. In contrast, the permanently-charged C6SLMeI is equally potent independent of pH. Electron spin resonance studies of C6SL- and C6SLMeI-labeled membranes show that these anesthetics interact electrostatically with components of the Acholeplasma membrane. Such electrostatic interaction between local anesthetics and anionic molecular components of the membrane has been reported previously (See Wang, H.H., Earnest, J., and Limbacher, H.P. 1983 Proc. Natl. Acad. Sci. USA 80:5297). This interaction is pH-dependent and is correlated with the pH-dependency of the anesthetic-induced enzyme stimulation in the Acholeplasma membranes. Further, studies using 5-doxylstearic acid labels and non-spin labeled C6SL at various pH values show that the membrane-fluidizing effect of anesthetics is not correlated with anesthetic-induced stimulation. Our observations are consistent with the hypothesis that electrostatic interactions between local anesthetics and anionic membrane components may lead to functional changes in membrane proteins. (Supported by NIH grant GM-28087).

W-Pos162 A MODEL FOR THE ACTIVATION OF PORCINE PANCREATIC PHOSPHOLIPASE A_2 FOR THE HYDROLYSIS OF DIPALMITOYLPHOSPHATIDYLCHOLINE LIPOSOMES. D. Lichtenberg, M. Menashe and R.L. Biltonen, Dept. of Biochemistry, Univ. of Virginia, Charlottesville, VA 22909 and Dept. of Physiology and Pharmacology, Tel Aviv Univ. School of Medicine, Ramat Aviv, Tel Aviv, Israel 69978.

The hydrolysis of dipalmitoylphosphatidyleholine (DPPC) unilamellar vesicles by bovine pancreatic phospholipase A_2 (PLA_2) has been studied under various conditions of temperature and enzyme and substrate concentrations. In the gel phase, addition of the enzyme to a dispersion of small unilamellar vesicles (SUV) in Ca^{2+}-containing medium results in instantaneous hydrolysis. However, no hydrolysis occurs when large unilamellar vesicles (LUV) are used as substrate. In mixtures of SUV and LUV no hydrolysis is observed, suggesting that LUV binds the enzyme but the E-S complex is inactive. The hydrolysis of SUV and LUV in their phase transition region is characterized by a phase of slow hydrolysis followed by an abrupt increase in the rate of hydrolysis. The latency phase (τ) is minimal near the phase transition temperature (t_m) and depends on the enzyme to substrate ratio. Preincubation of a mixture of enzyme and substrate vesicles of any size at a temperature below t_m followed by dilution into a medium in the transition region results in instantaneous hydrolysis. This hydrolysis is independent of the presence of Ca^{2+} in the preincubation medium. These results suggest the following scheme for the activation of PLA_2: The enzyme binds to the lipid bilayer in a Ca^{2+}-independent step which occurs best in the gel phase. This is followed by activation of the initially formed enzyme-substrate complex which requires Ca^{2+} and occurs only if dynamic structural irregularities exist in the membrane. This situation exists in the gel phase of SUV and in the thermal transition range of vesicles of any size.

W-Pos163 CALORIMETRIC STUDIES OF PROTEIN-PHOSPHOLIPIDS INTERACTION IN THE UBIQUINOL CYTOCHROME C REDUCTASE. Sung-Hee Gwak, Chang-An Yu, and Linda Yu; Department of Biochemistry, Oklahoma State University, Stillwater, Oklahoma, 74078.

Differential scanning calorimetry was used to investigate the interaction between highly purified delipidated ubiquinol-cytochrome c reductase (QCR), ubiquinone and phospholipids under various conditions. The reduced form of intact QCR was found to be more stable toward thermodenaturation than the oxidized form. The T_m for reduced and oxidized reductase were 341 K and 337.3 K respectively. The delipidated QCR, as expected, was less stable toward thermodenaturation than intact QCR. The thermodenaturation temperature of the delipidated QCR was, however, less redox state dependent. Ubiquinone showed little effect on the thermostability of QCR, but phospholipids significantly stabilized the QCR toward thermodenaturation. The intact, delipidated, and delipidated QCR reconstituted with phospholipids, such as dipalmitoyl phosphatidylcholine, dipalmitoyl phosphatidylethanolamine or azolectin showed typical endothermic thermograms. When the concentration of azolectin used for reconstitution was greater than 0.5 mg/mg protein, the reconstituted system showed an unexpected exothermic transition. This exothermic transition was also observed when a phosphatidylcholine containing unsaturated fatty acids was used in the reconstitution. This work was supported by grants from NIH (GM 30721), OAES, and American Heart, Tulsa chapter.

W-Pos164 CALORIMETRIC INVESTIGATION OF CYTOCHROME c OXIDASE-PHOSPHOLIPID INTERACTION: EVIDENCE OF TWO LIPID ENVIRONMENTS, Chang-Hwei Chen and Deborah Guard-Friar, Center for Laboratories and Research, New York State Department of Health, Albany, New York 12201, and Chang-An Yu, Department of Biochemistry, Oklahoma State University, Stillwater, OK 74078.

Highly sensitive differential scanning microcalorimetry was used to investigate the cytochrome c oxidase-phospholipid interaction. In the presence of cytochrome c oxidase, the thermogram of 1,2-dimyristoyl phosphatidylcholine (DMPC) vesicles exhibited a second endothermic peak, which was adjacent to the main lipid phase-transition peak and appeared at a higher temperature. As the concentration of added protein increased, the two endothermic peaks became further separated and the transition temperatures corresponding to both of the endothermic peaks decreased.

These two peaks are interpreted as representing two different environments of lipids: a fluid lipid component (at the lower temperature) and an immobilized lipid component (at the higher temperature). The higher temperature peak is not thermally reversible. Treatment of sample well above the transition temperature leads to changes in the lipid-protein interaction and consequently reduces the magnitude of the higher-temperature peak. These observations support the premise that "boundary lipids" occur in the presence of cytochrome c oxidase.

The possibility of impurities contributing to the higher-temperature peak was discussed and ruled out.

W-Pos165 DESIGN AND SYNTHESIS OF A MEMBRANE-ANCHORING PEPTIDE. Heather K. B. Simmerman, and Frank R. N. Gurd, Department of Chemistry, Indiana University, Bloomington, Indiana 47405.

A synthetic membrane-anchoring peptide has been designed to examine the spontaneous insertion of peptides into lipid bilayer systems. The peptide sequence is based on an analysis of the minimum structural requirements for non-lytic penetration of a lipid bilayer and models the membrane-binding segment of cytochrome b_5. The eicosahexamer NH_2-Gly-Ala-Glu-Ala-Ala-Glu-(Leu-Tyr)$_3$-Leu_{14}-COOH has been synthesized by solid phase techniques using the N^{α}-fluorenylmethoxycarbonyl form of all residues except the NH_2-terminal glycine, which carried the N^{α}-t-butyloxycarbonyl group. Side chains of glutamic acid and tyrosine also bore the t-butyloxycarbonyl group. The stepwise couplings were mediated by dicyclohexylcarbodiimide/1-hydroxybenzotriazole and were monitored by the Kaiser test and amino acid analysis. Cleavage from the p-benzyloxybenzyl ester resin with 55% trifuoroacetic acid in methylene chloride yielded the complete, deprotected peptide in preparation for HPLC purification. This peptide and other closely related variants may be used to evaluate the structural parameters by experimentally assessing the type and extent of interaction of each peptide with various hydrophobic media. (Supported by USPHS NIH Grant HL-14680).

W-Pos166 FUSION OF SONICATED VESICLES AND "PROPER" INSERTION OF CYTOCHROME b_5 Susan F. Greenhut, Steven M. Wietstock and Mark A. Roseman, Department of Biochemistry, Uniformed Services University, 4301 Jones Bridge Road, Bethesda, MD 20814.

When cyt b_5 is added to pre-formed vesicles, it binds in a "loose" or "transferrable" configuration in which the C-terminus of the hydrophobic tail loops back to the same side of the membrane as the catalytic domain. Incorporation by detergent dialysis or co-sonication results in a "tight" or "nontransferrable " configuration in which the tail spans the bilayer. Endogenous cyt b_5 in microsomes is bound in the tight configuration. We have found that one of our earlier preparations of purified cyt b_5 causes fusion of a small fraction of the vesicles to which it is added. This only occurs when the ratio of protein to lipid is low (i.e., 3 cyt b_5/vesicle) and the buffer contains moderate levels of salt (0.05-0.10 M). The large fused vesicles, collected from a Sepharose 2B column, were shown by negative stain EM to be single walled and about 800Å in diameter. Treatment with trypsin showed that the heme fragment was on the outside. Protein bound to the large vesicles was not degraded by carboxypeptidase Y, nor did it spontaneously transfer to small vesicles. From these results we conclude that the protein in the fused vesicles is "properly" inserted in the transmembrane configuration. Cyt b_5-vesicle complexes prepared in low salt (0.01 M) do not fuse. Addition of salt to these complexes causes fusion suggesting that fusion is not intimately linked with initial binding of the purified protein. Subsequent experiments indicate that the fusogenic activity is caused by a contaminating protein. The signficant conclusion is that membrane fusion may be one mechanism for properly inserting proteins into membranes. Support by NIH Grant #G27128 and USUHS Grants #C07117 and #C07138.

W-Pos167 THERMOTROPIC BEHAVIOR AND DYNAMICS OF CHOLERA TOXIN AND CHOLERA TOXIN SUBUNITS BOUND TO PHOSPHOLIPID VESICLES CONTAINING GANGLIOSIDE GM_1. B. Goins and E. Freire, Department of Biochemistry, University of Tennessee, Knoxville, TN 37996-0840

The interactions of Cholera Toxin and their isolated A and B subunits with large unilamellar DPPC vesicles containing ganglioside GM_1 on their outer surface have been investigated using high sensitivity scanning calorimetry, fluorescence and phosphorescence spectroscopy. Previously, we have shown that in the presence of Ca^{2+}, Cholera Toxin has a twofold effect on the thermotropic behavior of the membrane: it induces phase separation and causes a decrease in the enthalpy change (ΔH) of the phospholipid transition. Experiments with isolated Cholera Toxin subunits have allowed us to identify the subunits responsible for these effects. The hydrophobic and bioactive A_1 subunit is responsible for the decrease in ΔH and does not require ganglioside to accomplish this effect. On the other hand, the ganglioside binding subunit (B_5) is able to induce phase separation without causing any change in ΔH. Each Cholera Toxin molecule affects ~100 lipid molecules including the GM_1 molecules to which it is specifically bound. Approximately 35 phospholipids are withdrawn from the transition and 60 phospholipids are sequestered into the phase separated domains. We have also performed rotational mobility studies by measuring the phosphorescence anisotropy decay of erythrosin isothiocyanate labelled toxin. These results indicate that upon binding to its receptor the rotational mobility of Cholera Toxin becomes severely restricted, being characterized by a rotational correlation time of ~1 ms. Excimer formation experiments using pyrene lipid derivatives further indicate that the association of the toxin induces a decrease in the lateral mobility of the phospholipid molecules (Supported by NIH Grant GM-30819.)

W-Pos168 INTERACTION OF BRAIN CLATHRIN WITH INTACT AND MODEL MEMBRANES: AN INFRARED AND RAMAN SPECTROSCOPIC STUDY. J. S. Vincent,[a] C. J. Steer,[b] R. Blumenthal[b] and I. W. Levin,[a] [a]Laboratory of Chemical Physics, NIADDK, and [b]Laboratory of Theoretical Biology, NCI, National Institutes of Health, Bethesda, MD 20205.

Clathrin, the major structural protein associated with both coated pits and coated vesicles, has been implicated in the dynamics of various endocytic processes. In an attempt to define the mechanisms involved in the transition from uncoated membranes to clathrin coated pits and then to coated vesicles, we investigated by vibrational spectroscopy the lipid perturbations arising from the interactions of clathrin with bilayers of both intact and model membrane assemblies. A comparison of the infrared spectral frequencies for the lipid acyl chain symmetric CH_2 stretching modes at $\sim$2850 cm^{-1} for intact clathrin coated vesicles, uncoated vesicles and synaptic membranes (at $\sim$21°C) indicate that clathrin significantly increases the number of gauche chain conformers in the bilayer matrix of the coated vesicle system. The increase in disorder for the observed 0.5 cm^{-1} shift is equivalent to approximately the disorder incurred in heating liquid crystalline DMPC multilayers by $\sim$10°C. Temperature profiles for unilamellar DPPC vesicles interacting with clathrin at lipid:protein mole ratios ranging from 2700:1 to 1000:1 were determined by Raman spectroscopy. Depressions in T_m from 1 to 8°C suggest significant hydrophobic interactions of clathrin with the bilayer acyl chains in the model system. In conclusion, the bilayer disorder induced by these clathrin interactions in both model and real membranes may represent a critical factor involved in the evolution of vesicular structures from planar membranes.

W-Pos169 THERMOTROPIC AND DYNAMIC CHARACTERIZATION OF INTERACTIONS OF ACYLATED α-BUNGAROTOXIN WITH PHOSPHOLIPID BILAYER MEMBRANES. B. Babbitt, L. Huang and E. Freire, Department of Biochemistry, University of Tennessee, Knoxville, TN 37996-0840.

The incorporation of palmitoyl-α-bungarotoxin (acylated 8000 dalton snake toxin polypeptide, PBGT) into large unilamellar dipalmitoyl phosphatidylcholine (DPPC) vesicles causes a decrease in the phospholipid phase transition temperature (T_m), a broadening of the heat capacity function, and a decrease in the enthalpy change (ΔH) associated with the phospholipid gel-liquid crystalline transition. Analysis of the dependence of ΔH on the PBGT:DPPC molar ratio indicates that each PBGT molecule prevents six phospholipid molecules from participating in the phase transition. The local nature of the perturbation suggests that the protein molecule interacts with the bilayer solely through the covalently attached fatty acid chain. Steady state depolarization measurements indicate that the association of PBGT with the bilayer has a disordering effect below T_m and an ordering effect above T_m. Rotational mobility measurements employing the time-dependent decay of delayed fluorescence and phosphorescence anisotropy of erythrosin labelled PBGT indicate that the protein is highly mobile above the lipid phase transition temperature and only slightly restricted below T_m. Additional lateral diffusion measurements using fluorescence photobleaching recovery indicate that the lateral mobility of PBGT is strongly dependent on the physical state of the bilayer. These studies provide useful information concerning the role of fatty acids in determining the properties and interactions of acylated membrane proteins. (Supported by NIH Grants GM-31724 and GM-30819.)

W-Pos170 LIPOSOME MEDIATED IMMUNOASSAY FOR SMALL HAPTENS INDEPENDENT OF COMPLEMENT.

J. William Freytag and William J. Litchfield. Clinical and Instrument Systems Division, E. I. du Pont de Nemours & Co., Inc., Glasgow Research Laboratory, Wilmington, DE 19898.

A lipid vesicle mediated immunoassay for small haptens such as digoxin is described. Using a detergent removal procedure for vesicle formation, a water-soluble marker enzyme like alkaline phosphatase is stably entrapped within 1500-2000 Å unilamellar lipid vesicles composed of egg yolk lecithin and cholesterol. Specific lysis of the lipid vesicles is achieved upon addition of a covalently synthesized hapten-melittin conjugate. Inhibition or modulation of this lysis by the hapten-melittin conjugate can then be achieved by adding stoichiometric amounts of high affinity antibody. Finally, the antibody inhibition of hapten-melittin lysis can be modulated by the addition of competing amounts of free hapten. This assay approach is simple, fast, highly sensitive, and versatile such that it can be carried out in either a homogeneous or heterogeneous mode. Furthermore, unlike all other liposome mediated immunoassays, complement is not required for lysis.

W-Pos171 DETERGENT EXCHANGE OF MEMBRANE PROTEINS USING PHENYL SEPHAROSE. Neal C. Robinson and Diane Wiginton, Department of Biochemistry, The University of Texas Health Science Center, San Antonio, TX 78284.

Intrinsic membrane proteins are often solubilized in 0.5-2.0% Triton X-100 (TX), Triton N-101 (TN), or Nonidet P-40 (NP-40); however, these detergents, especially at high concentrations, often interfere with subsequent experiments, e.g., measurement of enzymatic activity, reconstitution of proteins into lipid vesicles, or high resolution SDS-PAGE. A method has been developed using Phenyl Sepharose to exchange one of several alkyl detergents, e.g., lauryl maltoside (LM), octyl glucoside (OG) or SDS for any of these solubilizing detergents. The method involves: 1) Saturating a 1-2 ml Phenyl Sepharose column with one of the alkyl detergents at pH 9, I = 0.02; 2) Applying a 0.5-1 ml solution of a TX, TN or NP-40 solubilized membrane protein containing as much as 20 mg/ml of detergent; and 3) Elution of the protein with buffer containing the alkyl detergent. The solubilizing detergent displaces the alkyl detergent from the column, leaving the protein in the alkyl detergent. Since the method involves conditions in which the protein does not bind to the matrix, protein recovery is maximized. By this approach, >99% of the solubilizing detergent was usually removed from solutions with a 85-90% recovery of protein. Examples of membrane protein solutions that have been used with this method are: cytochrome c oxidase, a total mixture of erythrocyte membrane proteins; and total inner mitochondrial membrane proteins. Supported by NIH Grant GM 24795 and Welch Foundation Grant AQ 907.

W-Pos172 STRUCTURAL TRANSFORMATION OF SPHINGOMYELIN VESICLES INDUCED BY APOLIPOPROTEIN C-III. Tareq Ahmad, John R. Guyton, James T. Sparrow, Antonio M. Gotto, Jr., and J.D. Morrisett. Baylor College of Medicine, The Methodist Hospital, Houston, Texas 77030

ApoC-III, unlike other human plasma apolipoproteins, has been shown to enhance the catalytic activity of sphingomyelinase (SMase) toward sphingomyelin bilayers. This might occur either by apoC-III induced alteration of 1) the enzyme, 2) the substrate, or both. To test hypothesis 2), the interaction of apoC-III with egg yolk SM single bilayer vesicles was studied. Vesicles prepared by probe sonication have a sharp DSC transition of 40^0 and a mean diameter of ~600Å as determined by gel filtration (GF) and electron microscopy (EM). Incubation of apoC-III with vesicles at 40^0 for 1 hr produces a rather homogeneous population of complexes whose composition, size, and hydrated density depend on the initial protein:lipid ratio (P/L). Mixtures with increasing initial P/L produce complexes of decreasing size, increasing density, and increasing final P/L until initial P/L = 1:100 beyond which protein is in apparent excess as indicated by GF and density gradient centrifugation. The complex formed at this ratio had MW ≃ 200,000, d = 1.085, and P/L = 1:110. Sedimentation velocity experiments indicate S_{obs} drops sigmoidally from 14.0 to 7.0; EM indicates the formation of discoidal complexes with dimensions 52 x 204 Å . These data suggest that apoC-III binds to SM vesicles, causing their collapse to smaller complexes which are better substrates for SMase. (Supported by HL-27341 (P-5) and Welch Fdn. Q-837).

W-Pos173 FACTORS CONTROLLING THE EXCHANGE RATE AND DISTRIBUTION OF CHOLESTEROL IN MEMBRANES, Philip L. Yeagle, Biochemistry Dept., SUNY/Buffalo School of Medicine, Buffalo, NY 14214.

The rate of transfer of cholesterol between phospholipid vesicles of different composition and size has been measured and the final equilibrium distribution of cholesterol has been determined. Small sonicated unilamellar vesicles and large unilamellar vesicles have been incubated at a defined temperature, and aliquots separated at selected times by differential centrifugation and analyzed. These data indicate that there is a larger barrier to leaving the vesicle surface when the large vesicle is the donar than when the small vesicle is the donar. These data also indicate that there is a strong preference of cholesterol for phosphatidylcholine over phosphatidylethanolamine at equilibrium. In contrast there is no indication of a preference of cholesterol for sphingomyelin over phosphatidylcholine at equilibrium when both membranes are in the liquid crystalline state. Inclusion of a small amount of phosphatidylserine in the membrane does not affect the distribution of cholesterol. The role of integral membrane proteins from the human erythrocyte membrane in controlling the distribution of cholesterol was also investigated using recombined membranes of purified band 3 . Band 3 reduced the incorporation of cholesterol into the vesicle containing the protein at equilibrium. These results suggest a model for the intracellular distribution of cholesterol in mammalian cells. This work was supported by a grant from NSF (PCM8207623).

W-Pos174 PROTEOLYTIC DEGRADATION OF D-β-HYDROXYBUTYRATE DEHYDROGENASE (BDH). Andreas Maurer, J. Oliver McIntyre and Sidney Fleischer. Dept. of Molecular Biology, Vanderbilt University, Nashville, TN 37235.

BDH is a lipid-requiring enzyme which has an absolute requirement for lecithin for function. The enzyme, purified from bovine heart mitochondria, is devoid of lipid (apo-BDH) and has no activity but can be reactivated with phospholipids. Apo-BDH can be inserted unidirectionally into mitochondrial phospholipid (MPL) vesicles and as such exhibits characteristics similar to the native membrane-bound enzyme. Apo-BDH is susceptible to proteolytic digestion with different proteases. Endopeptidases (trypsin, chymotrypsin, staphylococcus aureaus protease) and exopeptidases (carboxypeptidases A, B and Y) degrade apo-BDH as monitored by both enzymic activity and polyacrylamide-gel electrophoresis (PAGE) in sodium dodecyl sulfate (SDS). However, BDH after insertion into MPL, is not inactivated by trypsin or the carboxypeptidases and still exhibits a single band at 32 kdalton comparable to untreated BDH, as judged by SDS-PAGE with silver staining. Pronase digests and inactivates BDH both in the absence of MPL and as the BDH-MPL complex. Chymotrypsin digestion of BDH in MPL gives rise to a 26 kdalton fragment, but retains enzymic activity. We conclude that: 1) BDH, when inserted into the phospholipid bilayer, is less accessible to proteases, i.e., the phospholipids provide protection against proteolytic degradation; 2) the C-terminal end of apo-BDH is accessible to proteases; and 3) the enzyme in the membrane can be cleaved without loss of activity. [Supported in part by NIH AM 14632]

W-Pos175 AN ELECTRIC BIREFRINGENCE STUDY OF PHOSPHOLIPID VESICLES.
Leo D. Kahn and Shu-I Tu. Eastern Regional Research Center, USDA, ARS, Philadelphia, PA 19118.

Synthetic vesicles of phosphatidyl choline display electric birefringence (EB) when a second phospholipid bearing excess electric charge (in this work either phosphatidic acid (PA) or phosphatidyl serine (PS)) is incorporated in them. In either case no permanent dipole moment is present at acid pH. Curves of EB versus concentration of either PA or PS pass through a maximum and thus suggest that the positioning of PA or PS during self-assembly of the vesicle is at first a random process, but later takes on order, probably because of buildup of electric charge. The maximum for PS occurs at a higher concentration than for PA, and thus shows a greater tendency for PS to enter the inner surface of the vesicle. Decay curves plotted on a semi-logarithmic scale show that vesicles incorporating PS are more uniform than those incorporating PA. Monovalent ions have no effect on the EB of vesicles, but divalent cations diminish it, with Ca^{2+} having a greater effect than Mg^{2+}. Once Ca^{2+} is bound to a vesicle it cannot be removed with EDTA. The binding of divalent cations to a vesicle creates a permanent dipole moment of opposite polarity to the already present induced dipole moment. This indicates that one cationic charge binds to the vesicle and the other is free to contribute to a permanent dipole. The pH dependence of EB passes through a maximum at pH 6.75. As the pH increases, deprotonation of the vesicle builds up the induced dipole; beyond the maximum it starts to create a permanent dipole moment.

W-Pos176 MODIFIED PERRIN EQUATION FOR FLUORESCENCE POLARIZATION FROM MEMBRANE PROBES
Wieb Van der Meer, Lab.for Physiology, P.O.Box 9604, NL-2300 RC Leiden, The Netherlands

The average rotational diffusion coefficient D of a fluorescent probe embedded in a membrane, where a steady-state fluorescence anisotropy r_s has been measured, is higher than that of the same probe in an isotropic fluid with the same r_s, because the r_s of the membrane contains an infinite time anisotropy r_∞. A modified Perrin equation takes this into account:

$$6D\tau = r_o/r_s - 1 + m$$

where τ is the fluorescence lifetime, r_o is the maximal anisotropy value and m expresses the difference between membranes and isotropic fluids. In a first approximation m is a constant for every probe. Assuming a single exponential for the fluorescence and a single exponential plus r_∞ for the anisotropy after δ-excitation, one obtains:

$$r_\infty = r_o r_s^2/(r_o r_s + m^{-1}(r_o - r_s)^2)$$

For diphenylhexatriene in the membranes quoted by Pottel *et.al.* (Biochim.Biophys.Acta.730(1983)181) 90% of the r_s, r_∞-data has $.1<1/m<2$. and the best fit yields $1/m = .65$. The corresponding relation reproduces that found by Van Blitterswijk *et.al.* (Biochim.Biophys.Acta.644(1981)323), which was confirmed by Pottel *et.al.* The r_s, r_∞-data of Kutchai *et.al.* (Biophys.J.41(1983)345a) for 5 anthroyloxy fatty acids 2AS, 7AS, 9AS, 12AS and 16AP in 4 different lecithins containing various amounts of cholesterol are very well described by the relation with $1/m = .60$; 90% of the data has $.3<1/m<1$.

W-Pos177 A FREEZE-FRACTURE STUDY OF THE SQUID AXON MEMBRANE. Donald C. Chang, Dept. Physiol., Baylor Coll. Med., Houston, TX 77030; Ichiji Tasaki and Tom S. Reese, NIH, Bethesda, MD 20205.

A classical preparation of excitable membrane is the membrane of the squid giant axon. The morphology of this membrane, however, is not well understood. We report here the first freeze-fracture study of this axon membrane. Our objective is to identify the membrane protein structures which are thought to be conductance pathways (i.e., "channels") for the ions.

We have examined axons after three different treatments: (1) Schwann cell layers left intact, (2) Schwann cells removed (by a microsurgical technique developed by Tasaki), and (3) Schwann cells detached (by trypsin) but not mechanically removed. When the Schwann cells were removed, the axolemma was easily recognized at the boundary between the external ice and the axoplasm. However, very little membrane was seen in these studies because the axolemma was usually cross-fractured without splitting it over any significant distance. The best results were obtained using axons with Schwann cells chemically detached from the axon but not mechanically removed. In several of these axons the fracture plane cut through a stack of Schwann cells and then exposed a large extent of axolemma, where both E-face and P-face of the membrane were clearly seen. Fracture faces through the axon membrane, unlike those through the membrane of Schwann cells, are marked by many small, P-face particles. In addition, there are large P-face particles distributed both randomly and in aggregates. Judging from their size (between 10 and 18 nm) and density ($\sim$ 1000 particles per μm^2), certain of these large P-face particles are likely candidates for the intramembrane component of the "sodium channels." (Work supported partially by an ONR contract).

W-Pos178 ROLE OF Mg^{+2} IN THE STRUCTURE AND FUNCTION OF GASTRIC MICROSOMES. Jyotirmoy Nandi, Robert Kozol and Tushar K. Ray, Department of Surgery, Upstate Medical Center, Syracuse, N.Y. 13210.

The present study was undertaken to explore the role of Mg^{+2} in gastric H^+, K^+-ATPase activity and associated intravesicular H^+ transport using gradient purified dog gastric microsomal vesicles. The vesicles have the ATP hydrolytic sites facing the bulk medium and the K^+ effector sites facing the vesicle interior. Since the vesicles are tightly sealed to K^+ permeation, valinomycin (K^+ ionophore) is needed for full expression of the H^+, K^+-ATPase activity and continued H^+ transport. As expected, the K^+-preloaded vesicles show a transient acidification of the vesicle interior in absence of valinomycin (val). When the val-stimulated ATPase and ATP-induced vesicular H^+ transport was studied as a function of free Mg^{+2} concentration using Mg^{+2}-CDTA buffer, a parallel relationship was found to exist. However, unlike the ATP-induced H^+ uptake, the val-dependent uptake of H^+ could not be demonstrated at very low ($1x10^{-6}$M) Mg^{+2} concentration. The data demonstrate a val-induced leakage of H^+ at 1 uM Mg^{+2} and the process could be reversed showing a net uptake of H^+ by increasing the Mg^{+2} to 25 uM. Studies with aminonapthol sulfonate (ANS) which gives fluorescence with gastric microsomes also indicate a cation dependent structural alteration as evidenced from the changes in fluorescence signal. Thus, 2-5 uM Mg^{+2} demonstrated a potentiation of the val-K^+ induced fluorescence enhancement of ANS with gastric microsomes. The data suggest a critical role of Mg^{+2} in the structure-function relationship of gastric microsomes.

W-Pos179 ASYMMETRY OF THE SARCOPLASMIC RETICULUM MEMBRANE. R.J.Bick, W.B.Van Winkle, C.A.Tate, L. Herbette [1], S. Fleischer [2] and M.L. Entman. Baylor College of Medicine and The Methodist Hospital, Houston, TX 77030, [1]University of Connecticut Health Center, Farmington, CT 06032 and [2] Dept. of Molecular Biology, Vanderbilt University, Nashville, TN.

We have employed two methods, neutron diffraction and digestion by phospholipase A_2, to examine the skeletal muscle sarcoplasmic reticulum (SR) membrane phospholipid distribution. Values obtained were essentially the same by each method and showed a small, but significant lipid asymmetry apparent within the SR membrane. A total phospholipid distribution of 46/54 $\pm$ 2% for the outer/inner monolayer of the SR bilayer was obtained. Distribution of the different phospholipid species was also asymmetric. Electron microscopy and x-ray diffraction/neutron diffraction have shown that the calcium pump protein ia asymmetrically distributed within the SR membrane consistent with this phospholipid asymmetry. This complimentary asymmetry of the protein and lipid components within the SR membrane bilayer preserves the total average cross-sectional area for the SR membrane, and is thought to be related to the vectorial properties of the calcium pump.

Supported by grants HL 22856, HL 13870 and HL 27630.

W-Pos180 HYPERTHERMIA INDUCES PROTEIN TRANSLOCATION FROM CYTOSOL TO OUTER MEMBRANE IN *E. COLI*. Milton B. Yatvin, Kendyle Smith and Frank L. Siegel. Departments of Human Oncology, Pediatrics and Physiological Chemistry, University of Wisconsin Medical School, Madison, Wisconsin 53706.

In a study of the effects of hyperthermia on synthesis and distribution of protein in *E. coli*, cells were grown to mid-log phase at 37°C and incubated for varying periods of time at either 37°C or 48°C in the presence of [^{35}S]-L-methionine. Cells were disrupted and fractionated to yield cytoplasmic, inner and outer membrane fractions. The protein content and specific radioactivity of each fraction was determined and proteins of each fraction were resolved by SDS-PAGE. Gels were stained with Coomassie Blue and autoradiography was used to detect radioactivity.

There was little difference in protein staining patterns of cytosolic or inner membrane fractions from cells exposed to 37° or 48°C for 5 min or 1 h. In contrast, there were marked time-dependent increases in the amounts of specific outer membrane proteins in cells incubated at 48°C. There were striking differences in the distribution of newly synthesized (radioactive) proteins between cytosolic and outer membrane fractions. Most newly synthesized cytoplasmic proteins were translocated to the outer membrane when cells were incubated at 48°C for either 5 min or 1 h. Three major radioactive cytoplasmic proteins were not translocated. The amounts of newly synthesized proteins in the inner membrane fraction clearly decreased following hyperthermia; this, too, was a time-dependent phenomenon. In a pulse chase experiment, it was shown that proteins synthesized at 37°C were not translocated during subsequent hyperthermia, whereas hyperthermia during amino acid incorporation did result in translocation. (Supported by NIH Grants CA 24872 and NS 11652).

W-Pos181 ARE NITROXIDE FATTY-ACID LABELS LOCATED PRIMARILY IN THE PLASMA MEMBRANE OF EUKARYOTIC CELLS? Morse, Philip D., and Swartz, Harold M. University of Illinois College of Medicine at Urbana-Champaign, Urbana, IL 61801.

Spin label studies of membranes of eukaryotic cells generally make the assumption that the spin labels are located in the plasma membrane of these cells. The experimental evidence for this assumption includes: 1) membrane-impermeable potassium ferricyanide rapidly reoxidizes membrane spin labels (1) and 2) nickel ions, which is also supposedly membrane-impermeable, broadens much of the membrane spin label signal (2).

There are, however, data at variance with the above interpretation. These include: 1) experiments using large unilamellar phospholipid liposomes (90% DPPC-10% DPPG) which show that nickel ions passes relatively quickly through liposomal membranes and that membrane spin label broadening by nickel ions is concentration dependent; 2) data showing that concentrations of 50-100 mM potassium ferricyanide, potassium tris(oxalato)chromiate, Ni-EDTA, or Ni-Tris do not broaden membrane associated spin label signals, and 3) that isolated plasma membranes do not reduce spin labels, while mitochondria do.

An alternative explanation that fits all the above data is that membrane spin labels are in very rapid equilibrium with all of the cellular membrane components.

(1) Kaplan, J., Canonico, P.G., and Caspary, W. J. PNAS USA 70, 66, 1973.

(2) Curtain, C.C., and Gordon, C.M. in Receptor Biochemistry and Methodology, Venter, J.C., and Harrison, L., eds. Alan R. Liss, 1983.

Supported by the National Foundation for Cancer Research, Washington, D.C.

W-Pos182 RESONANCE RAMAN STUDIES OF CYANIDE BINDING TO STERICALLY HINDERED "STRAPPED HEMES". T. Tanaka, Nai-Teng Yu and C. K. Chang* (Intr. by P. Fong), School of Chemistry, Georgia Inst. of Tech. Atlanta, GA 30332; *Department of Chemistry, Michigan State University, East Lansing, MI 48824.

Soret-excited resonance Raman spectroscopy has been employed to investigate the nature of bonding interactions between Fe(III) and cyanide in heme model complexes with and without steric hindrance. The steric hindrance is provided by a hydrocarbon chain strapped across one face of the heme. We have detected the Fe(III)-CN^- stretching vibration in Fe(III)(heme-5)(N-MeIm)(CN^-)(in benzene) at 453 cm^{-1}, which is 42 cm^{-1} lower than the Fe(II)-CO stretching frequency at 495 cm^{-1} in Fe(II)(heme-5)(N-MeIm)(CO)[1]. Thus the Fe(III)-CN^- bond is weaker than the Fe(II)-CO bond, consistent with the x-ray structural data of Fe(III)(TPP)(Py)(CN^-)[2] and Fe(II)(TPP)(Py)(CO)[3], which reveal that the Fe(III)-CN^- bond distance (1.908 Å) is longer than the Fe(II)-CO bond (1.77 Å).

Previously, it was found[1] that an increase in steric hindrance (by decreasing the chain length) causes an increase in the Fe(II)-CO stretching frequency. In contrast, we found that the Fe(III)-CN^- stretching frequency decreases with increasing steric hindrance: heme-5 (unstrapped), 453 cm^{-1}; Fe(III)SP-15, 447 cm^{-1}; Fe(III)SP-14, 447 cm^{-1}; and Fe(III)SP-13, 445 cm^{-1}. The origin of this different behavior between cyanide and carbonmonoxy complexes will be discussed.

1. N.-T. Yu, E. A. Kerr, B. Ward and C. K. Chang (1983) Biochemistry 22, 4534.
2. W. R. Scheidt, Y. J. Lee, W. Luangdilok, K. J. Haller, K. Anzai and K. Hatano (1983) Inorg. Chem. 22, 1516. 3. S. Peng and J. A. Ibers (1976) J. Am. Chem. Soc. 98, 8032.

W-Pos183 THE TEMPERATURE DEPENDENCE OF LIGAND PHOTOLYSIS AND RECOMBINATION IN HEMOGLOBINS AT CRYOGENIC TEMPERATURES." M. R. Ondrias, Department of Chemistry, University of New Mexico; T. W. Scott and J. M. Friedman, Bell Laboratories, Murray Hill, NJ 07974.

The binding and release of small molecular weight ligands by heme proteins is a complex process, governed ultimately by the overall energetics of a number of constituent steps. Obviously, heme--ligand interactions are a major influence on ligand binding. However, evidence strongly sugguests that heme-protein and protein-ligand interactions play specific and important roles in this fundamental biological process. We present the results of a study that is the first to employ low-temperature, transient resonance Raman spectroscopy for the elucidation of geminate recombination kinetics. Spectra were generated with the 20 Hz output of an excimer pumped dye laser which produced ~1 mJ pulses at ~435 nm of ~10 ns duration. Single pulses were used to both photolyze the sample and generate the resonance Raman spectrum. The relative populations of liganded and transient deoxy hemoglobin species were determined by monitoring a heme vibrational mode sensitive to ligation (ν_4). The temperature dependencies of heme-ligand recombination were found to be CO>O_2>NO indicating a larger barrier to recombination for CO at cryogenic as well as physiological temperatures. Hb Zurich, which lacks a distal histidine in its α-chains was found to exhibit a lower barrier to CO-heme recombination than HbA. At temperatures below 100K a marked temperature dependence in CO but not O_2 or NO photolysis quantum yield was observed. This suggests that the nature of low energy nonradiative decay pathways, is ligand specific. The interpretation of these results in the context of dynamic heme-ligand and protein-ligand interactions will be discussed.

W-Pos184 A RESONANCE RAMAN STUDY OF AMBYSTOMA TIGRINUM HEMOGLOBINS: EVIDENCE FOR INTRASPECIES HEMEPOCKET VARIATIONS, S. D. Carson and M. R. Ondrias, Department of Chemistry; S. C. Wood, Department of Physiology, University of New Mexico, Albuquerque, NM 87131; and J. A. Shelnutt, Sandia National Laboratories, Albuquerque, NM 87185.

Resonance Raman spectroscopy is a most useful tool for the elucidation of structural differences at the heme in hemoglobins. The use of Raman difference spectrsocopy to compare the local heme environments in hemoglobins which exhibit variations in ligand affinity as a result of species differentiation, chemical alteration or genetic mutation has been particularly successful. We present here the results of a Raman difference comparison of the vibrational modes of hemoglobins from adult, neotenic and larval forms of the salamander Ambystoma tigrinum to each other and to human hemoglobin. This species is of interest because it has a high (40 mm Hg) P_{50}, the O_2 pressure at which half the O_2 binding sites are saturated, coupled with a negative Bohr effect ($\Delta \log P_{50}/\Delta pH$ = -0.08 vs. ≈0.5 for humans). Since P_{50} is one measure of the oxygen binding affinity in hemoglobins, it was felt that these unique physiological properties might be correlated with differences in the heme Raman vibrational spectra. Results indicate the local heme environments of the adult and neotenic proteins were identical and differed from that of the larval protein. Differences were observed in modes sensitive to phorphyrin π electron density and axial ligation. Systematic differences were also observed between human and adult salamander hemoglobins, particularly in modes sensitive to the heme vinyl environment. The relationship between these environmental differences, O_2 binding affinity and the effects of allosteric modulators are discussed.

W-Pos185 METASTABLE FORMS OF MYOGLOBIN EXAMINED BY RESONANCE RAMAN SCATTERING.
P. V. Argade, T. W. Scott, J. M. Friedman and D. L. Rousseau, AT&T Bell Laboratories, Murray Hill, NJ 07974

To understand the molecular basis governing the binding and release of ligands from heme proteins, it is necessary to examine the intermediate forms in the binding pathway. Such intermediates may be prepared by photodissociation of the liganded protein and then examined by transient spectroscopy or by steady state spectroscopy at cryogenic temperatures. We have generated metastable intermediates of myoglobin (Mb*) by photodissociating carbon monoxide and studied them by transient and cryogenic resonance Raman spectroscopy. The results of the two techniques are in agreement and show that there are no significant differences between the chemical deoxy preparation and Mb*. In contrast, such experiments on hemoglobin reveal differences in the iron-histidine vibrational mode as well as in modes of the porphyrin macrocycle. Furthermore, no differences were detected between experiments carried out at $2^{o}K$ and those done at $20^{o}K$. We conclude that photodissociation generates a deoxy heme that is indistinguishable from the chemical deoxy heme; that the protein environment of the liganded myoglobin exerts no strain on the metastable five-coordinate heme; and that any possible binding of the photodissociated CO to the heme does not influence the molecular or electronic structure of the heme.

W-Pos186 RESONANCE RAMAN SPECTRA OF REDUCED CYTOCHROME OXIDASE. Y. Ching,
P. V. Argade, and D. L. Rousseau, AT&T Bell Laboratories, Murray Hill, NJ 07974
The resonance Raman spectra of reduced cytochrome oxidase with Soret excitation have been compared to those of the reduced enzyme in the presence of CO and CN^{-}. Upon binding exogenous ligands, the line in the fully reduced enzyme at 214 cm^{-1} disappeared, consistent with its assignment as the iron-histidine stretching mode. Two modes observed at 520 and 586 cm^{-1} in CO-bound cytochrome oxidase were found to shift down by 4 and 15 cm^{-1} respectively on ^{13}CO isotopic substitution. By analogy to similar behavior in myoglobin, hemoglobin, and model compounds, we assign these lines as the Fe-CO stretching mode (520 cm^{-1}) and the Fe-C-O bending mode (586 cm^{-1}). The intensity of the bending mode is greater than 50% of that of the stretching mode, a higher ratio than heretofore detected in hemes. These results indicate that the Fe-C-O grouping is tilted with respect to the heme plane. Furthermore, the frequencies suggest that either the proximal histidine of the a_3 heme is severly strained or the back donation from the porphyrin macrocycle differs significantly from that of other hemes. The carbonyl frequency of the formyl group of reduced heme a_3 is at 1665 cm^{-1}. This frequency is unaffected by CO binding to the heme, but shifts significantly upon CN^{-} binding. The other porphyrin modes are very similar when these ligands are bound. Since the carbonyl frequency of the formyl group is unaffected by CO binding, the electronic structure and the conformation are insensitive to six-coordination. Thus, the change found with CN^{-} binding indicates that the charged CN^{-} group either directly or indirectly influences the protein environment on the heme periphery.

W-Pos187 EVIDENCE FOR DISTRIBUTED COOPERATIVE ENERGY IN HEMOGLOBIN. D. L. Rousseau, AT&T Bell Laboratories, Murray Hill, NJ 07974 and M. R. Ondrias, Department of Chemistry, University of New Mexico, Albuquerque, NM, 87131

The molecular mechanism for the control of oxygen binding in hemoglobin has been a topic of extensive study and much controversy. A major problem has centered on determining whether the free energy of cooperativity is localized at the heme or distributed over many bonds in the protein. To date, support for the distributed energy model has relied on the absence of clear cut evidence for localized interactions. We report cryogenic spectra of photodissociated hemoglobins (Hb*) stabilized in both the R and the T states. We find substantial differences between the photodissociated intermediates and the corresponding chemical deoxy forms. Such differences are not detected in equivalent experiments on myoglobin. The implications of these results on the localized and the distributed energy models for hemoglobin cooperativity are considered. It is concluded that the differences that have been found are positive evidence for a contribution to cooperativity from sources that are not localized at the heme and are, thus, the first confirmation of the distributed energy model put forward several years ago by Shulman and Hopfield.

W-Pos188 ARE SPIN-STATE AND QUATERNARY STRUCTURE LINKED FOR HUMAN METHEMOGLOBINS? John S. Philo, Ulrich Dreyer, and Todd M. Schuster, Biochemistry and Biophysics, The University of Connecticut, Storrs, CT 06268.

We have investigated by direct magnetic susceptibility measurements the effects of changes in quaternary structure on the spin states of mixed-spin human methemoglobins. Equilibrium studies of the changes in magnetism when IHP is used to switch the quaternary structure from R to T reveal that this change has only a very small effect on the high-spin $\rightleftharpoons$ low-spin equilibrium ($\lesssim$ 200 cal/mol). This is a much smaller effect than that predicted by the Perutz stereochemical model, and is much smaller than the effects in carp methemoglobins as measured by both Noble et al. (Eur. J. Biochem. 133, 475 (1983) and ourselves.

A second approach to the same problem (and one which avoids the use of IHP) is to monitor the changes in spin-state of the ferric subunits in valence hybrids when the quaternary structure is switched by removing ligand from the ferrous subunits. We will report preliminary results of time-resolved magnetic studies of flash photolysis of carbonmonoxy valence hybrids. (Supported by NSF PCM 8111320 and 8211437 and NIH HL-24644. U. Dreyer has been supported by an E.M.B.O. long-term postdoctoral fellowship.)

W-Pos189 **CONFORMATIONAL HETEROGENEITY OF HUMAN HEMOGLOBIN REVEALED BY FLUORESCENCE DECAY STUDIES OF THE TRYPTOPHAN RESIDUES.** **A. G. Szabo, M. Zuker, D. T. Krajcarski and B. Alpert (Intr. by L. Brand), National Research Council of Canada, Division of Biological Sciences, Ottawa Canada, K1A 0R6; and Universite Paris VII, Paris France.**

Using time correlated single photon counting detection and a sync-pumped dye laser excitation source the fluorescenc e decay of the tryptophan residues in four hemoglobin derivatives, HbO_2, Hb(deoxy), HbCO, and Hb(Met) was measured. The tryptophan fluorescence obeyed triple exponential decay kinetics in each derivative. Two of the decay times were similar in each derivative having values of 60-90 ps, and 1.75-1.95 ns. The third long lifetime component had a value between 4.9 - 5.5 ns. Most importantly the fractional fluorescence contribution of each component was different for each hemoglobin derivative. Our rationalization of the results suggests that there are at least three average conformations in each hemoglobin derivative and the relative proportions of each conformer depends on the nature of the heme ligand.

W-Pos190 KINETICS OF INITIAL AND TERMINAL PHASES OF LIGATION IN HEMOGLOBIN. Lawrence J. Parkhurst, Wang Guang-Xin, and Thomas M. Zamis, Dept. of Chemistry, University of Nebraska, Lincoln, NE 68588-0304.

The initial phases of CO binding to Hb have been studied in double-mixing and rapid quenching exeriments where the ligated intermediates have been trapped either at low temperature or by rapid solid-phase methods. In either case, the object was to determine the distribution of CO molecules among the alpha and beta heme sites for early stages of ligation in both human and beef hemoglobins to see if this distribution and the well-known lag phase in CO association kinetics could be reconciled with various models for ligation. Initial binding of CO is predominantly to the alpha chains in Hb. A two-state heterogeneous model is not adequate to accommodate the results, but a three state ($T \rightarrow T' \rightarrow R$) model that allows alpha-beta heterogeneity gives excellent agreement with absorbance change kinetics and CO population analyses. This model appears inadequate, however, for the later phases of ligation. We have carried out oxygen equilibrium measurements on very concentrated solutions of valency hybrids to obtain precise values for the Adair constants for a dimer. Laser photolysis measurements allowed us to obtain the dimer allosteric parameters. For either hybrid, the distribution of rapid (R) and slow (T) phases of CO binding measured by stopped-flow is in marked disagreement, however, with a two-state allosteric model for the final two steps of ligation.

Grant Support: NIH HL 15,284, NSF PCM 8003655, and Research Council, U. of Nebraska.

W-Pos191 STRUCTURES OF GEMINATE STATES OF MYOGLOBIN AND HEMOGLOBIN. Chance, B., Korszun, R., Kumar, C., Zhou, Y., Inst. Struc. & Func. Studies, Univ. City Science Ctr., Phila., PA 19104 and Dept. Biochem/Biophys, Univ. of Penna., Phila., PA 19104

Low temperature stabilization of the geminate state of photolyzed MbCO (Mb*CO) at 4 K permits structure determinations by X-ray absorption spectroscopy (EXAFS). (1,2) However this structure has not been identified by X-ray studies in the physiological function of hemoglobin. Flow flash kinetics at room temperature for EXAFS studies require stabilization of the intermediate here proposed by continuous light pumping of the equilibrium: $HbCO \rightleftharpoons Hb^*CO \rightleftharpoons Hb+CO$. X-ray photon counting during the pump flash is feasible with Be window X-ray detectors. Sample photolysis at 5mM concentration is possible with 100 um thick samples using 300 Joule flash input with durations up to 10 msec at repetition intervals of 1-10/sec corresponding to duty ratios of up to 10%. Efficient X-ray fluorometry of about ten sample cells brings the X-ray thickness up to the equivalent of 1 mm. X-ray beam photon damage (10^{12} photons/sec) and heating from the flash lamps (μ1 Kw) require rapid flow through the sample holders ($\sim$10 M/sec) The X-ray fluorescence signal is obtained from the ratio of counts during the flash to an equal time immediately preceeding the flasn affording an equivalent carrier frequency of 100 Hz therby to avoid low frequency noise in the Synchrotron beam.

Experimental tests using 1 mM MbCO at 23° as a model indicate effective pumping of this system over a 5 msec interval give X-ray fluorescence changes consistent with MbCO -> Mb structure changes

(1) Chance, B. et al Biochem. 22:3820 (1983); (2) Chance, B. et al Biophys. J 41:416a (1983)
HL18708; Gm31992, RR01633 and SSRL (Proj: 660B) by NSF through DMR & NIH through BRP in DRR, DOE.

W-Pos192 STATIC AND DYNAMIC CONTROL OF HEMOGLOBIN REACTIVITY. J. M. Friedman and T. W. Scott, AT&T Bell Laboratories, Murray Hill, N. J. 07974

The frequency of the iron-proximal histidine stretching mode has been shown to be sensitive to the tertiary changes arising both from quaternary structure and ligation. Photolysis studies on the 10 ns time scale indicate a direct relationship between the configurational determinants of this frequency and such basic ligand binding processes as geminate recombination and spontaneous dissociation. Comparative studies on hemoglobins derived from a wide variety of animal sources including fish, reptiles and mammals reveal a systematic spread of R and T state frequencies which correlate with ligand binding properties. Also observed is a well defined ligated and deoxy tertiary structure within each quaternary state. Transient Raman studies indicated that the relaxation of this tertiary structure is both solution dependent and, under low pH conditions, fast enough to influence geminate recombination. The emerging picture is one in which solution and evolution dependent influences upon both the static and the dynamic heme-protein interactions modulate ligand reactivity through the iron-proximal histidine linkage.

W-Pos193 MIXED ASSOCIATION OF DEOXYGENATED HEMOGLOBINS OF THE ADULT BULLFROG. D. R. Manning, L.-T. Tam, D. J. Cox, and A. F. Riggs, Dept. of Biochemistry, Kansas State Univ., Manhattan, KA 66506, and Dept. of Zoology, Univ. of Texas, Austin, TX 78712.

The bullfrog, Rana catesbeiana, has two major tetrameric hemoglobins, B and C, which undergo a mixed association only when deoxygenated (Tam, L.-T., and Riggs, A. F., (1983) J.Biol.Chem., in press). The association is responsible for unusually high cooperativity in the O_2-binding of hemolysates. We have analyzed the association quantitatively by computer simulation of sedimentation velocity experiments. Very slight dimerization of components B (K=0.027 1/g) and of C (K=0.013 1/g) are detected by this method. Models for the velocity of sedimentation of B-C mixtures took account of the slight self-association of each component, the presence of about 5 % of a fixed disulfide-bound dimer, and the hydrodynamic interaction between all sedimenting species as well as the mixed association reaction. We neglected possible pressure dependence of the association. The simplest model, $B + C \rightleftharpoons BC$, is qualitatively impossible. The experiments can be fit by the two-step process, $B + C \rightleftharpoons BC \rightleftharpoons BC_2$, provided that the nominal component ratio for the experiment was adjusted. The best fits were obtained with association constants of K_1=1.25 1/g and K_2=1.12 1/g by using the most plausible values for the frictional coefficients for the aggregates. The constants varied slightly with the value chosen for the hydrodynamic concentration dependence of the sedimentation coefficients. Since a ratio of K_2 to K_1 would be 3/16 if the association were noncooperative, a ratio of 0.90 indicates some cooperativity. The model predicts at least 90 % aggregate in deoxygenated red cells with a 2:1 ratio of C to B. Investigation is continuing with better defined mixtures and other models including BC_n species with $n>2$. (Supported by NIH grant GM22243 (D.J.C.), NSF grant PCM8202760 (A.F.R.), and R.A.Welch Foundation grant F213 (A.F.R.).)

W-Pos194 COMPARISON OF HEME-POCKET DYNAMICS IN HEMOGLOBIN AND MYOGLOBIN. A. Levy, K. Alston* and J. M. Rifkind**. Johns Hopkins University, Physics Department, Baltimore, MD 21218; *Benedict College, Division of Health and Natural Sciences, Columbia, SC 29204; and **NIH/National Institute on Aging, Laboratory of Cellular & Molecular Biology, Baltimore, MD 21224.

It has been demonstrated that heme pocket dynamics plays an important role in regulating ligand binding to heme-proteins. The temperature dependence of the Lamb-Mössbauer factor for ferrous forms of hemoglobin shows that the conformational contribution to the mean square displacement of the iron are much greater for liganded hemoglobin than deoxyhemoglobin. This observation shows that the conformational changes which occur during ligand binding influence heme dynamics. On the other hand, the Lamb-Mössbauer factor for myoglobin, which does not undergo major ligand induced conformational changes, is independent of ligand binding. It is, however, surprising that the magnitude of the heme iron fluctuations for myoglobin, which has a high ligand affinity, are similar to or even smaller than those of deoxyhemoglobin. Using Mössbauer and ESR spectroscopy, we have recently shown (J. Appl. Phys. 53, 2066, 1982; Biophys. J. 41, 9a, 1983) that ligand pocket conformational fluctuations in deoxyhemoglobin and methemoglobin permit the reversible formation of a distal histidine bond with the iron. Similar studies on myoglobin show that these ligand pocket conformational fluctuations are not possible with myoglobin. Both the studies on the Lamb-Mössbauer factor and the formation of a distal-histidine bond indicate much more restricted heme pocket dynamics in myoglobin than in hemoglobin. The possible significance of these findings for the cooperative binding of ligands to hemoglobin will be discussed.

W-Pos195 STRUCTURES OF PHOTOLYZED CARBOXYMYOGLOBIN. J.O. Alben and F.G. Fiamingo, Department of Physiological Chemistry, Ohio State University, Columbus, OH 43210.

The structures of photoactivated carboxymyoglobin (Mb*CO) at temperatures to 10 K have been investigated by Fourier transform infrared (FT-IR) spectroscopy, visible, and near infrared spectroscopy. Two energy states for *CO are observed by FT-IR which are altered 94% and 88% from the ground state heme CO toward free CO gas (Alben, et al, (1982) PNAS 79, 3744). Ground state MbCO shows no absorption in the near infrared from 700 nm-1200 nm. Conversely Mb*CO shows an absorption near 766 nm, similar to that of deoxy Mb at 758 nm. These data are compared with Moessbauer isomer shifts and quadupole splitting which clearly indicate that the iron in both Mb*CO and deoxy Mb is in the high spin Fe(II) state (Spartalian, et al. (1976) BBA 428, 281), as does the heme transition in the Soret (Iizuka et al. (1974) BBA 371, 126). Thus the electronic structure of iron in Mb*CO is nearly identical to that of deoxy Mb, and *CO is only slightly perturbed from the free gas.

These data appear to be at odds with a recent interpretation of EXAFS structural data for Mb*CO reported by Chance, et al. (Biochem. (1983) 23, 3820). Possible reasons for these discrepancies will be presented, along with structural models that are consistent with all spectroscopic data.

W-Pos196 STRUCTURES RELATED TO THE FUNCTION OF HRP COMPOUND I AND II. Powers, L., Ching, G. Bell Labs, Murray Hill, NJ 97974, Chance, B., Inst. Struc. & Func. Studies, Univ. City Sci. Ctr., Phila PA; Yamazaki, I., Res.Inst. Appl. Electricity, Sapporo, Japan and; & Paul, K.G. Umea Univ. Sweden

The key role of intermediate compounds of horseradish peroxidase and peroxides in catalytic activity (1) focuses interest on their structures. X-ray absorption spectroscopy (EXAFS) has contributed specific and distinctive structures of the two electron (I) and one electron (II) oxidized states of the enzyme. They were prepared with hydrogen and alkyl peroxides from a highly purified preparation which is completely converted to a stable Compound I. Electron donor (ascorbate) added in stoichiometric amounts converts it mainly to Compound II. Compound III was prepared by addition of excess H_2O_2 to Compound II and their conversions were monitored optically. These compounds were freeze trapped and maintained at -100° in order to avoid their reduction by hydrated electrons. Compound I was found to have intermediate spin structure with a covalently linked oxygen atom (1.64 Å) and iron to pyrrole nitrogen distances of 2.02 Å and iron to proximal histidine distance of 1.93 Å (cf. ref. 2). Compound II is low spin and with corresponding distances of 1.93, 2.00, and 2.10 Å while Compound III of intermediate spin has corresponding distances of 1.72, 2.02 and 1.92 Å and the resting enzyme is high spin 2.39, 2.04 and 1.90 Å respectively. We regard the last values to be essential to push electrons to the Fe and enable Compound I formation. Indicator energy (3) intensity is linearly related to volume magnetic susceptibility from 2 to 6 Bohr magnetons providing convincing evidence that the spin state of hemoproteins may be determined directly from the amplitude of the X-ray absorption intensity in the XANES region. (1) Chance, B, J. Biol. Chem 151:553-577(1943); Hahn, J.E., et al. SSRL Activity Rpt. 83/01, Prop. 699B (1983); (3) Chance, B. el al. Biophys. J. 44:353-363(1983) Support in Part: GM31992, RR01633, HL18708, GM33165, HL3k1909 and SSRL (Proj. 632B) by NSF through DMR & NIH through BRP in DRR, DOE.

W-Pos197 CHLORIDE IONS AS THE PRINCIPAL ALLOSTERIC REGULATORS IN BOVINE HEMOGLOBIN. By Clara Fronticelli, Enrico Bucci and Charles Orth* Department of Biochemistry, University of Maryland Medical School, Baltimore, Maryland 21201.

In the presence of 0.15 M Cl^--Tris buffer at pH 7.4 at 37°C, the P50 of human and bovine hemoglobins is 18 and 33 mm Hg respectively. The lower oxygen affinity of bovine hemoglobin is due to a very high sensitivity of this system to Cl^- ions. In fact, when the Cl^- concentration is lowered to 0.02 M the oxygen affinity of the two proteins becomes similar with P50's of 18 and 13 mm Hg respectively. At this low Cl^- concentrations the response of human and bovine hemoglobins to increasing amounts of 2,3-DPG is practically superimposable. When the two systems are saturated with 2,3-DPG (1 mM), addition of 0.15 NaCl further decreases the oxygen affinity of bovine but not of human hemoglobin. Conversely in 0.15 M Cl^-, addition of 1 mM 2,3-DPG further decreases the oxygen affinity of human but not of bovine hemoglobin. The Bohr effect of bovine hemoglobin is strongly dependent on Cl^- concentrations.

In all probability the modulator in vivo of oxygen transport in bovine hemoglobin are Cl^- ions. This may be a common characteristic of all of those hemoglobins (sheep, goat, cat B) in which the residues val β1 and his β2 are substituted by a methionine.

W-Pos198 ROTATIONAL MODES OF HEME-FREE HEMOGLOBIN. By Massimo Sassaroli*, Enrico Bucci, and Robert F. Steiner, Department of Biochemistry, University of Maryland, School of Medicine, and Department of Chemistry, University of Maryland Baltimore County.

Human heme-free hemoglobin (apohemoglobin) was labeled in position β93 with either fluorescein-iodoacetamide (apoFIA) or with N-iodoacetylaminoethyl-5-naphtilamine-1-sulfonate (apoAEDANS). Also 1-anilino-8-naphthalene sulfonate was used to label the free heme pokets of the protein (apoANS). The correlation times associated with the probes were measured using time-resolved pulsed fluorimetry. In 0.1 M Tris or phosphate buffers at pH 7.0 to 7.2 at 5°C, the correlation times of apoFIA were near 12 nsec, with a minor component near 1 nsec or less; those of apoAEDANS were near 15 nsec, also with a minor component near 1 nsec or less and those of apoANS were near 18 nsec. Addition of IHP had a non detectable effect on these parameters. The expected correlation times for the entire apohemoglobin molecule (an αβ dimer) is expected to be near 20 nsec. On this basis it appears that the rotational modes of the proteins go from those of a single subunit, which dominate the rotations in apoFIA, to those of the entire dimer in apoANS. The very short correlation times of 1 nsec or less probably represents the localized mobility of the probes attachment to the protein. Totally missing from these systems are the correlation time near 5 nsec which Oton et al (J. Biol. Chem. 256: 7248 (1981)) and Sassaroli et al (J. Biol. Chem. 257: 10136 (1982)) have found in hemoglobin and in the isolated heme-containing β subunits labeled with AEDANS at β93.

W-Pos199 PRESSURE-JUMP KINETICS OF SUBUNIT INTERACTIONS IN HEMOGLOBIN A
Herbert R. Halvorson and William R. Johnston
Division of Biochemical Research, Henry Ford Hospital, Detroit, Michigan 48202

Pressure-jump relaxation experiments, using 8 atm perturbations, on partially (90%) saturated hemoglobin A provide the rate constants for the process $2\ \alpha\beta \rightleftharpoons (\alpha\beta)_2$. At pH 7.4, 0.1 M Tris-Cl, 0.1 M NaCl, and 21.5 °C the association rate constant is $5 \times 10^6\ M^{-1}\ s^{-1}$ and the dissociation rate constant is $5.5\ s^{-1}$ (fully oxygenated species). ΔV^o (assoc) is about +50 mL/mole. From experiments over the range 10 to 30 °C, $\Delta H^{\ddagger}$ (dissoc) is estimated to be 26 kcal/mole at 21.5 °C, with a significant $\Delta Cp^{\ddagger}$. The corresponding quantity for deoxy hemoglobin, 33 kcal/mole (Ip and Ackers, JBC 252:82) differs by the difference between the free energies of association for the two liganded forms. In contrast, the activation enthalpies for association are 22 kcal/mole (oxy) and 4 kcal/mole (deoxy). Experiments over the pH range 7.0 to 8.0 show a specific effect of proton binding, in agreement with the equilibrium data. Varying the chloride concentration from 0.08 to 0.29 M produces a nonspecific (ionic strength) effect on both association and dissociation rate constants. Based on these and other data, we propose a two-step model for the association of deoxy subunits to form 'T-state' tetramers.

Supported by NIH GM 23302

W-Pos200 THREE DIMENSIONAL RECONSTRUCTION OF LUMBRICUS TERRESTRIS HEMOGLOBIN FROM A RESTRICTED NUMBER OF STEM PROJECTIONS. A.V. Crewe, D.A. Crewe and O.H. Kapp Intr. by S.N. Vinogradov, Enrico Fermi Institute, University of Chicago, Chicago, Ill. 60637.

The extracellular hemoglobin of Lumbricus terrestris is composed of multiple copies of six polypeptides by SDS-PAGE. It was prepared for observation in the field emission scanning transmission electron microscope (STEM) by application to thin (15Å) carbon films and negative stained with 2% uranyl acetate. Images were recorded directly on tape (512 x 512 pixel, 8 bit precision). Images corresponding to "top" and "side" views were aligned, rotationally averaged and summed followed by gray scale expansion (Crewe, A.V., Science 221, pp. 325-330) and reduction to 32 x 32 element arrays for reconstruction. A third, diagonal view was obtained by averaging images which appeared to represent the molecule with a 45 degree inclination. A fourth view was generated by inversion of the array corresponding to this diagonal view. The reconstruction program was written in APL2 and provides a semi-empirical stochastic approach to the problem of reconstructing an object from a limited number of projections (Crewe, A.V. and Crewe, D.A., Ultramicroscopy, in press). Basically this involves the formation of four normalized arrays which are multiplied together to form a probability matrix which in turn is used to specify a Boolean matrix indicating the presence (1) or absence (0) of protein in two dimensional cross-sections through the molecule. The reconstructed model of Lumbricus hemoglobin compared favorably with the original projections but also contained some apparent artefacts which may have been introduced by the negative stain and/or the uncertainty of the actual angular position of the inclined orientation. The model suggests the presence of large (~50 x 90Å) gaps between the central regions of adjacent 1/12th subunits of opposite tiers.

W-Pos201 A PROTON NUCLEAR MAGNETIC RESONANCE INVESTIGATION OF THE ANTISICKLING ACTIVITY OF L-AMINO ACIDS AND RELATED COMPOUNDS. Irina M. Russu, Claudio Dalvit, Allison K.-L. C. Lin, Chao-Ping Yang, and Chien Ho. Department of Biological Sciences, Carnegie-Mellon University, Pittsburgh, PA 15213.

Proton nuclear magnetic resonance (NMR) spectroscopy has been used to investigate the binding sites of p-bromobenzylalcohol and of several L-amino acids such as phenylalanine, tryptophan, and valine to sickle hemoglobin (Hb S, β6Glu→Val) and human normal adult hemoglobin (Hb A). With the exception of L-valine, all these molecules are known to inhibit the polymerization of Hb S. The binding of these compounds to Hb S and Hb A was monitored by measuring the longitudinal relaxation rates (T_1^{-1}) for each of their proton resonances and the transferred nuclear Overhauser effects, in hemoglobin solutions in the deoxy form. The specific binding sites on the Hb S and Hb A molecules were identified by T_1^{-1} measurements for individual Hb protons and by intermolecular truncated nuclear Overhauser effect measurements. The results indicate that, for all the antisickling compounds investigated, there are at least two binding sites to the Hb S molecule. One binding site is in the region around the β6 mutation site. This binding site is specific to Hb S. The results suggest that the binding of a given compound to the region around the β6 site in Hb S can be directly correlated to its antisickling activity. The second binding site is located at or close to the heme pockets of the α and β chains and is present in both Hb S and Hb A molecules. The relationship between these NMR results and the mechanism for antisickling activity of these compounds will be discussed. (Supported by a research grant from the National Institutes of Health).

W-Pos202 THE IDENTITY OF THE PULSED FORM OF CYTOCHROME OXIDASE. C. Kumar, A. Naqui, & B. Chance. Department of Biochem/Biophys, Univ. of Penna., Phila, PA 19104 & Institute for Structural and Functional Studies, 3401 Market St., Phila. PA. 19104

Reduction and reoxidation of resting solubilized cytochrome oxidase (Soret maximum at 418 nm) normally produces the so-called oxygenated enzyme with the Soret peak at 428 nm. Such oxygen "pulsed" enzyme has been shown to posess greater enzymatic activity than the resting form (1).

We report here experiments that show that reduction and reoxidation of beef heart cytochrome oxidase under conditions that ensure the strict absence of hydrogen peroxide produces a fully oxidized form of the enzyme that has the Soret band at 420 nm, as opposed to the 428 nm band normally associated with the pulsed or oxygenated enzyme. The 420 nm form shows the enhancement of catalytic activity associated with the pulsed enzyme. Addition of hydrogen peroxide to the 420 nm form gives rise to the 428 nm band of the oxygenated enzyme, thereby clearly establishing that the 428 nm form is a peroxide derivative of the fully oxidized enzyme. The 420 nm form is produced both when oxygen or other chemical oxidants (ammonium chloroiridate) are used for producing the oxidized enzyme. We present a critical reevaluation of past work on this subject in the light of our results and discuss the relevance of these forms to turnover intermediates.

(1) Antonini, E., et al Proc.Natl.Acad.Sci.USA 74:3128-3132 (1977).

Partial Support: GM33165, HL31909 HL18708, GM31992, RR01633 and SSRL (Proj. 632B) by NSF through DMR & NIH through BRP in DRR, DOE. We also acknowledge the interest and assistance in this work of Drs. M. Brunori and L. Powers.

W-Pos203 COPPER INVOLVEMENT IN LIGAND BINDING TO HEART CYTOCHROME c OXIDASE, S. Yoshikawa, O. Einarsdottir, and W.S. Caughey, Department of Biochemistry, Colorado State University, Fort Collins, CO 80523.

Infrared spectra of cyanide bound to cytochrome c oxidase (CcO) indicate that cyanide can bind to either Cu^{+} or Cu^{2+} in all redox states and to Fe^{2+} or Fe^{3+} in all but the fully oxidized state. In fully oxidized enzyme CN^{-} binds only at Cu^{2+} (ν_{CN} = 2152 cm^{-1}). Upon one electron reduction CN^{-} binds at both Fe^{3+} and Cu^{2+} with ν_{CN} at 2131 and 2152 cm^{-1} respectively. Two and three electron reduction results in bands at 2131 and 2092 cm^{-1} assigned to $Fe^{3+}CN$ and $Cu^{+}CN$ respectively. Four electron reduction results in bands at 2060 cm^{-1} ($Fe^{2+}CN$) and 2092 cm^{-1} ($Cu^{+}CN$). Effects of replacement of H_2O with D_2O and of isotopic substitution (^{13}C and ^{15}N) on IR band parameters in each case show the ligand bound to be the CN^{-} anion and not HCN. CO always binds only to Fe^{2+}. CN^{-} displaces CO from $Fe^{2+}CO$ in the one, two and three electron reduced enzyme to give $Fe^{3+}CN$; CO displaces CN^{-} from $Fe^{2+}CN$, but not from $Cu^{+}CN$, in the fully reduced enzyme to give $Fe^{2+}CO$ and $Cu^{+}CN$. To which metal and to which oxidation state of the metal CN^{-} binds thus depends on the overall oxidation state of the enzyme and whether CO is present or not. The 2152 cm^{-1} band is unlikely to involve bridging. ν_{CN} values for $Cu^{2+}CN$ in laccase, ascorbate oxidase, and Cu(II) leu-leu-leu cyanides are near 2168 cm^{-1}. ν_{CN} for CcO $Fe^{3+}CN$ at 2130 cm^{-1} is near values for metHb, metMb, and peroxidase cyanides. Support of 2092 cm^{-1} band as $Cu^{+}CN$ comes from isotope effects (^{13}C and D_2O) and ν_{CN} of 2092 cm^{-1} for Cu(I) leu-leu-leu cyanide. CcO $Fe^{2+}CN$ is at 2060 cm^{-1} compared with 2030 cm^{-1} for reduced horseradish peroxidase cyanide. These data provide the first direct evidence for participation of Cu in ligand binding at the O_2 reaction site of CcO under physiological conditions. (Supported by U.S.P.H.S. grant No. HL-15890).

W-Pos204 INTERACTION OF LOCAL ANESTHETICS WITH CYTOCHROME c. H. James Harmon, Departments of Zoology and Physics, Oklahoma State University, Stillwater, OK 74078.

Local anesthetics, particularly lidocaine, have been shown to alter the physico-chemical properties of cytochrome c (1). Lidocaine alters the midpotential while tetracaine, dibucaine, and procaine are without effect. Lidocaine causes a decrease in CO binding to ferrocytochrome c. At 77°K procaine causes a 6-7 nm bathochromic shift to 423 nm in the Soret of ferrocytochrome c with an increase in absorbance at 432 nm. Alterations in low temperature spectra are also observed with dibucaine, tetracaine, and lidocaine and generally involve absorbances at the 446 and 552 nm shoulders of the alpha band. Using proton-NMR the location of lidocaine interaction with cyt c has been determined. Lidocaine alters resonances of phe-36, trp-59, phe-46, and met-65 in ferricytochrome c; lidocaine interacts with hydrophobic residues around ring 4 of the heme plane. Perturbation of these residues is consistent with the observed alteration in midpotential, absorbance spectrum, and CO binding.

This research was supported by a grant-in-aid from the American Heart Association and by a grant-in-aid from the American Heart Association, Oklahoma Affiliate.

1. Harmon, H.J. (1983) Biophys. J. 41, 406a

W-Pos205 SOME PROPERTIES OF THE ACTIVATED CYTOCHROME OXIDASE SPECIES--THE 420 nm FORM. A. Naqui, C. Kumar & B. Chance. Dept. Biochem/Biophys, Univ. of Penna., Phila., PA 19104 & Institute for Structural & Functional Studies, University City Science Center, Phila., PA 19104

Recently we have reported (Kumar, et al, this meeting) that reduction and reoxidation of beef heart cytochrome oxidase in the absence of H_2O_2 produces a fully oxidized form of the oxidase that has a Soret maxima at 420 nm (from now on referred to as 420 nm form) and has an enhanced catalytic activity. This form binds H_2O_2 and CH_3CH_2OOH with relative ease and also binds cyanide monoexponentially with rate constants much higher than resting oxidase.

The 655 nm band so far attributed to resting state only (and absent in the oxygenated form) is present in the 420 nm form. THis band is substantially decreased upon addition of H_2O_2 and CH_3CH_2OOH. There are other spectral differences also. In the Soret region it has a maxima at 420 nm as opposed to 417 nm for the resting (prepared by Yonetani or Volpe-Caughey method) and 428 nm for its H_2O_2 complex. Unlike the resting form and like its H_2O_2 complex, the 420 nm form has an enhanced α band. Only upon addition of H_2O_2 or CH_3CH_2OOH, a new broad band around 580 nm is formed. The possible explanation of these spectral differences will be discussed. Other ligand binding properties (spectral changes and kinetics), EPR characteristics of the 420 nm form will also be reported.

Partial Support: GM33165, HL31909 HL18708, GM31992, RR01633 and SSRL (Proj. 632B) by NSF through DMR & NIH through BRP in DRR, DOE. We acknowledge the interest of Drs. M. Brunori and L. Powers in this work.

W-Pos206 EPR ANALYSIS OF CHLOROPEROXIDASE COMPOUND I; A SPIN COUPLED Fe(IV) PORPHYRIN CATION COMPLEX. H. L. Dhonau, M. P. Hendrich, R. Rutter#, P. G. Debrunner and L. P. Hager#, Departments of Physics and Biochemistry#, University of Illinois, Urbana, IL 61801.

The reaction sequence of chloroperoxidase (CPO) involves the formation of the intermediate Compound I (CPOI) which is two electrons more oxidized than the native enzyme. Optical, magnetic and Mössbauer studies have indicated that in CPOI the heme iron is in a Fe(IV) S = 1 state and that the remaining oxidizing equivalent consists of a porphyrin pi cation radical (1). We present rapid passage and power saturation X-band EPR studies on freeze-quenched samples of CPOI from Caldariomyces fumago. We have been able to resolve the CPOI pi cation signal from other EPR active impurities, thereby obtaining the entire .12 T wide absorption signal with $g_{\perp} \tilde{=} 1.73$ and $g_{//} \tilde{=} 2.0$. We model the electronic state of the complex using the Hamiltonian $H = H_o + H_z$ with $H_o = D(S_z^2-2/3) + E(S_x^2-S_y^2) + \vec{S}\cdot\tilde{J}\cdot\vec{S}'$, and $H_z = \beta(\vec{S}\cdot\tilde{g} + g'\vec{S}')\cdot\vec{B}$ as in (2). Diagonalization of this Hamiltonian is used to relate the observed g values to the parameters J/D and E. The magnitude of D is found through analysis of the power saturation as a function of temperature. The parameters $J/D \tilde{=} 1.02$, $D/k \tilde{=} 52$ K, E/D < .1, J > 0 (antiferromagnetic coupling) yield a good simulation of the EPR spectrum. These parameters are consistent with Mössbauer measurements and show CPOI to have a larger zero-field splitting D and stronger spin-coupling than observed in horseradish peroxidase Compound I.

References: 1) Rutter, R. and Hager, L. P. (1982) J. Biol. Chem. 257, 7958-7961.
2) Schulz, C. E. et al., (1979) F.E.B.S. Lett. 103, 102-105.

Supported in part by GM-16406.

W-Pos207 CHARACTERIZATION OF OLIGOMERS OF TUBULIN BY TWO-DIMENSIONAL NATIVE PAGE. J.J. Correia and R.C. Williams, Jr., Dept. of Molecular Biology, Vanderbilt University, Nashville, Tenn., 37235

We and others (Kravit et al., J. Cell Biol. 95, 344a, 1982; Lee et al., J.B.C. 248, 7253, 1973) have observed oligomers of tubulin by native PAGE, even when they are not evident in sedimentation velocity or gel exclusion chromatography experiments under comparable conditions. Tubulin aggregates are also seen on native starch gels. Tubulins purified from calf brain, sea urchin egg (Strongylocentrotus purpuratus) and antartic fish brain (Pagothenia borchgrevinki) give rise to similar distributions of aggregates. Unlike microtubules, these oligomers are relatively insensitive to temperature (5-25°C), pH (6.1-8.8), the absence of excess GTP and/or Mg^{2+}, stoichiometric concentrations of colchicine, reduction and carboxymethylation in 8M urea, lyophilization, and a variety of electrophoresis buffers. These aggregates, once formed during electrophoresis, associate and dissociate slowly. Depending upon the incubation conditions, they give rise to kinetically controlled distributions that are visualized in two-dimensional native PAGE as a square array of discrete polymeric species. The fastest migrating species (monomers) are often observed to preferentially re-equilibrate into the second band (dimers), dimers into the fourth band, the third band into the sixth, the fourth into the eighth, etc. (The assignment of molecular weights to these species by Ferguson analysis is tentative due to their slow re-equilibration.) Thus a feature of the re-equilibration is that association occurs more rapidly than dissociation with a kinetic preference for a pseudo dimerization reaction for all species. Although they may be related to protofilaments, these oligomers appear to be another example of nonmicrotubular, polymorphic aggregates of tubulin. (Supported by NIH grant GM 25638.)

W-Pos208 INCLUSION OF TYPE IV COLLAGEN AND LAMININ INTO TYPE I COLLAGEN MATRICES. L. Thornburg, V. Glushko, E. Hujanen and V. Terranova. Helitrex Inc., Princeton, NJ 08540; Dept. of Biochem., Temple Univ. School of Med., Philadelphia, PA 19140; Lab. of Develop. Biol. and Anomalies, NIDR-NIH, Bethesda, MD 20205.

The presence of type IV collagen and laminin in basement membranes may prevent the migration of normal cells from one tissue to another. In order to study the effect of these proteins on cell migration under controlled conditions, compositionally defined matrices of collagen with and without laminin were prepared. These matrices were then used in a modified Boyden chamber as a barrier to cell penetration. Type I collagen was purified from bovine Achilles tendon; type IV collagen and laminin were isolated from EHS tumor. An open matrix with a density of 0.013 and pore size of ~40 microns was formed from a dispersion of type I collagen. Human skin fibroblasts penetrated this matrix when platelet-derived growth factor was used as an attractant. Incorporation of laminin and type IV collagen into the matrix increased its effective density and reduced cell penetration by over 98%. Since this effect could be due to the formation of a passive barrier, the ultrastructure of these matrices was examined by SEM. The inclusion of type IV collagen and laminin with type I collagen yielded a matrix containing much larger pores. In addition, SEM revealed an overlying network of thin twisted filaments or ruffles not present in the type I collagen matrix. Shrink temperature, which reflects intermolecular interactions of the collagen matrix, was not affected by the presence of either protein. It appears that the barrier to cell migration imposed by type IV collagen and laminin is not simply due to passive obstruction, but is the result of a more complex biochemical process.

W-Pos209 ANTIBODY CRYSTALLIZATION IN TWO DIMENSIONS: DIFFERENCES IN MOLECULAR PACKING AND INTERACTIONS BETWEEN THE IgG AND THE IgE CLASSES. **E.E. Uzgiris, General Electric Research and Development Center, Schenectady, NY 12301**

Monoclonal mouse IgG forms two dimensional crystals of two types:[1] 1) a linear strand array of poor order obtained usually from high antibody concentration conditions and 2) a hexagonal array of high order obtained from low antibody concentration conditions. In the hexagonal array, the lattice is composed of hexamers of F_{ab} contacts with an intricate network of interconnecting F_c domains. These domains are directly visualized in the images of the 2-D crystals. The mouse monoclonal IgE antibody arrays that have been obtained to date are different from these. Only one type of lattice has been observed to date, a hexagonal type of P3 symmetry. The crystalline domains are large, extending for up to 5 microns. However, the optical diffraction peaks, although sharp, drop of rapidly in intensity with increasing order of diffraction. This suggests some degree of local disorder in the lattice. The F_c domains do not form an interconnecting network as in the IgG crystals. Furthermore, in the ordering of the 2-D lattices, there are significant differences in the dependence on temperature and solution pH.

1. E.E. Uzgiris and R.D. Kornberg, Nature 301, 134-136 (1983)

W-Pos210 STRUCTURAL ANALYSIS OF THE SURFACE LAYER PROTEIN OF AQUASPIRILLUM SERPENS BY HIGH RESOLUTION ELECTRON MICROSCOPY

WENNIE WU and ROBERT GLAESER,(Intr. by Richard Lozier)
Department of Biophysics and Medical Physics, and Donner Laboratory, Lawrence Berkeley Laboratory, University of California, Berkeley, CA 94720

Aquaspirillum serpens possesses a surface layer protein which exibits a regular hexagonal packing of the morphological subunits(HP-protein). A method was developed to isolate large quantities of the outer wall fragments, which appeared to be dark patches with symmetrical optical diffraction patterns. The outer wall fragments were manipulated to form large, light arrays with good crystalline order, of which the optical diffraction patterns always show "handedness". I concluded that these light arrays were real single layer protein arrays.

Low dose, low temperature electron microscopy has been applied to the frozen hydrated specimens of HP-protein. A computer processed image was obtained with a resolution of 13.70 Å. It was also noted that 6.9 Å structural details were preserved and retrieved in the image of the frozen hydrated specimen.

An "NSFT" method was developed and a computer processed image was obtained with a resolution of 13.70 Å for the specimen prepared by the NSFT method. It was noted that 5.7 Å structural details were preserved and retrieved in the image by the NSFT method.

A physical-mathematical model was derived to interpret the images constructed by the two methods. A major advantage of the NSFT method is easiness of getting high quality micrographs.
(supported by NIH GM23325 and US Department of Energy Contract No. DE-AC03-76SF00098.)

W-Pos211 ISOLATION OF MITOCHONDRIAL INNER MEMBRANE PROTEIN COMPLEXES

G. Georgevich* and Randall Mrsny. Institute of Molecular Biology, University of Oregon, Eugene, OR 97403. *Present address: Abbott Labs, North Chicago, IL 60064

Beef heart inner mitochondrial membranes were solubilized in 4-5% lauryldimethylamine oxide and subjected to density gradient centrifugation. Cytochrome c oxidase was recovered (∿80%) from a single gradient band which had a A_{280}/A_{420} of 3.1 - 3.5 and was free of other spectrally detectable cytochromes. Although this preparation was active in electron transfer, it lacked subunit III. Sedimentation velocity analysis indicates that the preparation is monomeric. These observations are consitent with recent reports of subunit III depleted cytochrome c oxidase and could comment on the range of detergent concentrations employed in such studies. Other bands in the gradient, such as an ATPase, had very low or no activity. The bulk of the protein loaded on the gradient remained at the origin suggesting that significant dissociation and denaturation of protein complexes other than the cytochrome c oxidase had taken place. This is a rapid procedure for the isolation of cytochrome c oxidase. Highly purified preparations were obtained with a subsequent ion exchange chromatography step. R. M. was supported by GM 08712.

W-Pos212 SITE SELECTION SPECTROSCOPY AND THE CONFORMATIONAL DYNAMICS OF PROTEINS. T. W. Scott and J. M. Friedman, AT&T Bell Laboratories, Murray Hill, N. J. 07974

Tryptophan containing proteins such as hemoglobin exhibit heterogeneous fluorescence at room temperature due to emission from a distribution microstates which fluctuate rapidly during the lifetime of their fluorescence. At sufficiently low temperatures (∿2K), these fluctuations are frozen out. Structured homogeneous fluorescence from specific microstates can then be observed by optical excitation at the red edge of the tryptophan absorption band. It will be shown now the temperature dependence of fluorescence line narrowing in proteins offers a useful probe of the energetics and dynamics of these microstates.

W-Pos213 INTERMEDIATES IN THIOREDOXIN-S_2 REFOLDING. Robert F. Kelley and Earle Stellwagen, Univ. of Iowa, Iowa City, IA 52242.

The small monomeric protein thioredoxin-S_2 is reversibly unfolded in a single cooperative transition centered at 2.5 M guanidine hydrochloride (Gdn-HCl) at pH 7.0 and 25°C as measured by peptide backbone CD and tryptophan fluorescence emission. Stopped-flow fluorescence measurements of unfolding in 4 M Gdn-HCl detect a single increasing kinetic phase with a τ of 7.1 ± 0.2 s. Refolding in 2 M denaturant occurs in three decreasing phases with τ values of 0.57 ± 0.15, 10.8 ± 0.4 and 560 ± 52 s with each phase accounting for 2.1 ± 0.4, 8.0 ± 0.7 and 88 ± 6% of the total change, respectively. The dominant slowest phase is generated in 4 M Gdn-HCl (τ=42 s) and has an activation enthalpy (22 kcal/mole) characteristic of peptide bond isomerization. Both the amplitude and τ of the slowest phase suggest that this peptide isomerization involves Pro-76 which is cis in the native protein. Peptide backbone CD measurements of refolding in 2 M Gdn-HCl indicate that 81 ± 4% of the secondary structure changes occur coincident with the slowest phase observed by fluorescence. However, about 50% of the viscosity decrease precedes the common slowest phase detected by CD and fluorescence measurements of refolding in 2 M Gdn-HCl. In contrast to the observed kinetics in 2 M Gdn-HCl, all of the CD changes and the majority of the fluorescence changes occur in the faster kinetic phases when refolding in less than 1 M Gdn-HCl. We suggest that thioredoxin-S_2 folding involves a hydrodynamic collapse preceding secondary structure formation and that isomerization of Pro-76 can occur in a globular intermediate having a transition midpoint at 1.7 M Gdn-HCl.
(Supported by USPHS grant GM 22109).

W-Pos214 THE NATURE OF ELECTROSTATIC INTERACTIONS IN MYOGLOBIN. Bertrand Garcia-Moreno E., Lin X. Chen, Frank R. N. Gurd, Department of Chemistry, Indiana University, Bloomington, Indiana 47405.

Structural-energetic relationships involving electrostatic free energy (ΔG_{el}) arising from charge-charge interactions were studied in sperm whale myoglobin. The crystallographic coordinates were divided into their constituent elements of secondary structure. A static accessibility-modified Tanford-Kirkwood model was used to study interactions between pairs of charged sites. The net ΔG_{el} of each structural element was calculated and divided into two terms, one arising from interactions within the structural element and another from interactions between the structural element and the rest of the protein. At pH 7.0 and I=0.01 M, the total ΔG_{el} of myoglobin is -18.63 kcal/mol. Approximately 50% of this ΔG_{el} arises from interactions between the structural elements. At this pH and ionic strength all structural elements experience net, favourable interactions. Each of the long helices (A,F,E,G,H) is stabilized by its interactions with the rest of the protein by more than -2.0 kcal/mol, the terminal helices (A,H) by more than -4.0 kcal/mol. The small helices C and D have weak interactions with other structural elements but strong ones within themselves. The F helix has a negligible, net ΔG_{el}. Most of the ΔG_{el} of each structural element derives from strong, specific, pairwise interactions. The conservation of the charges in these interactions throughout evolution suggests their importance in the function, folding and stability of myoglobin.
(Supported by U.S. Public Health Service Research Grant HL-05556.)

W-Pos215 PREDICTION OF SUBUNIT SECONDARY STRUCTURE IN FILAMENTOUS VIRUSES AND COMPARISON WITH EXPERIMENTAL RESULTS. B. Prescott and G.J. Thomas, Jr., Department of Chemistry, Southeastern Massachusetts University, N. Dartmouth, MA 02747.

The algorithm of Garnier, Osguthorpe and Robson (J. Mol. Biol. (1978) 120, 97-120) for prediction of protein secondary structure has been applied to the coat protein sequences of six filamentous bacteriophages: fd, If1, IKe, Pf1, Xf and Pf3. For subunits of the Class I virions (fd, If1, IKe), the algorithm predicts a very high percentage of α-helix in comparison to other structure types, which is in accord with the results of circular dichroism and laser Raman measurements. Agreement with experiment is particularly good when the algorithm is biased in favor of α-helix. On the other hand, for subunits of the Class II virions (Pf1, Xf, Pf3), the algorithm consistently predicts a predominance of β-strand structure, which is not in accord with the presumed native structures, but is compatible with the demonstrated facility for conversion of Class I subunits from α-helix to β-strand under appropriate experimental conditions (Thomas et al., J. Mol. Biol. (1983) 165, 321-356). Even when the algorithm is biased to favor α-helix, the Class II virion subunits are predicted to contain considerably more strand than helix. Therefore, both predictive and empirical methods indicate a distinction between Class I and II subunits, which is reflected in a greater tendency of the latter to adopt other than uniform α-helix conformation. Application of the Chou-Fasman algorithm (Adv. Enzym. (1978) 47, 45-148) to the same sequences also distinguishes the Class I and II structures from one another, but absolute structure predictions by the Chou-Fasman algorithm are in less favorable agreement with experimental data.

Supported by N.I.H. Grant AI 11855.

W-Pos216 COLLECTIVE MOTIONS IN PROTEINS: ANALYSIS OF MOLECULAR DYNAMICS SIMULATIONS OF BOVINE PANCREATIC TRYPSIN INHIBITOR. Toshiko Ichiye and Martin Karplus, Department of Chemistry, Harvard University, Cambridge, MA 02138

The collective motions of atoms in proteins, which are believed to be important in their biological function, are studied by the molecular dynamics method. Two simulations of bovine pancreatic inhibitor are analyzed: one for the protein in a vacuum and the other for the protein in a van der Waals solvent with atom size and density corresponding to water. The analysis indicates that the atomic fluctuations have two components: local, high-frequency oscillations which have roughly the same magnitude throughout the protein and collective, lower frequency modes which contribute to the variations in the magnitude of the fluctuations in different parts of the protein.

Collective groups corresponding to the low frequency modes in the protein are determined by the degree of correlation between the fluctuations, as measured by equal-time cross-correlations, of all possible Cα atom pairs and by similarities in the time-correlation functions of individual atoms. These collective groups may range from a few neighboring atoms (for instance, a side chain) up to many atoms which may be far apart in sequence. We also examine the cross-correlations of the fluctuations of pairs of atoms as a function of their separation, which demonstrates the range of the collective effects, and with respect to their location in the protein structure, which shows that areas of secondary structure move as collective groups. In addition, we have calculated the time-series and correlation functions of the positions of the centers of mass of various groups and of individual atoms in these groups with respect to the group center-of-mass. From these calculations, the collective behavior as well as the separability of local and collective behavior is clearly demonstrated.

W-Pos217 SEQUENCE EVIDENCE FOR MITOCHONDRIAL EVOLUTION D.G. George, L.T. Hunt, L.-S. Yeh, and W.C. Barker, National Biomedical Research Fnd., Georgetown Univ. Med. Ctr., Washington, D.C.

We have previously presented sequence evidence, based mainly on cytochrome c-type protein and 5S rRNA sequences, that indicates an endosymbiotic origin for mitochondria and chloroplasts. Cytochrome c is a mitochondrial protein that is encoded in the nucleus. Presumably, the cytochrome c gene is of mitochondrial origin and is one of a number of mitochondrial genes that were transferred to the host nucleus subsequent to the symbiotic invasion. Animal mitochondria have the capacity to code for 13 proteins. Of these, the function is known for five: protein 6 of the mitochondrial ATPase complex, polypeptides I, II, and III of cytochrome oxidase, and cytochrome b. Although the remaining eight are believed to be expressed, no functions have yet been assigned. In addition, the genomes of animal mitochondria code for 12S and 16S rRNAs. These rRNAs contain about 1,000 and 1,600 nucleotides, respectively, and thus are a much more detailed source of phylogenetic information than the 5S rRNAs. There is now sufficient sequence evidence to derive phylogenetic trees for the five mitochondrially encoded proteins of known function, at least one of the hypothetical proteins, and the 12S rRNA and 16S rRNA sequences. These trees contain, in addition to animal mitochondria, information from insect, plant, and fungal mitochondrial sequences and in one case from a related E. coli sequence. These trees will be compared and contrasted with trees derived from the products of nuclear genes. The evolution of nuclear- and mitochondrial-encoded proteins will be assessed with respect to changes in the environment accompanying gene transfer.

This work was partially supported by NASA contract NASW3317 and NIH grant GM08710.

W-Pos218 STUDY OF PROTEINS WITH MAJOR INTRASEQUENCE HOMOLOGIES. Winona C. Barker and David G. George. National Biomedical Research Fnd., Georgetown University Medical Center, Washington, DC 20007

We have made a comprehensive study of protein sequences for evidence of homologies resulting from internal gene duplication. Representatives of over 1100 protein families (sequences in different families are more than 50% different) were tested using programs RELATE, DOTMATRIX, and ALIGN. Here we summarize the major results of this study and present examples of well-established internal duplications. For many of the proteins exhibiting sequence duplication, other evidence, such as gene structure or X-ray crystallography, also reveals that the protein structure is organized into discrete domains. Duplicated domains are generally repeated 2-5 times in the protein structure, they usually represent a major portion of the protein sequence, and they may be several hundred residues long. Another major type of duplication produces many tandem repeats of a short length. Proteins with this type of repeat may have an unusual amino acid composition and a highly ordered secondary structure. A tabulation of the proteins containing these two major types of intrasequence homologies will be presented and their characteristics will be summarized.

This work was supported by NIH grant HD09547.

W-Pos219 BIOMOLECULAR ADSORPTION ON TUNGSTEN†, J. A. Panitz, Sandia National Laboratories, Albq., NM. Biomolecular films adsorbed onto metal substrates from solution may have important technological application ranging from novel solid-state chemical sensors to high capacitance electrodes and coatings for surface passivation. We have been studying the adsorption properties and the morphology of ferritin and DNA monolayers on tungsten substrates by direct visualization of the layers using Field-Ion Tomography. For flexible molecules like DNA, the molecular conformation which we observe for the adsorbed species depends upon its adhesion to the surface. Preadsorption of poly-l-lysine or post adsorption of spermidine can be used to improve surface adhesion. Our observations will be discussed in the context of obtaining close-packed, well characterized biomolecular layers on metallic substrates.

†This work supported by the Defense Advanced Research projects agency under contract # 4597 and the U.S. Department of Energy under contract # DE-AC04-76DP00789.

W-Pos220 PACKING OF CYLINDRICAL COLLAGEN FIBRILS OF UNIFORM DIAMETER IN CONNECTIVE TISSUES.

Eric F. Eikenberry and Barbara Brodsky, Rutgers Medical School, Piscataway, N.J. 08854

Low angle equatorial x-ray scattering has been used to characterize the average diameter and lateral arrangement of cylindrical collagen fibrils in several connective tissues that feature a relatively homogeneous population of fibril diameters. The following values for hydrated tissues were determined from the cylinder transform and the interfibrillar interference function:

	lamprey notochord	bovine cornea	chick tendon	lamprey skin
Fibril diameter	17 nm	36 nm	56 nm	67 nm
Center-to-center separation	31 nm	68 nm*	90 nm	83 nm
Packing fraction	0.26	0.24	0.34	0.57

The fibrils in each case are packed on a disordered hexagonal array such that each fibril has five or six nearest neighbors. Although the fibril separation and size varies, the packing fraction is approximately the same for the first three tissues listed, giving rise to a geometrical similarity differing only in scale. The average center-to-center separation of the fibrils is nearly twice the diameter, and the minimum separation is close to the average, giving an even distribution of fibrils at relatively low density. In the case of lamprey skin, the fibrils are packed at much higher density. We are examining fibril organization as a function of water and proteoglycan content to investigate the factors responsible for stabilizing the structure in these tissues. This system offers an opportunity to extend the studies on forces that stabilize arrays of cylinders in biological systems.

* calculated from Sayers, et al., J. Mol. Biol. 160 (1982) 593.

W-Pos221 PHOTOCHEMICAL DISSOCIATION IN OPTICALLY DENSE SOLUTIONS: APPPLICATIONS TO CARBOXYMYOGLOBIN. F.G. Fiamingo and J.O. Alben, Dept. of Physiological Chemistry, Ohio State University, Columbus, OH 43210

Photodissociation of ligands has made important contributions to the understanding of function and structure in heme proteins. We present a theory for photochemical dissociation that is not limited by the assumption of previous analyses of optically thin samples, and compare it with experimental results from the photolysis of carboxymyoglobin. Equations are derived and presented in terms of the effects of absorbance, A ($\log_{10}(I_0/I)$ = probability of absorption of light quanta per unit surface area), and the potential for dissociation, D (maximum probability of photodissociation per unit surface area; a linear function in time of photolysis) for both monochromatic and polychromatic light sources. When monochromatic light is used, we show that for large absorbances (A > 2) the fractional photolysis increases as log(D)/A, and may appear to "saturate" even though well below completion. For polychromatic light intensities and absorbances the theory predicts that the near infrared tail of the absorbance band of carboxymyoglobin should be sufficiently transparent to allow the radiation to penetrate the sample, yet still have a significant absorptivity such that complete photodissociation is possible. An optically thick myoglobin-CO sample illuminated with a tungsten lamp was observed to behave somewhere between these two theories. These theoretical relations may be useful in the analysis of photolysis data from optically dense solutions and as a guide for future experimental design.

W-Pos222 ARTIFACTS IN THE DECAY OF THE FLUORESCENCE ANISOTROPY: THE EFFECT OF MULTIPLE LIFETIMES. Richard D. Ludescher, Institute of Molecular Biology, University of Oregon, Eugene, OR 97403.

The fluorescence anisotropy decay is generally recognized to be a faithful measure of the rate and amplitude of fluorophore motion during the lifetime of the excited state. Certain situations can exist, however, in which the correspondence between curvature in a measured r(t) decay and molecular rotation fails. When the total decay [I(t)] is the sum of fluorescence from two species with different lifetimes, $r(t) = f_1(t)r_1(t) + f_2(t)r_2(t)$ where $f_i(t) = a_i\exp(-t/\tau_i)/I(t)$. The time dependence of the two weighting factors differs radically: at long time $f_i(t)$ goes to 0 and 1 for the short and long lifetime species, respectively. If the functional forms of the component $r_i(t)$ decays are different, then the sum r(t) curve will reflect different linear combinations of the two components at different times. Simulation of the effects of such a model have been calculated using a two component approximation to the component anisotropy decays: $r_i(t) = r(0)[\alpha_i\exp(-t/\phi_i) + (1 - \alpha_i)]\exp(-t/\phi_p)$. The model simulations result in r(t) decays with very unusual and sometimes physically impossible curvature. For example, if $\phi_p >> \tau_2$ (where 2 is the long lifetime) then r(t) will decay to a constant and either rise at long time ($\alpha_1 > \alpha_2$) or decay further ($\alpha_1 < \alpha_2$). When $\phi_p \cong \tau_2$, the decays can have a plateau at intermediate time ($\alpha_1 > \alpha_2$) or appear to accelerate at long time ($\alpha_1 < \alpha_2$). An especially insidious situation exists when $\alpha_1 < \alpha_2$ and the two lifetimes are nearly equal. This results in a spurious decay in the sum r(t) curve which appears linear when plotted on a logarithmic scale. The natural history of this phenomenon will be illustrated with model simulations and with actual data which display some of the various possible artifacts.

W-Pos223 2-PHENYLBENZOXAZOLE: ITS EXCITED STATE REACTIONS WITH N_3^- AND I^-. A FLUORESCENCE AND ESR STUDY. R.D. Hall, K. Reszka, and C.F. Chignell, National Institute of Environmental Health Sciences, Laboratory of Molecular Biophysics, PO Box 12233, Research Triangle Park, North Carolina 27709.

We have investigated the photosensitizing properties of 2-phenylbenzoxazole (P) as part of a more general study of benzoxazole derivatives of environmental significance. Irradiation of P at 300 nm in deoxygenated ethanol with 2,2,6,6-tetramethylpiperidinooxy (TEMPO) and the electron donors, I^- and N_3^-, produces a decrease in the intensity of the nitroxide ESR signal. At the same time a study of the fluorescence quenching of $^1P^*$ gives quenching rate constants near the diffusion limit [$k_q(N_3^-) = 6 \times 10^9 M^{-1}sec^{-1}$; $k_q(I^-) = 1 \times 10^{10} M^{-1}sec^{-1}$] consistent with electron transfer from the quencher (Q^-) to $^1P^*$. Irradiation of P and N_3^- in the presence of 5,5-dimethyl-1-pyrrolidine-1-oxide (DMPO) leads to detection of the azido adduct of DMPO: evidence for the formation of the azide radical, $N_3^\cdot$. The following sequence of photo-initiated redox reactions explains our observations:

$$P \xrightarrow{h\nu} {}^1P^* \xrightarrow{[Q^-]} {}^{1,3}(P^{\cdot-}....Q^\cdot) \longrightarrow P^{\cdot-} + Q^\cdot$$

$$P^{\cdot-} + \text{TEMPO} \longrightarrow P + \text{TEMPO}^-$$

I^- quenches $^1P^*$ more effectively than N_3^- but the reduction of TEMPO proceeds more rapidly with N_3^- present instead of I^-. We propose that the iodide radical, $I^\cdot$, through its strong spin-orbit coupling with $P^{\cdot-}$, more efficiently facilitates deactivation of its respective geminate radical pair with $P^{\cdot-}$. As a result, both the rate of formation of the free radical $P^{\cdot-}$ and the rate of reduction of TEMPO are lower for the photo-induced reaction of P with I^-.

W-Pos224 LOCAL MOTIONS IN PROTEINS AS INVESTIGATED BY THE THERMAL COEFFICIENT OF THE FRICTIONAL RESISTANCE TO ROTATION. S. Scarlata, M. Rholam and G. Weber, Department of Biochemistry, Univ. of IL, Urbana, IL 61801.

We have measured the thermal coefficient of the frictional resistance to rotation (α) through the fluorescence polarization of Tryptophan and Tyrosine both free in solution and as intrinsic protein chromophores. For free fluorophores (Tyr, Trp, PRODAN and Perylene) we found: 1) α is a function of the solvent viscosity only and is independent of the chromophore used in its measurement, 2) The values of α are equal to those determined by flow viscometry. In proteins we observe two distinct values of α; one at lower temperatures (α_s) equal to the thermal coefficient of the solvent viscosity and at higher temperatures a second, reduced value (α_p) is seen, the magnitude of which is distinctive of the individual protein. The transition from α_s to α_p occurs at the rotational amplitude at which the motions of the chromophore become limited by the surrounding peptide. The magnitude of α_p appears to depend on the extent of coupling between the two motions of the chromophore and those of the protein subdomain that surrounds it. Simple cyclicpeptides (oxytocin, vasopresin) and several globular proteins show essentially similar patterns in indicating the importance of the immediate peptide environment in the determination of the observed behavior. A two-fluid thermodynamic model that can simulate the observed behavior is presented. This work was supported by RO1-GM11223.

W-Pos225 LOW TEMPERATURE CONFORMATION OF Mg^{++} -POLY(U) IN D_2O AS REVEALED BY IR, RAMAN SPECTROSCOPY AND NORMAL COORDINATE ANALYSIS. Jagdeesh BANDEKAR and Georg ZUNDEL, Institute of Physical Chemistry, The University of Munich, MUNICH, West Germany (Introduced by P.K. Sengupta)

IR and Raman spectra of the Mg^{++} salt of poly(U) in D_2O were recorded in the 1600-1800 cm^{-1} region and between 1° C and 15° C. The IR spectra showed a melting curve similar to UV curves with a temperature of transition of 7° C. This spectral change is assumed to be connected with the formation of the secondary structure of Mg^{++} -poly(U) in D_2O below 7° C. Three double-helical and two triple-helical structures were used as inputs to compute the normal modes of vibration. A double-helical structure was found to give the best agreement with the observations. Knowledge of the C=O eigenvectors and of the expression for transition probability from quantum mechanics was used to explain the so far unanswered question of Miles (Miles, H. T. (1964) Proc. Natl. Acad. Sci. 51, 1104) as to why there is an increase in the IR vibrational frequency of a carbonyl band when that group is H-bonded to another polynucleotide chain in a helix. Such considerations also explain why a predicted band at about 1648 cm^{-1} is not to be seen in the IR spectra but is present in the Raman spectra. The model incorporating the C=O transition dipole-dipole coupling interaction is able to successfully explain also the higher intensity of the higher wave number band (H-bonding would cause the opposite effect). The experimental results demonstrate that the complete picture of structure and vibrational dynamics of Mg^{++} -poly(U) in D_2O is obtained only by looking simultaneously at IR and Raman spectra and not at only one of them. Weak IR bands were found to be as useful as the strong ones in understanding vibrational dynamics and structure.

W-Pos226 EFFECT OF ROTATIONAL DIFFUSION ON FLUORESCENCE QUENCHING BY IODIDE: ASSESSMENT OF SOLUTE ASSESSABILITY TO N^{ϵ}-FLUORESCEIN ISOTHIOCYANATE-LYSINE-23-COBRA α-TOXIN BOUND TO THE ACETYLCHOLINE RECEPTOR. David A. Johnson, Juan Yguerabide, and Palmer Taylor*, Divison of Pharmacology, Depts. of Medicine and Biology, University of California, San Diego, La Jolla, California 92093

Fluorescence quenching by certain ions and small molecules is a technique widely used to assess the exposure of intrinsic and extrinsic fluorophores associated with proteins. Results are usually interpreted in terms of collisional quenching using the Stern-Volmer equation, and differences in quenching rate constants between protein and fluorophore free in solution or between different binding states of the protein are attributed to differences in local accessibility to the quenching agents. These interpretations implicitly assume that every collision between protein and quenching molecules can produce quenching if the fluorophore is locally accessible and are correct only if the protein molecule rotates at a rate much faster than the collision rate. To incorporate orientational and rotational effects in the interpretation of the fluorescence quenching experiment we have modified the formulations of Shoup et al. (Biophys. J. 36:697, 1981) for the calculation of bimolecular rate constants for diffusion-limited reactions between asymmetric molecules with comparable rotational and collisional rates. The effect of rotational diffusion, molecular weight and fluorescence lifetime on the bimolecular quenching rate were analyzed numerically. The experimentally observed iodide quenching constants for fluorescein, FITC-toxin, and FITC-toxin bound to the Torpedo acetylcholine receptor are 13.8, 5.0 and 3.0 M^{-1}, respectively. Using our treatment we find that these differential quenching constants can be largely explained in terms of a reduced rotational diffusion induced by toxin conjugation and receptor binding.

W-Pos227 MODELING THE MAGNETIC CIRCULAR DICHROISM OF LOW SYMMETRY CUPRIC SITES. B.S. Gerstman and A.S. Brill, Dept. of Physics, Univ. of Virginia.

We describe here the use of hybrid atomic orbital models of the cupric ion in low symmetry sites, such as in the blue proteins, for the calculation of MCD spectra. Two fold spin degeneracy of the ground state together with spin-orbit mixing of the excited electronic states produces C-terms that should dominate the MCD spectra below 100 K and possibly at room temperature. Such effects have been observed experimentally (D.G. Eglinton, Ph.D. dissertation Univ. of East Anglia, 1981; Prof. A.J. Thomson, personal communication).

The energies of the excited states not only determine the positioning of the MCD bands, but also influence their strengths. Further, if spin-orbit coupling of the excited states with the ground state is ignored, the sum of C-values over all bands is zero. With the assumption that the vibrational intensities for all the transitions are the same, the C-values summing to zero results in MCD spectra that are balanced with respect to the baseline. When admixing of the ground state with excited states by spin-orbit coupling is included, the extent of which depends inversely upon the excited state energies, the sum of the C terms is no longer zero and the MCD spectra are imbalanced. We report on the formulation of these effects and on factors which influence the importance of the imbalance relative to the contributions which sum to zero.

W-Pos228 INTERACTION OF THE ADRIAMYCIN-IRON COMPLEX WITH MODEL MEMBRANE SYSTEMS. A. Samuni, P. Chong, Y. Barenholz and T.E. Thompson, Department of Biochemistry , University of Virginia, Charlottesville, VA 22908.

The anthracycline drug adriamycin (ADR) is widely used in cancer chemotherapy despite its cardiotoxic effects. Neither the mechanism of its antitumor activity nor that of its cytotoxic side-effects have been adequately elucidated. Much evidence indicates the involvement of free radicals as well as metal ions in ADR toxicity. Although most studies have been focused on ADR-induced damage in DNA, more recent work points to cellular membranes as the vital target. The effect of ADR on membranes together with the key role of transition metal ions in causing biological damage and their high affinity for ADR, prompted us to examine the interaction of ADR-metal complexes with membranes. We have compared the nature and kinetics of the interaction of ADR and of ADR-iron complexes with vesicles formed from synthetic saturated phospholipids, using the characteristic fluorescence of the ADR-Fe complex. ADR-Fe, like ADR, preferentially partitions into the vesicles. This partition is accompanied by a corresponding fluorescence enhancement, an inaccessibility to hydrophylic quenchers, an increase in fluorescence polarization and, unlike ADR, by a significant blue shift. Iron ions avidly bind to ADR prior or subsequent to its incorporation into vesicles. This binding can be blocked, though not reversed, by chelating agents. The primary instantaneous association of ADR-Fe complex with vesicles is followed by a slower process. This process is faster above the lipid transition temperature and is facilitated by higher [metal]. These features permit study of ADR-Fe within the vesicle bilayer, its permeation across the bilayer and its transfer between bilayers. (Supported by USPHS grants HL-17576 and GM-14628.)

W-Pos229 SPECTROSCOPIC CHARACTERIZATION OF A FLUORESCENT GDP ANALOG INTERACTING WITH ELONGATION FACTOR TU. John F. Eccleston, Department of Biochemistry and Biophysics, University of Pennsylvania, Philadelphia, PA. 19082. David M. Jameson, Department of Pharmacology, University of Texas Health Science Center at Dallas, Dallas, TX 75235 and Enrico Gratton, Department of Physics, University of Illinois at Urbana-Champaign, Urbana, Il. 61801.

A fluorescent derivative of GDP was prepared by the reaction of 2'-amino-2'-deoxy GDP with fluorescamine (reaction occurs at the 2'-amino group of the nucleotide). The emission properties, including spectra, polarizations and lifetimes, for this compound free in buffer (50 mM tris·HCl, 10 mM $MgCl_2$, pH 7.6) and bound to elongation factor Tu (EF-Tu) from *E.coli* are presented. Emission data on the fluorescamine-ethylamine conjugate are also given. A multifrequency phase and modulation lifetime study (using nine modulation frequencies over the range of 2 MHz to 80 MHz) indicate that the emissions of these three systems are best characterized by single exponsntial decays corresponding to 1.5 nanoseconds for the fluorescamine-ethylamine derivative in buffer, and 7.7 and 11.0 nanoseconds for the fluorescamine-GDP derivative free in buffer and bound to EF-Tu respectively. These results indicate a homogeneous, non-relaxing environment for the probe on the protein. The results of both steady state and multifrequency differential polarized phase fluorometry further indicate the absence of local rotation of the protein bound probe. Addition of excess GDP to the EF-Tu probe complex leads to displacement of the fluorescamine-GDP derivative as evidenced by the change in both the steady state and dynamic polarization measurements. These results demonstrate the utility of the fluorescamine-GDP derivative as a probe of guanosine nucleotide dependent systems as well as the general applicability of multifrequency phase and modulation fluorometry. Supported in part by NIH grant GM 29603 and NSF grant 79-18646 and ICR Physics 1-2-22190.

W-Pos230 EXCITED-STATE MIXING BY LOCAL ELECTROSTATIC FIELDS IN MOLECULAR CRYSTALS: TRANSITION MOMENT DIRECTIONS IN 9-ETHYLGUANINE, Robert W. Woody, Dept. of Biochemistry, Colorado State University, Fort Collins, Colorado 80523

Previous analyses of the crystal spectra of heterocyclic bases such as the biological purines and pyrimidines have neglected the effects of local electrostatic fields. The permanent dipole field of the crystal can modify the spectrum in two ways: (1) shifting the energies of gas-phase states due to the change in charge distribution upon excitation; (2) electrostatically induced mixing of gas-phase states. In extreme cases, the first effect can reverse the ordering of states in a polar molecular crystal relative to the gas phase. The second effect can lead to significant reorientation of transition moments in the crystal. Both effects are most significant in cases of near degeneracy, such as the near uv spectrum of purines. Guanine has a large ground-state dipole moment, which according to MO theory, decreases markedly on excitation to the first excited state (gas-phase), but increases somewhat on excitation to the second excited state. Calculations on 9-ethyl-guanine crystals indicate that the effect of local electrostatic fields is to reverse the order of the first two excited states in the crystal relative to the gas phase. This eliminates a serious discrepancy between theoretical and experimental transition moment directions in the case of guanine. The effect is also likely to be important in adenine and indole and perhaps in the pyrimidines. Such effects must be considered in improved treatments of the optical properties of nucleic acids and may help resolve difficulties in accounting for the CD of Z-DNA. (Supported by USPH GM-22994.)

W-Pos231 Interpretation of the Raman spectrum observed on a contracted muscle cell. J.-P. Caillé, Dép. de Biophysique, Université de Sherbrooke, Sherbrooke, M. Pigeon-Gosselin and M. Pézolet, Dép. de Chimie, Université Laval, Québec, Canada.

Recently we reported that the internal perfusion of a barnacle muscle fiber with an electrolyte solution containing 10^{-4} M Ca^{++} induced an increase of the characteristic Raman bands of the α-helical conformation and a decrease of a band at 1045 cm^{-1} (Caillé et al., 1983. Biochim. Biophys. Acta 758, 121-127). Following this observation we looked for a relation between these changes of intensities in the Raman spectra obtained from barnacle muscle fibers and from samples of myoplasm prepared from these giant cells. In order to specify the attribution of the band at 1045 cm^{-1}, different experimental conditions were explored. A contribution of taurine to the Raman spectrum of these cells at 1045 cm^{-1} was also investigated and a reversible reduction of the intensity of this band was observed on contracting isolated muscle cells. On isolated muscle fibers in isotonic solution with zero Ca^{++} an increase of the band at 1045 cm^{-1} and a reduction of the amide I band at 1650 cm^{-1} were observed. A rotation (90°) of the myoplasmic sample reduced the intensity of the amide I band, this observation confirms that the molecules with an α-helical conformation are oriented. It is postulated from these observations that taurine which is present in almost all muscle cells, contributes to the Raman spectrum of the barnacle muscle fibers and interacts with the contractile proteins during muscular contraction.

This work was supported by the Medical Research Council of Canada, the National Research Council of Canada and the "Fondation de la Recherche en santé du Québec".

W-Pos232 ANALYSIS OF LIGHT SCATTERING AND ABSORPTION FLATTENING EFFECTS IN THE CIRCULAR DICHROISM SPECTRA OF SMALL UNILAMELLAR VESICLES. D. Mao and B.A. Wallace, Dept. of Biochemistry, Columbia University, 630 West 168th Street, New York, N.Y. 10032.

The large size of membrane particles and the high local concentrations of proteins in these particles give rise to differential scattering and absorption flattening effects. These result in significant distortion of the circular dichroism spectra of membrane proteins and produce erroneous estimates of secondary structure.

In an attempt to find a membrane system in which scattering and flattening are minimal, but in which native protein conformation is retained, several methods of fragmentation, including sonication, solubilization and incorporation into small unilamellar vesicles (SUVs) were examined. Bacteriorhodopsin in purple membrane sheets was used as a test system for the effectiveness of the procedures since its secondary structure is known from independent physical measurements and these large membranes produce considerable distortions, as seen by comparison of observed and calculated spectra for the protein. While sonication decreased differential scattering, it had little effect on the total distortion; solubilization in octyl glucoside tended to decrease both differential scattering and flattening, but induced some conformational change in the protein. However, when bacteriorhodopsin was incorporated in active form into small unilamellar vesicles, which serve to both decrease particle size and dilute the concentration of protein, the spectrum produced was nearly identical to the calculated one, suggesting SUVs may be appropriate vehicles for use with membrane proteins and may be a facile method for eliminating optical artifacts.

Supported by NIH Grant GM 27292.

W-Pos233 RESONANCE RAMAN CHARACTERIZATION OF A NOVEL, OXYGEN BINDING HEME PROTEIN FROM C. VINOSUM. E. W. Findsen and M. R. Ondrias, Department of Chemistry, University of New Mexico, Albuquerque, NM 87131; D. F. Gaul and D. B. Knaff, Department of Chemistry, Texas Tech University, Lubbock, TX, 79409.

Recently a high-spin-oxygen binding heme protein was isolated from the purple sulphur bacterium, Chromatium vinosum. This protein has been found to bind oxygen and CO when the heme is in the ferrous state. Resonance Raman spectroscopy has been employed to study the heme moiety. The results are compared to adult human hemoglobin (HbA). Resonance Raman spectra have been obtained for the ferrous and ferric resting enzyme and a ligand bound species, using O + B band excitation. Qualitative comparison of the high frequency regions of the Chromatium high spin heme protein (CHP) and hemoglobin confirms previous studies which indicated that the resting ferrous enzyme is high-spin and five-coordinate. Bands due to peripheral vinyl interactions with the protein matrix are not observed in the spectra of CHP indicating that the method of interaction of the heme moiety with the protein matrix is very different from that of HbA. The heme-core sensitive modes may indicate distortions of the heme geometry of CHP relative to HbA. Spectra of liganded species of CHP indicate that the access of exogenous ligands to the heme pocket is more restricted in ferric CHP than in ferrous CHP. This suggests that substantial conformational changes take place in the protein near the heme pocket between the oxidized and reduced resting enzyme.

W-Pos234 UO_2^{2+} AS A BIOPHYSICAL PROBE: MAGNETIC CIRCULAR DICHROISM SPECTRUM OF URANYL PHOSPHATE. Robert Renthal and Paul Friedman, U. of Texas at San Antonio, San Antonio, Texas 78285

Recent studies have employed UO_2^{2+} as a structural probe in low angle X-ray scattering of membranes and dark field electron microscopy of ribosomes, and as a spectroscopic probe in NMR of phospholipids and fluorescence quenching at membrane surfaces. However, the nature of the uranyl binding sites in these experiments has not been clearly demonstrated. We now report a quantitative spectroscopic method for identifying uranyl phosphate complexes, using magnetic circular dichroism (MCD). The dissociation constants of uranyl phosphates were determined by Thamer (JACS 79:4278, 1957) in 0.9 M $HClO_4$. Under these same conditions, we measured the uranyl phosphate MCD spectrum. Uranyl perchlorate displays a weak A-term MCD spectrum centered at 332 nm. As the phosphoric acid concentration is increased, the peaks intensify and sharpen into pairs, with a slight red shift. We have compared the change in ellipticity as a function of phosphoric acid concentration with the dissociation constants measured by Thamer. We find that the phosphate-induced change in the MCD signal at 332 nm is directly proportional to the number of phosphate ligands of UO_2^{2+} ($\Delta\varepsilon_M$ = 0.01). No significant spectral change is observed at this wavelength if acetic acid is added instead of phosphoric. We have also measured the MCD spectrum of uranyl ATP at pH 6. Positive and negative peaks were observed at the same wavelengths as for uranyl phosphate. Uranyl at 0.2 mM was found to be fully complexed to 3 phosphates in 10 mM ATP. Sensitivity to microcmolar concentrations of uranyl phosphate complexes in macromolecules might be achieved with luminescence detection of MCD.
(Supported by grants from the Robert A. Welch Foundation and NIH)